The United Nations University

ORKUSTOFNUN

UNIVERSITY OF ICELAND

Corrosive species and scaling in wells at Olkaria, Kenya and Reykjanes, Svartsengi and Nesjavellir, Iceland

MSc Thesis
Department of Geology and Geography,
Faculty of Science
University of Iceland

by

KIZITO M. OPONDO
Kenya Electricity Generating Co., Ltd.
Olkaria Geothermal Project
P.O. Box 785, Naivasha
KENYA

United Nations University
Geothermal Training Programme
2006 - Report 2
Published in March 2007

The United Nations University

GEOTHERMAL TRAINING PROGRAMME
Orkustofnun, Grensásvegur 9,
IS-108 Reykjavík, Iceland

Reports 2006
Number 2

CORROSIVE SPECIES AND SCALING IN WELLS AT OLKARIA, KENYA AND REYKJANES, SVARTSENGI AND NESJAVELLIR, ICELAND

MSc thesis
Department of Geology and Geography, Faculty of Science
University of Iceland

by

Kizito M. Opondo
Kenya Electricity Generating Co., Ltd. - KenGen
Olkaria Geothermal Project
P.O. Box 785
Naivasha
KENYA

United Nations University
Geothermal Training Programme
Reykjavík, Iceland
Published in March 2007

ISBN 978-9979-68-210-3

This MSc thesis has also been published in August 2006 by the
Department of Geology and Geography,
University of Iceland

INTRODUCTION

The Geothermal Training Programme of the United Nations University (UNU) has operated in Iceland since 1979 with six month annual courses for professionals from developing countries. The aim is to assist developing countries with significant geothermal potential to build up groups of specialists that cover most aspects of geothermal exploration and development. During 1979-2006, 359 scientists and engineers from 40 countries have completed the six month courses. They have come from Asia (44%), Africa (26%), Central America (14%), and Central and Eastern Europe (16%). There is a steady flow of requests from all over the world for the six month training and we can only meet a portion of the requests. Most of the trainees are awarded UNU Fellowships financed by the UNU and the Government of Iceland.

Candidates for the six month specialized training must have at least a BSc degree and a minimum of one year practical experience in geothermal work in their home countries prior to the training. Many of our trainees have already completed their MSc or PhD degrees when they come to Iceland, but several excellent students who have only BSc degrees have made requests to come again to Iceland for a higher academic degree. In 1999, it was decided to start admitting UNU Fellows to continue their studies and study for MSc degrees in geothermal science or engineering in co-operation with the University of Iceland. An agreement to this effect was signed with the University of Iceland. The six month studies at the UNU Geothermal Training Programme form a part of the graduate programme.

It is a pleasure to introduce the ninth UNU Fellow to complete the MSc studies at the University of Iceland under the co-operation agreement. Mr. Kizito M. Opondo, BSc in Chemistry, of the Kenya Electricity Generating Co. Ltd KenGen, completed the six month specialized training at the UNU Geothermal Training Programme in October 2002. His research report was entitled "Corrosion tests in cooling circuit water at Olkaria I plant and scale predictions for Olkaria and Reykjanes fluids". After two years of geothermal research work in Kenya, he came back to Iceland for MSc studies at the Faculty of Science of the University of Iceland in February 2005. In August 2006, he defended his MSc thesis presented here, entitled "Corrosive species and scaling in wells at Olkaria, Kenya, and Reykjanes, Svartsengi and Nesjavellir, Iceland". His studies in Iceland were financed by a fellowship from the Government of Iceland through the UNU Geothermal Training Programme. We congratulate him on his achievements and wish him all the best for the future. We thank the Faculty of Science of the University of Iceland for the co-operation, and his supervisors for the dedication.

Finally, I would like to mention that Kizito's MSc thesis with the photos in colour is available for downloading on our website at page *www.os.is/unugtp/yearbook/2006.*

With warmest wishes from Iceland,

Ingvar B. Fridleifsson, director
United Nations University
Geothermal Training Programme

DEDICATION

I would like to dedicate this work to my parents, my late father Peter Opondo Mutanda and my late mother Christine Nasike Opondo for showing me the way of school at a very early stage in life and to all those who may not be mentioned here but who made immense contributions in my early schooling life.

ACKNOWLEDGEMENTS

I would like to express my gratitude to Dr. Ingvar Birgir Fridleifsson, the Director, United Nations University (UNU) Geothermal Training Programme (GTP) for having offered me the opportunity to attend the MSc. Programme under the University of Iceland-UNU GTP co-operation programme and for his encouragement and guidance throughout the entire course, but also to Mr. Lúdvík S.Georgsson and Gudrún Bjarnadóttir of UNU (GTP) for being of great help whenever I needed it.

I extend my gratitude and indebtedness to my supervisors Prof. Stefán Arnórsson and Mr. Sverrir Thórhallsson for having been there the whole way and providing a very supportive environment for my research along with much guidance. The lecturers at the University of Iceland provided a great learning experience and my sincere gratitude to them. My sincere appreciation to Gestur Gíslason and Grétar Ívarsson of Orkuveita Reykjavíkur for assistance with all the field work at Nesjavellir, to Dr. Sigurdur Jakobsson for analysis and interpretation of infrared spectroscopy, to Ingvi Gunnarsson and Jón Matthíasson for analysis with the Inductively Coupled Plasma (ICP) and the Scanning Electron Microscope (SEM) and Sigurdur Jónsson for the X-Ray Diffraction spectra (XRD), to the staff of Iceland Geosurvey (ISOR) and Orkustofnun (OS) with whom interaction was of great help. To Niels Giroud for providing chemical data for Nesjavellir well fluids and Halldór Ármannsson for chemical data for Reykjanes and Svartsengi well fluids. Special thanks are extended to my fellow students with whom interaction was very encouraging throughout my study.

I would like to thank institutions and organisations that funded and supported my studies; The Government of Iceland through the UNU Geothermal Training Programme (UNU-GTP) and Orkuveita Reykjavíkur (Iceland). To my employer, the Kenya Electricity Generating Company Ltd (KenGen) for granting me study leave to carry out this study.

My deepest thanks to my wife, Eunice who played dad and mum during my long period of absence, my daughters Christine Nasike, Esther Narotso, Lynn Nabwire all who had to bare with my long absence. You all were of great encouragement whenever I phoned and talked to you. To almighty God for keeping me in good health during my entire stay.

ABSTRACT

The Olkaria geothermal system in Kenya is located within the Okaria volcanic complex in the central sector of the Kenya Rift Valley. Reykjanes, Svarstengi and Nesjavellir geothermal fields are located in southwest Iceland and fall on a continuous earthquake epicentric line extending through the Reykjanes Penninsula that stretches northeast to Langjökull. These four geothermal fields are all high-temperature. Measured temperatures in Olkaria are as high as 350°C, Reykjanes 320°C, Svartsengi 240°C and Nesjavellir > 380°C. The reservoir waters in the four fields vary. The water type at Olkaria is mainly dilute near neutral pH sodium -chloride and sodium-bicarbonate waters with chloride ranging between 50 and 4000 ppm at atmospheric pressure. At Reykjanes and Svartsengi these are saline sodium-chloride waters with chloride being 20,000 and 13,000 ppm, respectively, while at Nesjavellir they are very dilute sodium chloride waters with chloride of ~ 150 ppm.

Gas concentrations in the fluids of all the four fields are low, except for fluids of the Olkaria West sector in Olkaria. Speciation calculations indicate that in Olkaria CO_2 partial pressures range between 0.5 bar and 5 bar except for fluids in the Olkaria West sector with > 90 bars a. At Reykjanes, Svartsengi and Nesjavellir the CO_2 partial pressures fall between 0.0867 to 1.66 bars a. The high CO_2 partial pressures cause CO_2 rich waters to develop when CO_2 in steam encounters shallower ground waters. This becomes corrosive in the process as the pH of the water is lowered. At Reykjanes and Svartsengi, well fluids are low in pH but this is little influenced by the partial pressures of CO_2. The pH of condensates that form due to dissolution of CO_2 at separation pressures range between 4.55 and 5.51 for Olkaria wells while at Reykjanes, Svartsengi and Nesjavellir these are between 5.20 and 5.55. Thermodynamic calculations of HCl concentrations using pH, chloride concentrations and aquifer temperature indicate high concentrations of HCl in the aquifer water of Reykjanes and Svartsengi (0.81 and 0.083 ppm) and low HCl concentrations in the Olkaria and Nesjavellir well fluids. In steam high HCl concentrations are derived for Reykjanes well fluids due to high wellhead pressures. Low pH and high chloride concentration coupled with high temperatures contribute to high HCl concentrations in fluid in the Reykjanes and Svartsengi fluids. In dry steam conveyed in steam gathering systems HCl becomes corrosive as steam condenses due to formation of H^+ and Cl^- ions.

Studies of scales formed during tests at Nesjavellir using the binocular microscope, FTIR, XRD, SEM, ICP and UV indicate that scales formed at the wellheads of wells NJ-14 and NJ-22 consisted mainly of sulphides at well NJ-14 and mixed sulphides and oxides at well NJ-22. In separated water after the heat exchangers, entry to retention tank and at injection well the scales consisted mainly of amorphous silica with some indication of clays. Crystalline phases were not prominent in the scales but traces of chalcopyrite were identified in scales formed at the wellhead of well NJ-14 and at the entry to the retention tank. Traces of clays formed in scales at the wellhead of well NJ-22. The highest amount of scale deposited at the entry to the retention tank, with a deposition rate of ~0.261mm/yr. At the injection well the rate was lower ~0.0168 mm/yr.

Olkaria well OW-34 has an enthalpy close to that of dry steam of 2672 kJ/kg and anomalous chemistry. Chloride concentration in the separated water is ~ 4000ppm at atmospheric pressure. The high solute content in well OW-34 fluids is influenced by evaporative effects due to the high discharge enthalpy. Scales formed in the wellhead equipment and studied by the same method above indicated they were prominently amorphous silica scales. Crystalline phases were absent from the scales.

TABLE OF CONTENTS

Page

LIST OF FIGURES

Page

1. INTRODUCTION

For many countries geothermal energy is an important resource. Utilisation, both direct and for power generation, is increasing faster than that of any other energy resource. Worldwide installed capacity of geothermal power plants has increased by ~ 10 % or more per year over the last two decades (Bertini, 2005). The technology needed to harness geothermal energy has advanced much over the last 20-30 years and steps have been taken to reduce the environmental impact of geothermal energy utilization, particularly by injection of spent fluid into wells and directional drilling. The main operational problems encountered when utilising high-temperature geothermal reservoirs for power generation involve the formation of various types of scales in production wells, surface equipment and injection wells. Corrosion is sometimes also a problem, both for high and low-temperature fluid utilisation.

The most common scales formed are amorphous silica and calcite. However, many other types of scales have been encountered including metal-sulphides, silicates of iron and aluminium and anhydrite. In geothermal fluids various species can be corrosive and these include chlorides, carbon dioxide, ammonia, hydrogen ion, dissolved oxygen, bisulphate, which dissociates into sulphate and H^+ upon cooling. Chloride ion breaks passive films that are protective on metal surfaces and can concentrate in crevices and cause pitting corrosion. Hydrogen chloride in steam can produce acid condensate and lead to severe corrosion. Dissolved carbon dioxide gas in geothermal water causes corrosion of low carbon steels, which is generally localized.

In this study special attention is given to assessing the conditions for the formation of amorphous silica and calcite scales, and the concentrations of the corrosive species CO_2 and HCl in geothermal water and steam. Special attention is given to scaling in wells and wellhead equipment that are in contact with slightly wet steam. The study is based on data from Olkaria, Kenya and Reykjanes, Svartsengi and Nesjavellir, Iceland. Further scaling tests were carried out at Nesjavellir, Iceland, both at wellheads and downstream, where the separated water was oversaturated with respect to amorphous silica.

1.1 Corrosion in geothermal environments

Corrosive attack in high-temperature geothermal installations is found mainly in well casings, condensate injection pipelines made of carbon steel, wellhead equipment and turbine blades. In generation of electricity by direct contact condensing turbines where a cooling water circuit is utilized, low pH (4-5) of the condensate is caused by the dissolution of CO_2 and H_2S gases present in the steam. In condensate injection pipelines made of carbon steel, Villa et al. (2001) and Villa and Salonga (2000) report rapid deterioration due to low pH of condensates. Oxygen ingress exacerbates the problem. When conductive heat losses occur along steam pipelines, steam may condense and through dissolution of CO_2 and H_2S, lower the pH (Thain et al., 1981; Henley et al., 1984). In Olkaria, Svartsengi and Nesjavellir direct contact condensing turbines are utilized and low pH condensates which are corrosive develop. Corrosion related to the low pH condensates on disposal is not reported.

In superheated steam where HCl is present Allegrini and Benvenuti (1970), Meeker and Haizlip (1990) and Truesdell (1991) describe severe corrosion in well casings, steam gathering systems and turbine blades, mainly caused by H^+ and Cl^-. Thórhallsson (2005) reported corrosion in steam pipelines due to HCl transported in the steam in a dry steam well at Svartsengi. In Svartsengi, Thórólfsson (2005) has reported various corrosion related problems observed during maintenance of the plant.

Corrosion of casing in high-temperature geothermal systems can also be related to low pH associated with acid-sulphate waters. In andesitic geothermal systems like those found in the Philippines, e.g. the Tiwi and Bacman fields, Sugiaman et al. (2004) and Rosell and Ramos (1998) report casing corrosion observed due to penetration by low pH acid sulphate water. Similar casing corrosion was reported in Cerro Prieto, Mexico by Dominquiz (1980) and Miravalles, Costa Rica by Moya et al. (2005). In

other cases, casing corrosion has been caused by CO_2 rich waters in geothermal fields. These waters form when ascending CO_2 rich steam dissolves in near surface shallow waters. In the Broadlands-Ohaaki geothermal field, New Zealand, Hedenquist and Stewart (1985) reported severe external well casing corrosion caused by CO_2 rich steam-heated water. Zarouk (2004) reviewed casing corrosion occurrences in New Zealand geothermal fields. In all cases, these are related to CO_2 rich dilute geothermal water. In Olkaria, Omenda (1998) and Karingithi (2002) report CO_2 rich fluids but the extent to which they are corrosive is not known.

Modes of corrosion attack in geothermal installations have been disscussed by Conover et al. (1979), Boulton and White (1983) and Corsi (1986). These are uniform (general) corrosion, pitting corrosion, crevice corrosion, stress corrosion cracking (SCC), sulphide stress cracking (SSC), intergranular corrosion, galvanic coupling, corrosion fatigue, microbiological by induced corrosion, erosion corrosion and cavitation.

1.2 Scale formation

The main drawbacks in the utilization of geothermal resources arise from the precipitation of solid scales from the geothermal fluid. In many cases the scales cause restriction in flow, e.g. in the boreholes, two phase pipelines, the separators and waste water lines and steam pipelines. Their formation often impedes the closing and opening of valves leading to leaks. Deposition on turbine blades is common which results in the turbine chest pressures increasing. Three main areas of scale deposition can be distinguished (Corsi, 1986). These are: deposition from a single phase fluid (injection pipelines), deposition from flashing fluid (wells, separators, two phase-pipelines) and deposition by steam carryover (separators, steam lines and turbines).

A great deal of work has been carried out on the nature of scales formed from geothermal fluids (Thórhallsson et al., 1975; Arnórsson, 1981; Gallup, 1989; Gallup, 1998; Simmons and Christenson 1993; Simmons and Christenson, 1994). Amorphous silica and calcium carbonate scales are the most extensively studied but metal sulphides and silicates to a lesser extent, although they are presently receiving more attention (Simmons and Christenson 1993; Simmons and Christenson, 1994; Ármannsson, 1989; Mecerdo et al., 1989; Benoit, 1989; Durak et al., 1993; Hardardóttir et al., 2001; Weissberg et al., 1979; D'Amore et al., 1998; Karebalas et al., 1989; Gallup, 1993; 1998).

1.2.1 Silica

Amorphous silica deposition is probably the most commonly encountered and troublesome scale formed from high-temperature geothermal water. Such scale has been studied by many workers (Weres and Tsao, 1981; Hurtado et al., 1989; Thórhallsson et al., 1975; Arnórsson, 1981; Gallup, 1989; Gallup, 1998; Mahon, 1966; Henley, 1983; Garcia et al., 1996, Yanagase et al., 1970; Itoi et al., 1989; Kato et al., 2003; Corsi, 1986). A lot of effort has been devoted to the study of silica scale formation. In the utilization of high-temperature geothermal resources the efficient extraction of energy is limited by the silica scale that may form as a consequence of cooling.

It has been established that aqueous silica concentrations in high-temperature geothermal fluids are controlled by close approach to equilibrium with quartz (e.g. Fournier and Rowe, 1966; Mahon, 1966; Fournier, 1973; Fournier and Rowe, 1977; Fournier and Potter, 1982, Gíslason et al., 1997; Gunnarsson and Arnórsson, 2000). The quartz solubility constant has been the subject of thorough experimental studies (Fournier, 1983; Fournier, 1985; Fournier and Potter, 1982; Fournier and Rowe, 1977). Quartz solubility increases with increasing temperature. Often quartz is not present as a primary mineral in geothermal systems but forms by precipitation from the water. Silica scales are only known to form if the extent of boiling and cooling of the aquifer water is sufficient to saturate it with amorphous silica, the reason being the fast rate of deposition for this phase but slow rate for quartz, particularly below 150°C. In contrast to calcite scale formation discussed below, amorphous silica

deposition does not occur at depth in production wells but characteristically in wellheads, surface pipings and injection wells.

The control of silica concentrations in high-temperature geothermal waters by quartz solubility implies that aqueous silica concentrations in producing aquifers increase with increasing temperature of the water. As a consequence, the temperature at which amorphous silica saturation is attained for particular well water depends on the temperature of the source aquifer. Thus amorphous silica scale formation is not a problem unless the reservoir temperature exceeds 250˚C.

The factors that affect the rate of amorphous silica precipitation and colloidal formation polymerisation) include the degree of supersaturation, pH, temperature and salinity. Aeration may also contribute. Reactions between silica molecules in amorphous silica oversaturated solutions may react between themselves to form colloidal silica or deposit from solution to form amorphous silica. The kinetics of amorphous silica precipitation and silica polymerisation have been studied by several workers (Rothbaum et al., 1979; Rimstidt and Barnes, 1980; Weres and Tsao, 1981; Gunnarsson and Arnórsson, 2005).

The solubility of pure amorphous silica has been the subject of many studies (Fournier and Marshall, 1983; Rimstidt and Barnes, 1980; Gunnarsson and Arnórsson, 2000; Marshall and Chen, 1982; Weres and Tsao, 1981; Rothbaum et al., 1979). [Amorphous silica solubility is dependent on ions that affect its surface charge]. Marshall and Warakomski (1980) and Chen and Marshall (1982) have studied the effects of dissolved salts of varying concentrations on the solubility of amorphous silica. Generally, they found that the effect of the cations of the salts had a decreasing effect on amorphous silica solubility in the order $Mg^{2+} > Ca^{2+} > Sr^{2+} > Li^{+} > Na^{+} > K^{+}$. Yokoyama et al. (1989) showed specifically that aluminium ion could have a strong influence on silica polymerisation rates. These effects are likely to be caused by complex formation between silica and cations in the salts but the salts will also affect the value of the activity coefficients taken by aqueous silica species. The presence of cations in solution may also affect the composition of and the precipitated amorphous silica and therefore its solubility. Thus aluminium and iron silicates deposition has been described in other saline geothermal systems such as Milos, Nissyros, Asal., Reykjanes, Salton sea, e.g. Karabelas et al. (1989), Virkir-Orkint (1990), Hardardóttir et al. (2001, 2004, 2005), and Gallup (1989, 1993, 1998).

Several methods have been adapted to reduce or eliminate deposition of amorphous silica in geothermal installations (Yanagase et al., 1970; Weres and Tsao, 1981; Kiyota et al., 2000; Arnórsson, 2000; Gunnarsson and Arnórsson, 2005). A method commonly adapted to reduce amorphous silica scaling in production wells and wellhead equipment is to maintain steam separation pressures (and temperatures), above amorphous silica saturation. Many other methods have been practiced including removal of silica from solution by its precipitation, silica polymerisation and by raising the pH of the separated water even at elevated temperature sufficiently to cause some of the silica to ionize. Acidification has also been applied. It reduces deposition rates. Polymeric silica has less tendency to precipitate out of solution than monomeric silica. The relative rates of the two reactions, amorphous silica deposition and silica polymerisation, and the rate at which polymeric silica settles from solution, determine how successful polymerisation treatment is in reducing amorphous silica deposition from spent geothermal waters.

Deposition of silica scales has been observed in Svartsengi, Reykjanes, Olkaria and Nesjavellir. In all the cases it is reported in wellhead equipment, separated water and in the plant. In Svartsengi, Thórólfsson (2005) reported maintenance problems associated with silica scale formation in heat exchangers, brine pipes and on 1st stage turbine nozzles. In Reykjanes amorphous silica is deposited from separated water at lower temepratures and exists as a mixed scale (Hardardóttir et al., 2001, 2004, 2005). In Olkaria, Opondo and Ofwona (2003) reported intense deposition of silica in the wellhead equipment of one well. At Nesjavellir studies on scale formation by Haukson (1996), Gíslason and Gunnlaugsson (1994-1995) and Kjartansson (1996) indicated problems in pilot heat exchangers. Little indication of silica polymerization or scaling was observed on fluidized heat

exchangers in pilot plant. Silica polymerization results of studies by (Hauksson, 1996) at different temperatures and in different fluid mixtures with condensed steam in pilot plant heat exchangers indicated that, when the residence time of the fluid in the heat exchangers was short, polymerisation took place to a small extent. Silica polymerization proceeded more slowly at low temperatures than high temperatures and amorphous silica saturation was reached in brine at Nesjavellir at about 180˚ C. Silica polymerization tests on a mixture of condensate and separated water showed that the mixture remained undersaturated. Separated waters cooled from ~188˚C to 83˚C (Gunnarson and Arnórsson, 2005), showed that amorphous silica polymerization by ageing the separated water, decreased the potential for amorphous silica deposition.

1.2.2 Calcite

Troublesome calcium carbonate scale formation is known to occur in many geothermal fields (e.g. Simmons and Christenson, 1993; Simmons and Christenson, 1994; Ármannsson,1989; Mecerdo et al., 1989, Benoit, 1989; Durak et al., 1993; Solis et al., 2000). The scale is often calcite but aragonite has also been reported.

According to Arnórsson (1978), (1989), Ármannsson (1989), Benoit (1989), Simmons and Christensen (1994) and Todaka et al. (1995) it is expected that scale formation of this kind is most intense at the depth level of first boiling. Such deposition may significantly decrease the output of production of wells or even clog them. In other rare occurrences calcite deposition has been observed in two-phase lines where fluids from two different wells mix (Solis et al., 2000). Calcite deposition could also occur due to heating of the re-injected fluid.

Waters in the aquifer of high-temperature geothermal systems are close to being calcite saturated (e.g. Arnórsson, 1989; Karingithi et al., 2006) but equilibrium between calcite and solution is rapidly attained (Busenberg and Plummer, 1986; Zhang and Dawe, 1998), certainly at the temperatures of high-temperature geothermal systems. Upon extensive boiling of the aquifer water and subsequent degassing with respect to CO_2, calcite saturated waters will become oversaturated. Calcite solubility increases with decreasing temperature counteracting the effect of degassing during adiabatic boiling.

Deposition of calcite has been observed in production wells at Svartsengi but not at Reykjanes Olkaria and Nesjavellir. In Svartsengi the calcite scaling (Björnsson and Steingrímsson, 1999) was severe during the early years of production. Calcite deposition in Svartsengi followed drawdown in reservoir pressures. In zones where the reservoir pressures decreased, boiling and hence deposition took place at subsequently greater depths in production wells. It was solved by regular mechanical cleaning of the wells and drilling of wider diameter wells that also gave higher yield than earlier wells. The scaling problem vanished when reservoir pressure draw down was sufficient to induce extensive boiling in producing aquifers. Worldwide, calcite scaling problems have been succesfully solved either by mechanical cleaning or by the use of inhibitors (Pieri et al., 1989; Parlaktuna and Okandan, 1989; Candaleria et al., 2000; Siega et al., 2005).

1.2.3 Other scales

Scales of sulphide minerals mostly pyrite, occur widely and are the rule rather than the exception in high-temperature geothermal installations. However, the quantity of the precipitate is generally limited due to low aqueous concentrations of the metals forming the sulphide phases. In brines of high-temperature geothermal fluids, such as in Reykjanes and Svartsengi, Iceland, Milos and Nissyros Greece, Asal Djibouti, and Salton Sea California, the concentrations of metals forming sulphide are high leading to extensive sulphide mineral deposition. By contrast, they are low in dilute fluids, e.g. at Broadlands, New Zealand (Weissberg et al., 1979). The metals are often transported as metal complexes. The state of pyrite saturation is largely affected by degassing of the boiling water, the pH change associated with boiling and the change of pyrite solubility with temperature. Increase in pH due to boiling results in a decrease in the solubility of pyrite.

The rate of sulphide precipitation is fast and is not a limiting factor for the rate of scale formation. Scales of metal sulphides are mechanically resistant. They are known to protect casing materials and pipings from corrosion by various components present in geothermal water and steam such as CO_2. Extensive sulphide scales, associated with saline fluids have been reported by Hardardóttir et al. (2001) at Reykjanes, Iceland, at Assal Djibouti by D'Amore et al. (1998), at Milos Greece by Karebalas et al. (1989), at Salton Sea California by Gallup et al (1990). At Reykjanes, Asal and Milos the sulphide scales were mainly composed of sulphides of lead, zinc, copper and iron. Amorphous phases mainly of silica and some oxides of iron were also formed mainly downstream of flash valves. Poorly crystalline or amorphous aluminium and iron silicate scales have also been identified in geothermal installations at Salton Sea (Gallup, 1993; 1998) as mixtures with metal sulphide scales. A mixture of aluminium-magnesium silicates in the scales at Reykjanes are reported by Hardardóttir et al. (2001) although the major scale is sulphide.

Formation of sulphide minerals from geothermal fluids is known to increase deposition of silica, probably because they act as nuclei for the growth of silica minerals. Thus deposition of silica from saline fluids can be a major problem. It has been arrested satisfactorily by acidification. By decreasing water pH, the silica precipitating reaction is slowed down and the amount of sulphide minerals precipitated reduced.

Extensive deposition of sulphides has been observed at Reykjanes but not Olkaria, Svartsengi and Nesjavellir. In Reykjanes, Hardardóttir et al. (2001, 2004, 2005) studied the formation of sulphide scales, mixed scales and amorphous silica scales from brine surface pipings at different pressures. They concluded that there was a relationship between the types of scales formed and pressure after orifice plates and sequential deposition with decrease in temperatures was observed. Sulphides deposited were relatively high at high temperatures while amorphous silica and mixed scales deposited at lower temperatures. The sulphide scales were enriched in heavy metal concentrations.

1.2.4 Objectives of the study

The study for the thesis focuses on the following objectives:

- Assess corrosive behaviour by calculations of CO_2 and HCl concentrations in the fluids in Olkaria, Reykjanes, Svartsengi and Nesjavellir.
- Evaluate potential calcite scaling of pre-boiled geothermal waters with different salinities, CO_2, temperature and pH.
- Evaluate scales deposits during scaling tests at Nesjavellir and scales from Olkaria well OW-34.

2. GEOLOGICAL FEATURES OF THE STUDY AREAS

2.1 The Greater Olkaria Geothermal System

The Olkaria geothermal system is located south of Lake Naivasha on the floor of the southern segment of the Kenya rift which is part of the East African Rift Valley. The East African rift runs from the Afar triple junction at the Gulf of Eden in the north to Beira in Mozambique in the south. It is a segment of the eastern arm of the rift that extends from Lake Turkana in the north to Lake Natron in northern Tanzania to the south. The rift system that falls within Kenya and the location of Olkaria is shown in Figure 1.

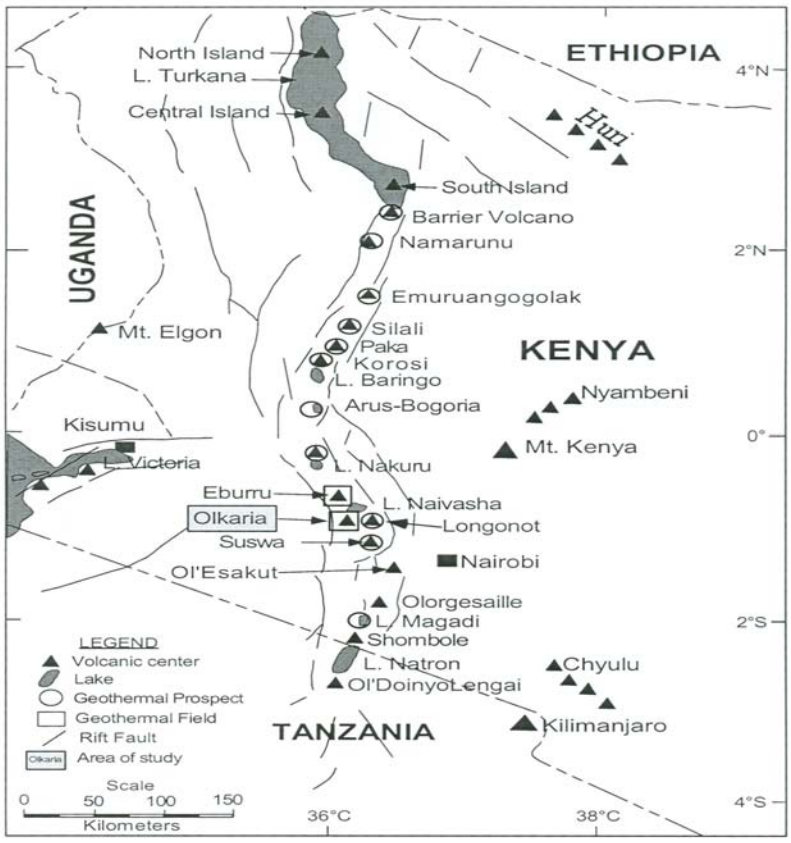

FIGURE 1: A map of the Kenya Rift showing the major geothermal prospects and the Olkaria geothermal field

The Olkaria geothermal system is about 120 km northwest of Nairobi, the Kenyan capital. Initial exploration work in Olkaria began in the 1950's and the first exploration wells were drilled around 1956. They did not successfully discharge. Systematic exploration was again began in 1970 under the initiative of the United Nations Development Programme (UNDP) and the Government of Kenya and drilling recommenced in 1973 after extensive surface work, by the drilling of Olkaria well OW-01. The well proved to have low temperatures. A second well, well OW-02 was drilled and this proved to be more successful. More drilling was undertaken and in 1976 a prefeasibility study to utilize geothermal steam for electricity generation was done by SWECO and VIRKIR consulting companies. The first unit of 15 MWe was constructed in 1981, the second in 1982 and the third in 1985. After the intial five years of steam production in Olkaria, steam decline was experienced in the steamfield. Make up wells were drilled based on reservoir simulation studies by (Bodvarsson and Preuss, 1987) to increase steam production.

The resource is hosted within the Olkaria volcanic complex which consists of a series of lava domes and ashes, the youngest of which has been dated at ~ 200 years (Clarke et al., 1990). This complex is estimated to be 50-80 km^2. Maximum temperatures in deep wells at Olkaria range between ~ 200°C and ~340°C. The area has been divided into seven sectors for purposes of development (Figure 2).

The sectors are named Olkaria East, Olkaria North East, Olkaria North West, Olkaria South West, Olkaria South East, Olkaria Central and Olkaria Domes. Four power plants are currently in operation in the Greater Olkaria Geothermal Area with a total generating capacity of ~ 129 MWe. Two plants are operated by KenGen, i.e. the Olkaria I and Olkaria II plants that generate ~ 115 MWe. The Olkaria I plant has a capacity of 45 MWe and receives its steam supply from the Olkaria East Production Field. The Olkaria II plant, which is about 3 years old, receives steam from the Olkaria North East Field. Two independent power producers generate about 14 megawatts of electricity from

the Western Sectors. The Olkaria III plant, operated by Orpower 4 Inc., a subsidiary of Ormat International generates 12 MWe and ~ 2 MWe are generated by a flower farm, Oserian Development Company from wells leased from KenGen. These two plants are organic Rankine Ormat cycle plants. Plans are underway to expand the capacity of Olkaria II plant in the Olkaria North East Field from 70 MWe to 105 MWe by the year 2007 (Mwangi, 2005) and the Orpower 4 Inc. plant from 12 Mwe to 48 Mwe by 2006 (Reshef and Citrin, 2003).

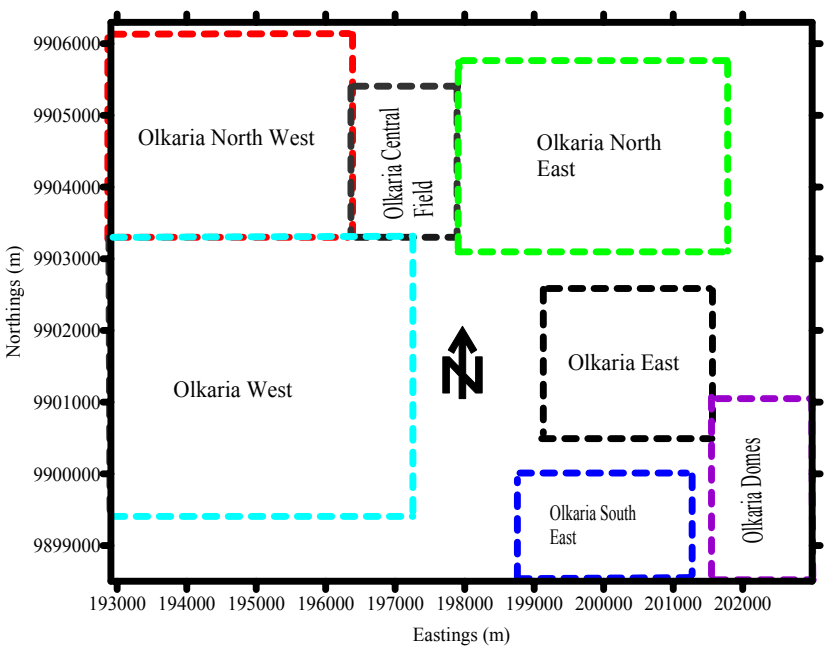

FIGURE 2: Location of the geothermal fields in the Greater Olkaria Geothermal Area

The geology around Olkaria has been studied by numerous workers (Naylor, 1972; Brown, 1984, Odongo, 1986; Clarke et al., 1990) and is described as being characterized by numerous eruptive volcanic centres of Quaternary age. The geothermal field is located within a remnant of a caldera complex intersected by N-S rifting faults. These faults are conduits for numerous eruptions that have formed pumice and ryholite domes within the Olkaria Volcanic complex. The area has a thick cover of pyroclastic ash which is thought to have been erupted from volcanic centres outside Olkaria namely Suswa and Longonot. The Olkaria Volcanic complex is considered to be bounded by arcuate faults forming a ring or a caldera structure. Within this structure a magmatic heat source might be represented by intrusions at depth. Faults and fractures are prominent in the area with general N-S and E-W trends but there are also some inferred faults striking NW-SE. Other structures in the Olkaria area include the Ol'Njorowa gorge that trends NW-SE and may represent a fault, the Ololbutot fault that trends N-S, the ENE-WSW trending Olkaria fault, the WNW-ESE trending Gorge Farm fault, and Olkaria fractures.

The general subsurface stratigraphy at Olkaria has been described by Brown (1984), Odongo (1986) and Mungania (1992). The rocks at the surface are composed of comendites and pantellerites and these also occur in the upper parts of the subsurface. Omenda (1998) has described the lithostratigraphy of the Olkaria geothermal area as it is revealed by data from the geothermal wells. These consist broadly of six main groups, namely proterozoic "basement" formations, pre-Mau volcanics, Mau tuffs, Plateau trachytes, Olkaria basalt and Upper Olkaria volcanics.

2.2 The Reykjanes and Svartsengi geothermal fields

The Reykjanes Peninsula is located in southwest Iceland and falls on the continuous earthquake epicentre line extending through the peninsula and further inland, reaching several more high-temperature geothermal fields (Saemundsson and Fridleifsson, 1980). Figure 3 shows a simplified geological map with the location of the Reykjanes, Svartsengi and Nesjavellir fields and other high-temperature fields in Iceland.

The Reykjanes geothermal field is one of the six geothermal fields on the Reykjanes Peninsula which make up the western volcanic zone. Initial development of the geothermal resources at Reykjanes dates back to around 1956, when the first exploratory well was drilled in the area. To evaluate the

geothermal reservoir for production of water and steam, extensive field investigations were carried out in the period between 1968 and 1970. This effort revealed a high-temperature geothermal resource. The reservoir temperatures are between 250˚ and 320°C. The stratigraphic succession of the Reykjanes geothermal field, revealed by drilling, consists of four main units, namely an upper strata (< 120 m) characterised by pillow basalt and on top by subaerial basalt flows of postglacial age. A more dominant sedimentary tuff formation above 1000 m and more crystallized basalt formations at greater depths have been identified (Tómasson, 1971). Thick hyaloclastite tuff formations have also been identified at depth.

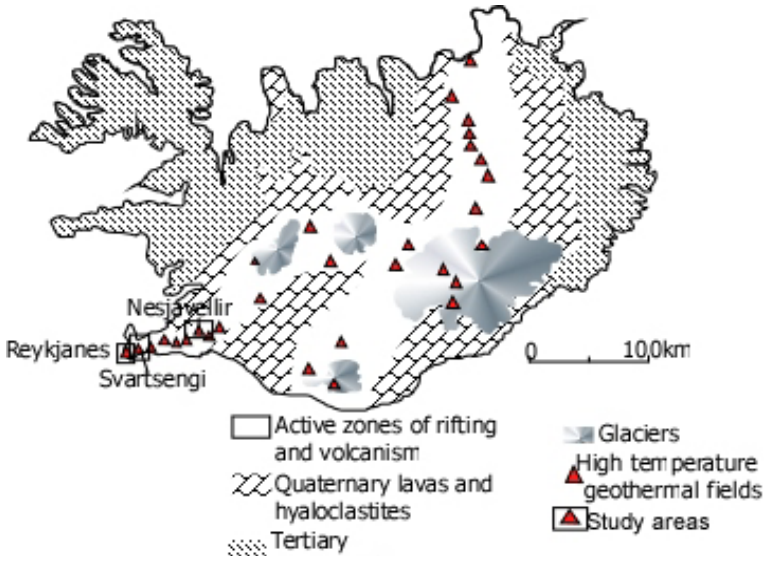

FIGURE 3: A simplified geological map with the locations of high-temperature geothermal fields in Iceland

The wells drilled produced high pressure brine and steam. The development of the Reykjanes geothermal area was based on an interest in producing common salt from brine. A salt production plant was set up in the early 1970's with a 0.5 MWe power plant. More recent surface resistivity studies (Karlsdóttir, 1997) delineate an area with an extent of ~ 10 km^2 for the Reykjanes geothermal system, whereas surface manifestations only cover about 1 km^2. Accelerated drilling was undertaken in Reykjanes during the period 2002 to 2005 and a total of 24 wells have been drilled for electricity production. A 100 MWe power plant was commissioned at Reykjanes in May 2006. The locations of wells drilled into the Reykjanes geothermal field are shown in Figure 4.

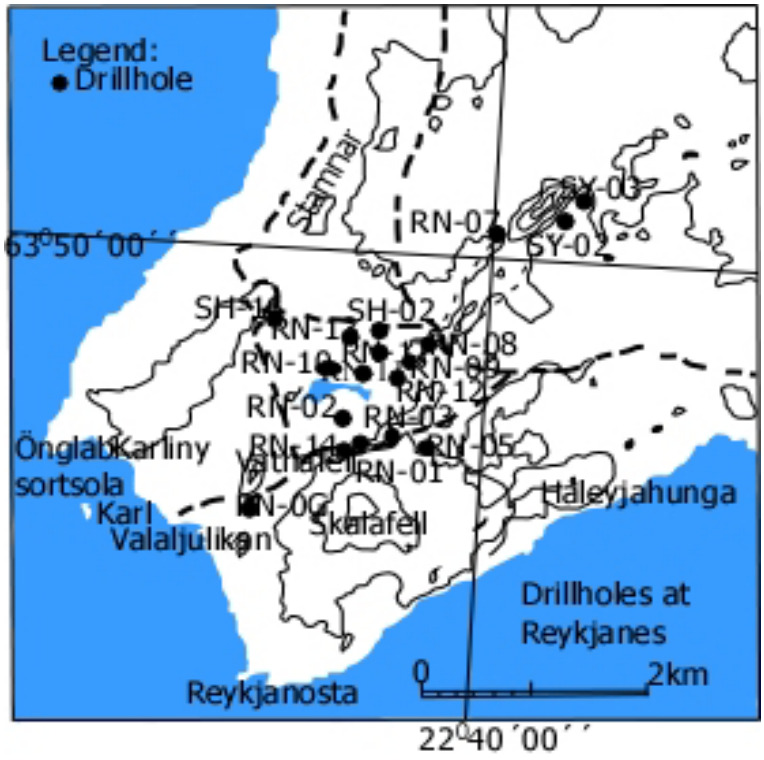

FIGURE 4: Location of wells in the Reykjanes geothermal field

The Svartsengi geothermal field (Figure 5) is located about 15 km to the east of the Reykjanes geothermal field. Stratigraphically it consists of basaltic formations down to ~300 m depth, followed by about 300 m thick hyaloclastite series, and this is the cap rock of the reservoir. Underneath the hyaloclastites there are flood basalts. At 1000-1300 m depth intrusions become dominant (Franzson, 1983; 1995). A fissure swarm crosses the reservoir in the eastern part of the well field. Surface manifestations are limited and mostly confined to fumaroles in a post-glacial lava field. Discharges to the surface are in the form of steaming fumaroles. Reservoir temperatures are uniform between 235 and 240°C (Björnsson, 1999). The field supports a geothermal combined heat and power plant with ~

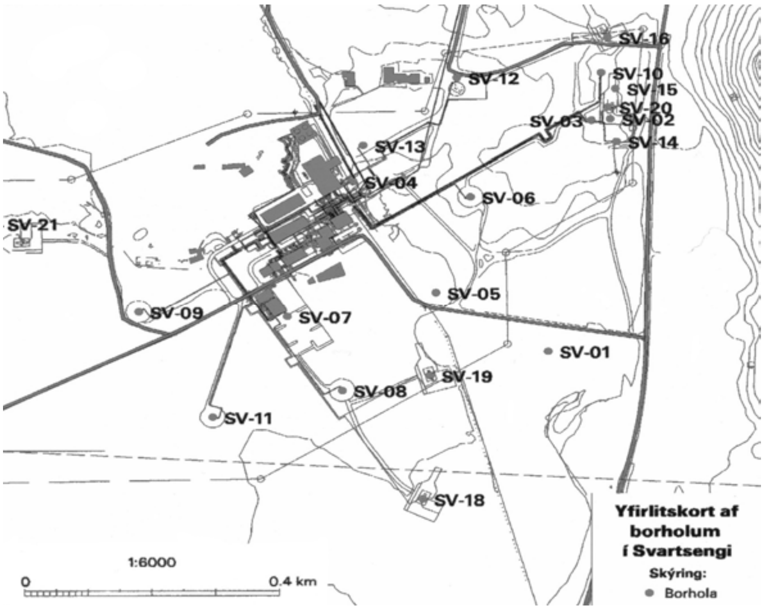

FIGURE 5: Well locations in the Svartsengi geothermal field

46.4 MWe and 125 MWt. A shallow steam zone has evolved with time at Svartsengi and this zone contributes substantially to the power production. The Svartsengi geothermal field has an areal extent of ~ 1 km^2. Well locations in the Svartsengi geothermal field are shown in Figure 5.

2.3 Nesjavellir geothermal field

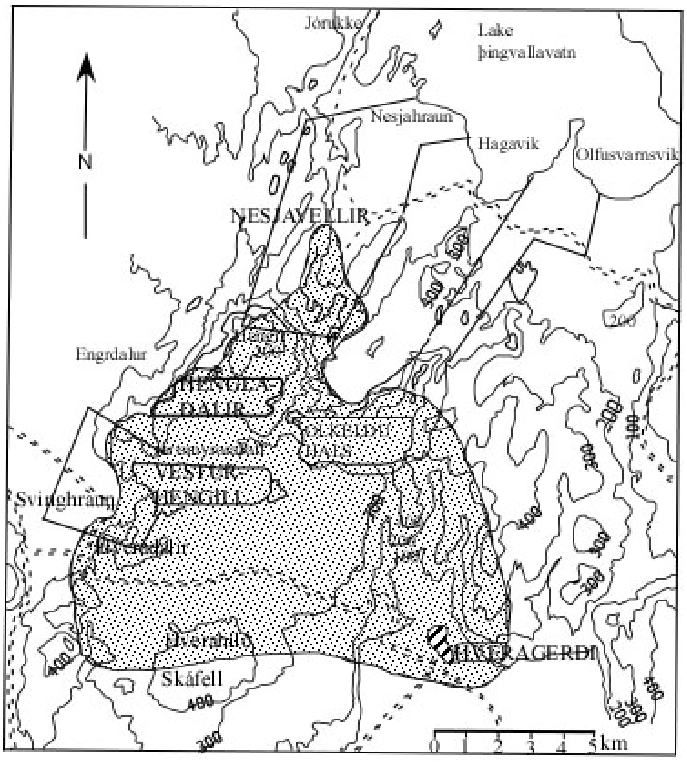

FIGURE 6: Resistivity map delineating the lateral extent of the Hengill geothermal area

The Nesjavellir geothermal field is located in the Hengill high-temperature geothermal area which is situated within the active volcanic zone in southwest Iceland. This belt is characterised by several NE-SW trending fissure swarms exhibiting normal faults and open fissures. The Hengill volcano is intersected by one of these fissure swarms. It is about 50 km long and has a structure of nested grabens. Faults are very abundant within the fissure swarm. Several eruptive fissures transect the centre of Hengill and extend to the northeast by Nesjavellir. Geothermal surface manifestations cover an area of about 40 km^2 (Figure 6).

These include fumaroles, mud pools, steaming ground and acid surface alteration as well as hot springs. From the Hengill there is a lineament of surface manifestations extending towards the SE into the Hveragerdi centre forming a continuation of the transcurrent faults dissecting the main fissure swarm.

Surface surveys for geothermal exploration in the Hengill area started in the 1940´s. Drilling started in the late 1950’s and early 1960’s. In 1990 the geothermal resource at Nesjavellir was harnessed for district heating in Reykjavík. This involved heating water using heat exchangers. The geothermal water could not be used directly due it its chemical content. At the time it was decided to harness the geothermal resource at Nesjavellir, 14 production wells had been drilled and all but one were successful (Gunnarsson et al., 1992). Wells drilled at Nesjavellir range in depth from 1,000 to 2,200 meters and the highest temperatures recorded are > 380 ˚ C (Gunnarsson et al., 1992).

The stratigraphy at Nesjavellir as revealed by drilling, consists mainly of volcanic rocks. These are divided into extrusive and intrusive rock formations. The extrusive rocks consist mainly of

hyaloclastites and basalt lavas. Nouralie (2000) described the stratigraphy as consisting mainly of hyaloclastites in the shallower parts of the system, < 730 m. In the deeper parts, > 730 m, basalt lavas are predominant. The hyaloclastites are mainly volcanics which are divided into four groups; Tuffs, Breccia lavas, Basaltic breccias and Pillow lavas. The intrusives are predominantly basalts and are found in the deeper parts of the system.

The thermal plant was initially commissioned to generate about 100 MWt of heat, but has since been progressively expanded in tandem with better utilization of the resource. In 1991 the capacity of the thermal plant was expanded to 150 MWt and in 1998 a further 250 MWt and 60 MWe were added. This started the Nesjavellir co-generation plant which has two main functions; to produce electricity from geothermal steam and to heat cold ground water for district heating. Currently, the installed capacity for electricity generation is 120 MWe from four steam cycle turbines of 30 MWe each and 290 MWt. The Nesjavellir geothermal field with well locations is shown in Figure 7.

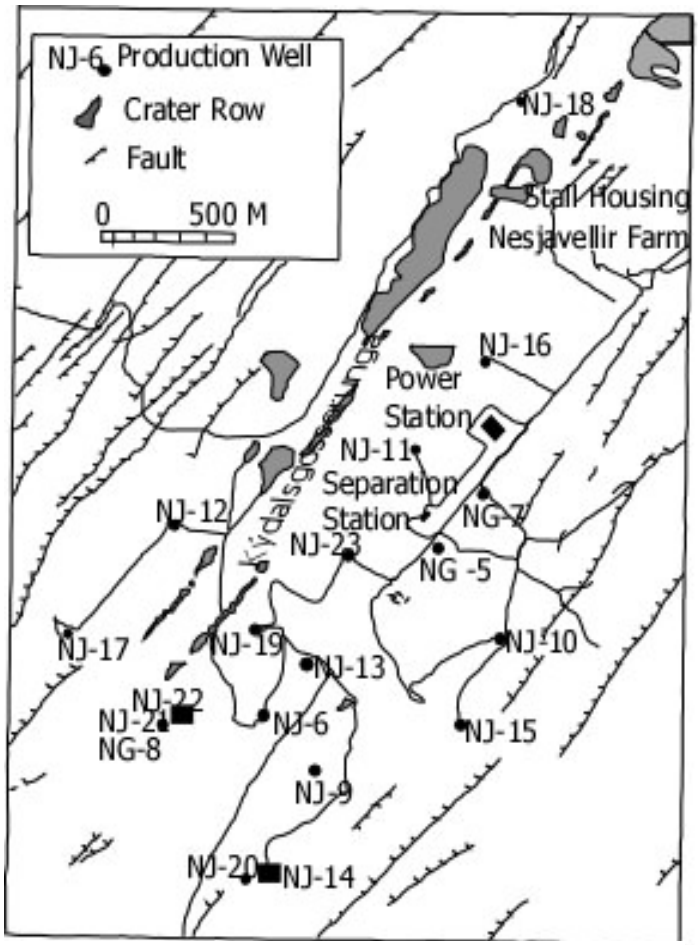

FIGURE 7: Well locations in the Nesjavellir geothermal field

3. SAMPLING AND ANALYSIS

3.1 Sample collection

At Reykjanes, Svartsengi and Nesjavellir,and other Icelandic fields both steam and water are collected at the same pressure using a Webre separator.

At Olkaria various methods have been applied to collect samples of water and steam from the wet-steam well discharges. Some of these methods are described by Ellis and Mahon (1977) and Arnórsson et al. (2000). One of the methods involves the use of a Webre separator, which is connected to a two-phase pipeline that conveys the total discharge to an atmospheric silencer (Figure 8).

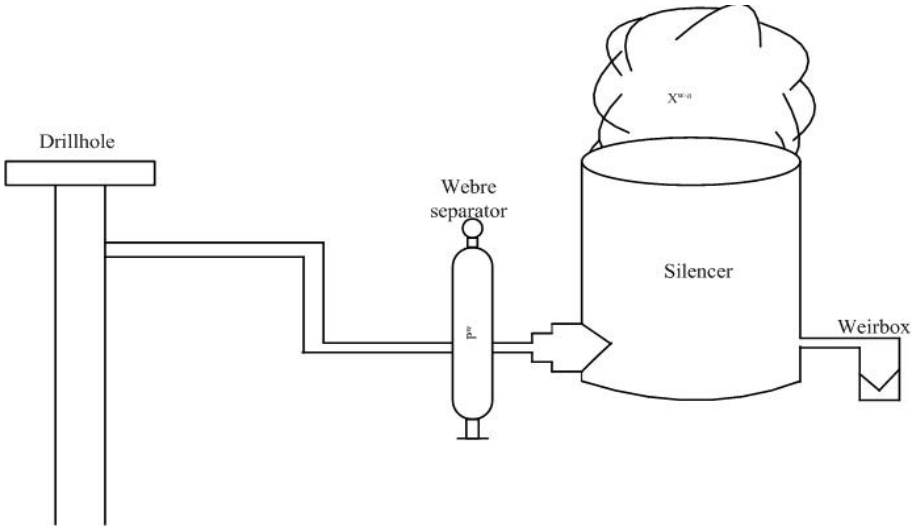

FIGURE 8: Steam is collected from a Webre separator on a two-phase pipeline upstream from the atmospheric silencer and water from the weirbox, a part of the steam (X^{w-a}) discharged from the atmospheric silencer is not sampled, i.e. the steam which forms by depressurisation boiling from the pressure in Webre separator to atmosphere

By this method sampling involves the collection of steam samples under pressure from the Webre separator and water from the weirbox. Steam samples collected in this way are mostly from the wells that are being discharge tested or exploration wells and a number of production wells in the Olkaria East production field that share a common separator station. In the Olkaria North East Field which produces steam for the Olkaria II power plant sampling of steam and water will be carried out by the use of a Webre separator. For production wells in the Olkaria East Production Field, steam samples were collected from the steam line downstream of the wellhead separator using a stainless steel tubing (Figure 9).

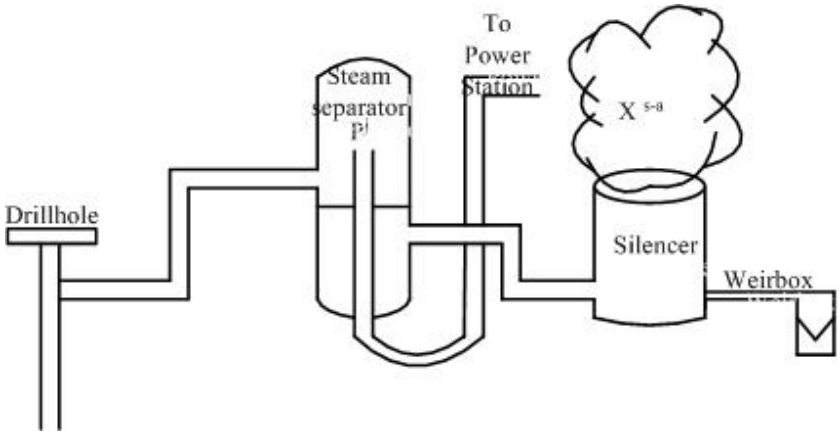

FIGURE 9: Steam is collected from the steam separator and water from the weirbox, the steam (X^{s-a}) discharged from the atmospheric silencer is not sampled. This steam forms by depressurisation boiling from pressure in the steam separator to atmospheric pressure

Water samples were collected from the weirbox. A fraction of the discharge is not sampled when the water and steam samples are collected at different pressures as explained in Figs. 8 and 9. As explained in section 5.2 below, it is assumed when calculating aquifer water composition that the

secondary steam not sampled is free of gas. When collecting water and steam samples from wet-steam well discharges using a Webre separator good phase separation is essential. Pipes from wells with low discharge enthalpy (less than 900 kJ/ kg) may experience slug flow and separation can be a problem. When the steam fraction is high, i.e. the discharge enthalpy approaches that of dry steam (above 2500 kJ/kg), the water flow rate into the Webre separator may not be sufficient for collecting a steam free water sample and when this is the case, the only alternative may be the collection of a water sample at atmospheric pressure (from the weirbox) or from a wellhead steam separator.

The sampling methods in case 3 were applied in Olkaria since the inception of the Olkaria East Production Field, but may change with total re-injection of separated water being a requirement in current power development schemes. This will require in the future that both water and steam are collected at the same pressure.

Steam samples were collected into two gas-sampling flasks, which had been evacuated in the laboratory after introducing 10 ml of freshly prepared 50 % w/w KOH in the case of Olkaria and the others 50 ml of 4M NaOH solution. The gas bulbs were weighed before and after sampling to record the amount of steam condensate collected. Water samples were filtered through 0.2 μm millipore membrane (cellulose acetate) into low density polyethylene bottles using a propylene filter holder. The entire filtration apparatus was thoroughly rinsed with deionised water before collecting a sample. A 100 ml sample was acidified with 1 ml of suprapure concentrated HNO_3 for ICP-AES analysis for Si, B, Na, K, Ca, Mg, Al, Fe and S(SO_4). Another 100 ml sample was collected for SO_4 analysis to which 1 ml of 1% zinc acetate solution was added to remove H_2S. A third 100 ml sample was collected and for the determination of Cl and F by ion chromatography only, 250 ml glass bottles with special caps that prevent entrapment of air were used to collect water samples for the determination of pH and total carbonate carbon. These two water samples, which were not filtered, were cooled to < 40˚C by passing them through a stainless steel cooling coil to prevent degassing of the sample that would otherwise occur upon storage due to thermal contraction of the water prior to analysis.

3.2 Analysis of water and steam samples

Steam samples were analysed for CO_2, H_2S, H_2, CH_4, N_2, and O_2 . The non-condensable gases (H_2, CH_4, N_2 and O_2) were analysed by gas chromatography, while CO_2 and H_2S were determined by titration of the NaOH-condensate solution with 0.1 M HCl and 0.001M $Hg(CH_3COO)_2$ standard solutions respectively (Arnórsson et al., 2000). Both CO_2 and H_2S disssolve quantitatively in the alkaline solutions. In this way, the non-condensable gases become concentrated in the gas phase making analysis for them more precise.

In water samples, H_2S was analysed for in the same way as in steam samples and determined on site to obtain its own concentration and again at the time of the total carbonate (TCC) titration for the purpose of subtraction. Total carbonate carbon (TCC) and pH were determined in the laboratory as soon as possible (1-2 hours) after sampling by titration with 0.1 M HCl. Interference from other bases was corrected for by back titration with 0.1M NaOH following the bubbling of N_2 through the solution to remove CO_2 and H_2S (Arnórsson et al., 2000). By this method, the difference of the two titrations gives the sum of TCC and total sulphide. The value for TCC was obtained by difference from independent measurements of total sulphide. The major aqueous cations (Na, K, Ca, Mg, Al, Fe,) plus Si, SO_4 (as S) and B were analysed for on a Thermo Jarrel Ash ICP-AES. Ion chromatography was used to determine SO_4, Cl, F.

4. FLUID COMPOSITIONS

The composition of fluid discharged from wells in the four areas is quite variable (Tables 1a and 1b in Appendix A). These are taken from different sources, namely Olkaria (Karingithi, 2002), Reykjanes and Svartsengi (Orkustofnun data base, Ármannsson, H., 2005, pers. comm.) and Nesjavellir (Giroud, N., 2006, pers. comm.). Within the Olkaria geothermal field the composition of discharged liquid water and steam is varied but less so at Nesjavellir. In Svartsengi and Reykjanes, fluid compositions are quite homogenous.

The fluid composition from the Greater Olkaria Geothermal Area, Reykjanes, Svartsengi and Nesjavellir is plotted on a Cl-SO_4-HCO_3 ternary diagram (Figure 10). The discharged waters in the Olkaria West Field are predominantly near neutral sodium-bicarbonate waters, while those of from the Olkaria East and Olkaria North East fields are dilute, near neutral-pH chloride waters. The waters from Reykjanes and Svartsengi, plot at the chloride apex. Waters from Nesjavellir are relatively enriched in chloride, like the Olkaria East waters. Waters discharged from wells in Olkaria Central and Olkaria Domes are mainly mixed sodium bicarbonate - sodium chloride waters.

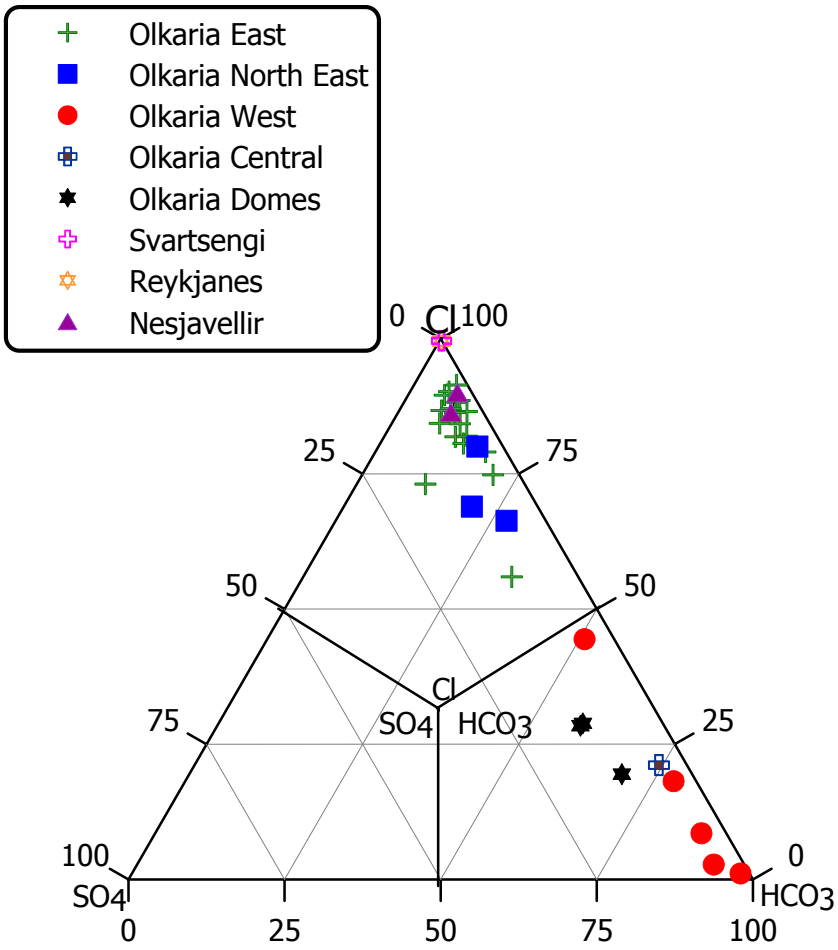

FIGURE 10: Cl-SO_4- HCO_3 ternary plot for fluids from different sectors of Olkaria, Reykjanes Svartsengi and Nesjavellir geothermal fields

Waters discharged from the weirbox of wells at Olkaria have chloride concentrations ranging from ~50 ppm to ~ 4000 ppm. The silica content varies between ~ 350 ppm and ~ 1000 ppm SiO_2. The total carbonate concentration is highly variable ranging from < 100 ppm to almost 2500 ppm as CO_2. Gas content in steam, especially carbon dioxide (CO_2) and hydrogen sulphide (H_2S) is generally low in the fluids of Olkaria except fluid discharged from Olkaria West which has a very high CO_2 gas content in steam ~ 10,000 mmoles/kg (Table 1a, Appendix A). Nitrogen content in steam is relatively high, but highest for well discharges in Olkaria Domes and Olkaria West which could suggest there is a high contribution of flow from the surface to the fluids.

At Reykjanes the water in the reservoir is sea water (Björnsson et al., 1972). The composition of the parent sea water has been modified by reactions with the basaltic rock. Slight loss of sodium has occurred but slight enrichment in silica, potassium and calcium, and almost complete depletion in sulphate and magnesium (Bjarnason, 1984). The chloride content of the geothermal water is close to

that of sea water. Carbon dioxide is the most abundant gas, > 95 %, corresponding to ~2000 ppm in the reservoir fluid. Compared to Olkaria, H_2S and H_2 concentrations are relatively low.

The reservoir water in Svartsengi is two-thirds sea water and one-third meteoric water by origin as indicated by its Cl content. This parent water has also been modified by reactions with the basaltic rock in a fashion similar to the water at Reykjanes. As at Reykjanes, CO_2 gas makes up the major gas in the steam , ~ 95 vol.% . The concentrations of H_2S and H_2 are low relative to Olkaria.

Water discharged from wells at Nesjavellir, which is meteoric by origin is very low in dissolved solids (Table 1 b in Appendix A). Silica is the most abundant dissolved solid. The chloride content is 100-200 ppm. The cause of the low Cl concentrations is the low Cl content of the basalts with which the water has interacted. Carbon dioxide is the major gas component in steam. Hydrogen sulphide and hydrogen concentrations are relatively elevated compared to well fluids at Olkaria, Reykjanes and Svartsengi.

5. CALCULATION OF AQUIFER FLUID COMPOSITIONS

5.1 Discharge enthalpy of wells

Production wells at Olkaria and Nesjavellir typically have "excess" enthalpy (Table 1a and b of Appendix A), i.e. the enthalpy of the fluid discharges is higher than that of steam saturated water at the respective aquifer temperature. At Svartsengi production wells have liquid enthalpy, i.e. their enthalpy equals that of liquid water at the temperature of producing aquifers except for shallow wells which have been drilled into the steam cap that has formed on top of the liquid dominated reservoir as a consequence of reservoir pressure decline following exploitation. At Reykjanes some wells have liquid enthalpy and some excess enthalpy. Excess enthalpy of wells poses problems in calculating component concentrations in the initial aquifer fluid from analytical data on samples of liquid water and steam collected at the wellhead.

Excess well discharge enthalpy in the Olkaria East Production Field may be produced by withdrawal of fluid from the steam zone and the underlying liquid dominated reservoir. In general it may, however, be produced by processes occurring in the depressurization zone around discharging wells where extensive boiling occurs. These processes are: (1) heat transfer from the aquifer rock to the fluid that migrates through the depressurization zone and (2) separation to the relative permeabilities of the liquid water and steam phases and their different flowing properties (e.g. Horne et al., 2000; Pruess, 2002; Li and Horne, 2004). Transfer of heat from the aquifer rock to the fluid flowing through the depressurization zone into wells tends to occur because depressurization leads to cooling of the fluid by boiling and hence generates a positive temperature gradient between the aquifer rock and this fluid. Production of excess well discharge enthalpy by phase segregation tends to occur because the liquid water is partially retained in the aquifer as a result of capillary forces, while the steam flows into wells. "Excess enthalpy" may be due to the presence of significant steam fraction in the initial aquifer fluid. Specifically at Olkaria, the "excess enthalpy" could, at least be due to contribution from the shallow steam zone which overlies the liquid dominated zone. The discharge could also be from multiple feeds, shallow vapour-dominated and deep liquid-dominated feeds.

If the excess discharge enthalpy is solely caused by conductive heat transfer from the aquifer to the fluid flowing into the well (conductive heat transfer model), the composition of the total well discharge will be the same as that of the aquifer fluid. Conservative components, such as Cl, which are concentrated in the liquid water phase, will increase in the phase and approach infinity when the discharge enthalpy approaches that of dry steam. On the other hand, if phase segregation were the cause of the excess discharge enthalpy (phase segregation model), Cl concentrations in the liquid water would be about constant but they would approach zero in the total discharge when the discharge enthalpy approached that of dry steam.

When excess well discharge enthalpy is produced by the conductive heat transfer model, total well discharge compositions can be used to calculate quartz and Na/K geothermometer temperatures. This is, however, not valid if the cause of the excess enthalpy is phase segregation. Total discharge composition will yield low quartz equilibrium temperatures, and the lower the higher the discharge enthalpy. The Na/K geothermometer, which is based on an elemental ratio, is independent of which model is responsible for the excess enthalpy.

Calculated temperatures of tqtz and tNaK from the equations given by Arnórsson (2000 a), for some of the selected wells at Olkaria, Reykjanes, Svartsengi and Nesjavellir are presented in Table 3 of Appendix A. At Olkaria, quartz equilibrium and Na/K geothermometer temperatures compare well when using the segregation model to calculate the aquifer water compositions (Karingithi et al., 2006). This also applies to Nesjavellir (Figure 11).

For the present study, therefore, the phase segregation model and the average of the quartz and the Na-K geothermometer results were used to represent aquifer temperature of wells at Olkaria and Nesjavellir. At Reykjanes, Na/K temperatures are somewhat lower than those of quartz. The cause is

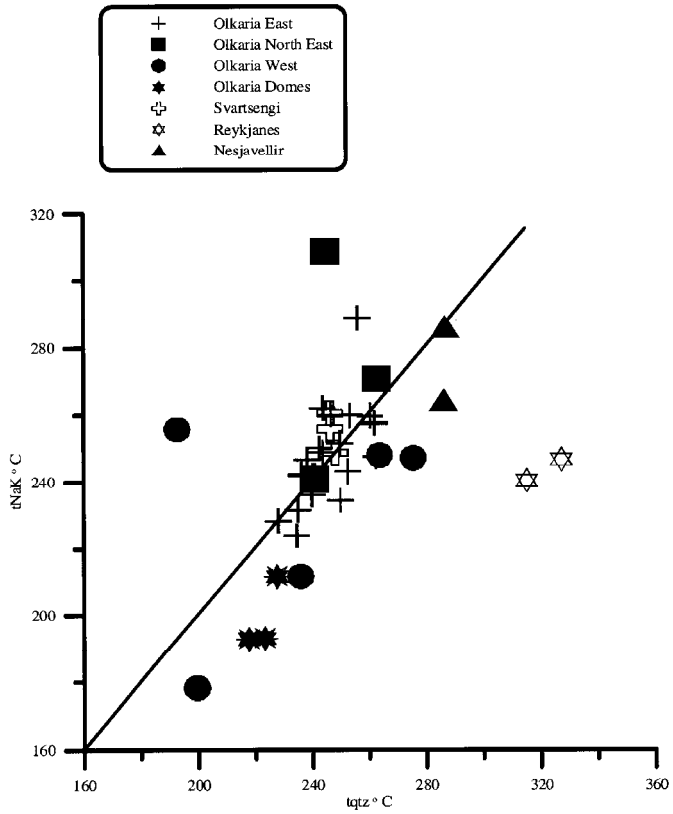

FIGURE 11: Relationship between tqtz vs. tNaK equilibrium

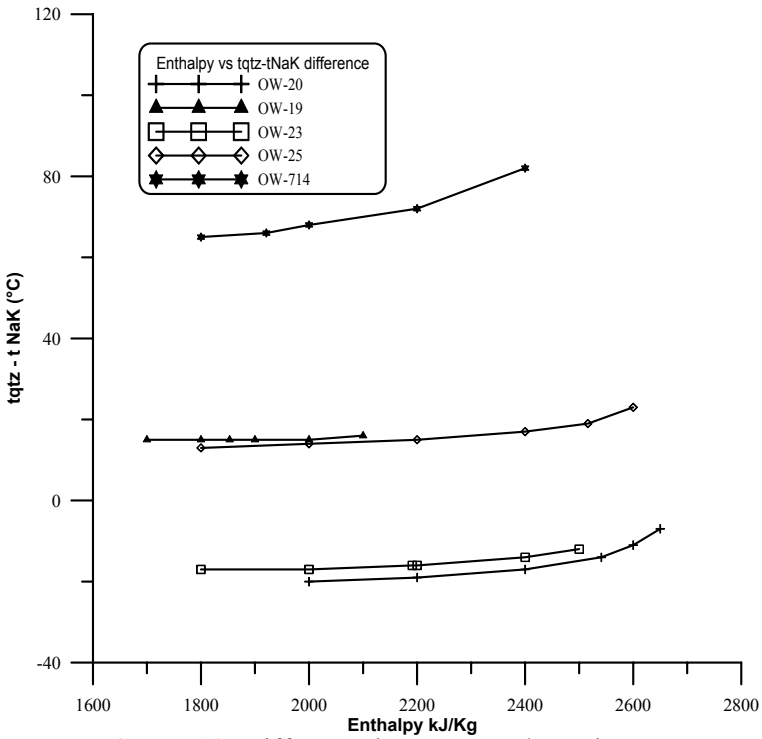

FIGURE 12: Difference between tNa/K and tqtz vs. various enthalpies for selected number of wells from Olkaria East and Olkaria North East

considered to be limited supply of K to the water. The geothermal seawater has about four times the K concentration of seawater and the basaltic rock with which the geothermal seawater has reacted is very low in K. At Reykjanes, measured downhole temperatures were selected taking total well discharge compositions to represent the aquifer water compositions. The enthalpy of the wells represents pure liquid and it is assumed they follow the boiling point with depth curve. In the sub-boiling reservoir at Svartsengi, measured temperatures downhole were selected. They compare well with both quartz equilibrium and Na/K geothermometer results.

A number of selected wells in Olkaria, Reykjanes and Nesjavellir indicate tqtz temperatures that are higher than tNaK. In Reykjanes as explained above, the difference could be due to limited supply of potassium in the water. In the case of a number of selected wells in Olkaria, and Nesjavellir, this could be caused by the model selected to calculate the aquifer water composition which could be wrong. The origin of the fluid composition could be due to conductive heat transfer from the aquifer rock to the fluid flowing into wells which contributes to the discharge enthalpy. Aquifer water composition may not be the source of the error. Other errors may arise from the selection of discharge enthalpy which is affected by measurements of water flow. Wells in the Olkaria Domes sector have enthalpies close to those of liquid enthalpy and tqtz is higher than tNaK. A similar observation is made for wells in the Olkaria West sector (Table 3, Appendix A). This difference may not be explained by the selected discharge enthalpy. A different temperature model may be applicable for temperature selection.

Figure 12 shows enthalpy vs temperature difference between tqtz and tNaK for a number of selected wells in Olkaria. As enthalpy

increases the difference in tNaK – tqtz increases because the enthalpy affects the value of calculated SiO_2 concentration in the liquid water phase.

The temperature difference between tNaK and tqtz in wells OW 709 and OW-202 is high and these stand out (Table 3 Appendix A). The high tNaK and tqtz differences for the fluids of wells OW-709 and OW-202 cannot be explained by enthalpy effects, but possibly by dilution of geothermal water. Such dilution would not affect Na/K temperatures but yield low quartz equilibrium temperatures relative to the temperature of the undiluted water. The high pH of the aquifer fluids of these two wells could affect the tqtz due to enhanced dissociation of the unionised silica, but this does not seem to be the case.

Another well with a high temperature difference between tNaK and tqtz is well OW-34. The well is much higher in mineral content and its enthalpy is high ~2672 kJ/Kg. High enthalpy affects silica concentrations. This could probably contribute to the large differences in tNaK and tqtz temperatures.

5.2 Calculation of gas concentrations in steam at atmospheric pressure

The WATCH chemical speciation program (Arnórsson et al., 1982), version 2.1A (Bjarnason, 1994), was used to calculate aquifer water composition and aqueous species distribution from data on liquid water and steam sample composition at wellhead conditions. This program assumes that both types of samples are collected at the same pressure. As explained in section 3, the Olkaria well samples were collected differently and therefore gas concentration in steam at atmospheric pressure was calculated assuming that the secondary steam not sampled is free of gas. Two cases need to be condsidered (Arnórsson and Stefansson, 2005). One is represented by steam samples collected from the wellhead steam separator and the other when there was no wellhead separator and the steam samples were collected with the aid of a Webre separator, which is connected to the two-phase pipeline discharging into the atmospheric silencer.

Case 1: Steam samples collected from the wellhead steam separator separating the total discharge.

The total steam fraction discharged from the well at atmospheric pressure according to this case is X^{al}, relative to the total well discharge is given by:

$$X^{al} = X^{s} + X^{s-a} \qquad 5.2.1$$

Here, X^{s}, represents the steam fraction in the wellhead separator. The fraction of steam which forms by depressurisation boiling of the separated water flowing from the wellhead steam separator to the atmospheric silencer, $X^{s\text{-}a}$, relative to the total discharge is given by:

$$X^{s-a} = \left(\frac{h^{l,s} - h^{l,a}}{L^{a}}\right)(1 - X^{s}) \qquad 5.2.2$$

$h^{l,s}$ is the enthalpy of liquid water at the vapour pressure in the wellhead separator, $h^{l,a}$ and L^{a} denote the enthalpy of steam saturated water and its latent heat of vaporisation at atmospheric pressure. X^{s} is the steam fraction in the wellhead separator. Hence, (1- X^{s}) is the water fraction.

The gas composition of the total steam discharged (m^{t}_{g}) is given by:

$$m^{t}{}_{g} = \frac{X^{s}}{X^{al}} m^{s}{}_{g} \qquad 5.2.3$$

where m^{s}_{g} represents the concentration of gas in the steam collected from the wellhead separator. For steam samples taken from most of the wells in the Olkaria East Production Field, this approach has to

be applied because the steam samples were collected at wellhead separator pressures and the water at the weir box.

Case 2: Webre separator on a two-phase pipeline discharging into an atmospheric silencer.

The total steam fraction relative to the total discharge is given by the following equation:

$$X^{a2} = X^{w} + X^{w-a} \qquad 5.2.4$$

Here, X^{a2} represents the total steam fraction of the well discharge at atmospheric pressure, X^{w} is the steam fraction in the Webre separator and $X^{w\text{-}a}$ represents the steam fraction that forms by depressurisation boiling from vapour pressure P^{w} to atmospheric pressure.

A portion of the steam is not sampled when using the Webre separator and this fraction is given by

$$X^{w-a} = \frac{h^{t} - h^{l,a}}{L^{a}} - \frac{h^{t} - h^{1,w}}{L^{w}} = X^{a} - X^{w} \qquad 5.2.5$$

$h^{l,\,w}$ and L^{w} represent the enthalpies of the steam saturated water at the vapour pressure in the Webre separator and its latent heat of vaporization, respectively.

For correction of gas composition of steam sampled by use of a Webre separator and depressurisation boiling from vapour pressure P^{w} to atmospheric pressure, the following equation was used:

$$m^{t}{}_{g} = \frac{X^{w}}{X^{al}} * m^{w}{}_{g} \qquad 5.2.6$$

where $m^{w}{}_{g}$ represents the concentrations of gas in a steam sample collected from the Webre separator.

This correction is applicable to steam samples collected from exploration wells, and for steam samples collected before 2001 from wells in the Olkaria North East Field, Olkaria Domes and Olkaria West Fields. The composition of Olkaria well fluids is shown in Table1a of Appendix A and calculated gas concentrations in steam are shown in Table 2a for production wells in Olkaria East and Table 2b of Appendix A for exploration wells in Olkaria North East, Olkaria West and Olkaria Domes.

5.3 Calculation of aquifer water compositions and speciation distribution

Component concentrations and aqueous species distribution in the water was calculated with the aid of the WATCH chemical speciation program (Arnórsson et al., 1982; Bjarnason, 1994), version 2.1A, on the assumption that excess discharge enthalpy was due to phase segregation only and that no equilibrium steam is present in the aquifer. It was further assumed that any phase segregation that has taken place occurs between 180°C and the initial aquifer temperature. For wells in the Olkaria East sector which have a steam separator at the wellhead the calculation involves three steps: Firstly the composition and speciation, including the pH, of the water in the wellhead separator was calculated from the analytical data on the water samples from the weirbox on the assumption that the secondary steam discharged from the atmospheric silencer was free of gas. Secondly, water composition and pH so obtained were used, together with steam analysis data and measured discharge enthalpy, to calculate liquid water and steam composition at 180°C (10 bars abs. vapour pressure). Thirdly, the calculated liquid water and steam composition at 180°C was used to calculate the composition and speciation distribution in the aquifer water taking the fluid enthalpy to be that of steam saturated water at the aquifer temperature, but this temperature was taken to be the average of the tNa/K and tqtz geothermometer temperatures, the latter being consistent with the phase segregation model.

The procedure for calculating aquifer water compositions for wells in other sectors than Olkaria East is somewhat different because the two phases of the discharges travel together to the atmospheric silencer. Firstly, the steam composition at atmospheric pressure was calculated from the analytical data in Table 1a of Appendix A taking the steam fraction, which forms by depressurisation boiling between the gas sampling pressure and atmospheric pressure. Steam and water composition was calculated at 180°C using the discharge enthalpy values, the water composition in Table 1a of Appendix A and calculated gas concentrations in the steam phase at atmospheric pressure. The third step is the same as that for Olkaria East wells.

The selection of the intermediate step at 180˚C is based on the following considerations: the enthalpy of saturated steam reaches maximum at around 235°C and in the range 180-270°C (10-55 bars-abs. vapour pressure) it has a value close to this maximum but at lower and higher temperatures it drops significantly. As a consequence of this, the steam to water ratio (enthalpy) of a fluid has little effect upon depressurisation of the liquid water in the interval 10-55 bars-abs. Below 10 bars abs. steam formation by depressurisation boiling is enhanced by decreasing steam enthalpy. The opposite is the case above 55 bars-abs. Most of the Olkaria wells have temperatures less than 270°C. The calculation procedure just described to retrieve the component concentrations in the initial aquifer water closely matches the phase segregation model.

6. POTENTIAL CORROSION BY CO_2 AND HCl

6.1 Carbon dioxide

The pH of geothermal water is largely controlled by silicate hydrolysis equilibria. In some cases high concentrations of dissolved carbon dioxide (CO_2) in geothermal fluids could have an influence on the pH. Carbonate carbon occurs mostly as dissolved CO_2 and bicarbonate. The partial pressures of CO_2 in the deep fluid of the study areas have been evaluated with the assistance of the WATCH computer code (Arnórsson et al., 1982; Bjarnason, 1994) version 2.1A. At Olkaria CO_2 partial pressures are quite variable being very high in the Olkaria West sector compared to the other sectors of Olkaria or 10-100 bar (Table 4 of Appendix A). In Olkaria North East they are 1-3 bar, 0.5 -5 bar in Olkaria East, and 2-4 bar in Olkaria Domes. In the reservoirs at Reykjanes and Svartsengi they are 0.5-0.9 bar and 0.6-1.7 bar respectively. At Nesjavellir the CO_2 partial pressures are even lower 0.07-0.09 bar for the wells selected (Figure 13).

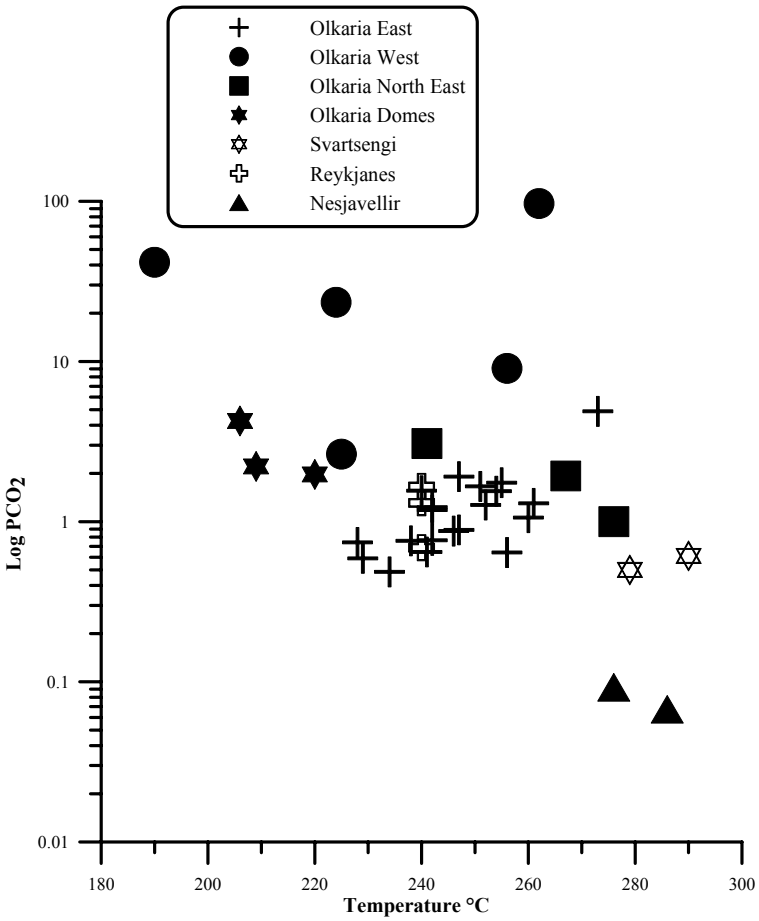

FIGURE 13: Aquifer temperature vs CO_2 partial pressures in the aquifer fluids

The carbon dioxide (CO_2) concentrations in high-temperature geothermal aquifer waters are highly variable. Essentially two factors control the aquifer water CO_2 concentrations, (1) the rate of supply of CO_2 to the water from magmatic heat sources and (2) equilibration with specific mineral buffers. In the study areas these buffers include epidote + prehnite + calcite + quartz and epidote + grossular + calcite + quartz (Karingithi et al., 2006; Fridriksson et al., 2006). In Olkaria West, the CO_2 in the reservoir water is considered to be controlled by the rate of supply of CO_2 from the magmatic heat source. Another possibility is that Olkaria West is on the periphery of the Olkaria geothermal system and the fluid is peripheral, i.e. it is in outflow from the system and has developed an excess CO_2 concentration. In other parts of Olkaria and in the other study areas, CO_2 aquifer water concentrations are on the other hand controlled by close approach to equilibrium with one of the mineral buffers mentioned above.

Shallow groundwaters, rich in CO_2, may form when CO_2-rich steam rising from the deeper reservoir condenses into such shallow water. Waters of this origin exist in Olkaria West, as evidenced by the discharge of well OW-304D. The pH of such waters could be lowered by the high CO_2 concentrations (Figure 14).

Waters of this type have also been reported from Broadlands in NewZealand (Hedenquist and Stewart, 1985). Shallow CO_2-rich groundwaters may cause corrosion on the outside of casings, at least if cementing of the casing is in adequate or if the water can dissolve the cement.

Concentrations of CO_2 at equilibrium between water and steam can be calculated using thermodynamic data on the equilibrium partial pressures of dissolved CO_2 and a given temperature, using Henry's law constant. The expression used is:

$$mCO_2 = kh*Pi,$$

where mCO_2 = concentration of CO_2 in moles/kg,
Kh = Henry's Law coefficient,
P i= Partial pressure of CO_2 at equilibrium in bars.

Arnórsson et al (1996) describe the temperature dependence of Henry's Law coefficient given by the function:

$$CO_2,g = CO_2,aq = -59.612 + 3448.59/T - 0.68640\times10^{-6}\ T^2 + 18.847\times log\ T$$

where T = Temperature in Kelvin.

Upon extensive boiling of geothermal water in producing aquifers and wells, the CO_2 initially dissolved in the aquifer water is largely transferred to the steam which forms. Figures 15 and 16 show how CO_2 concentrations in the boiling water and the steam change during one step adiabatic boiling of water from selected wells in the study areas.

The separated water at the surface contains 0.5-5 ppm dissolved CO_2 and the separated steam 0.2-24 ppm. These are theoretically calculated using Henry's law constants for CO_2 at equilibrium. One might expect that the separated water would cause corrosion of mild steel due to its relatively high CO_2 content. Such corrosion is, however, generally not observed in geothermal installations. The reason is considered to be the formation of protective sulphides, carbonates and silicate coating (Jones, 1996).

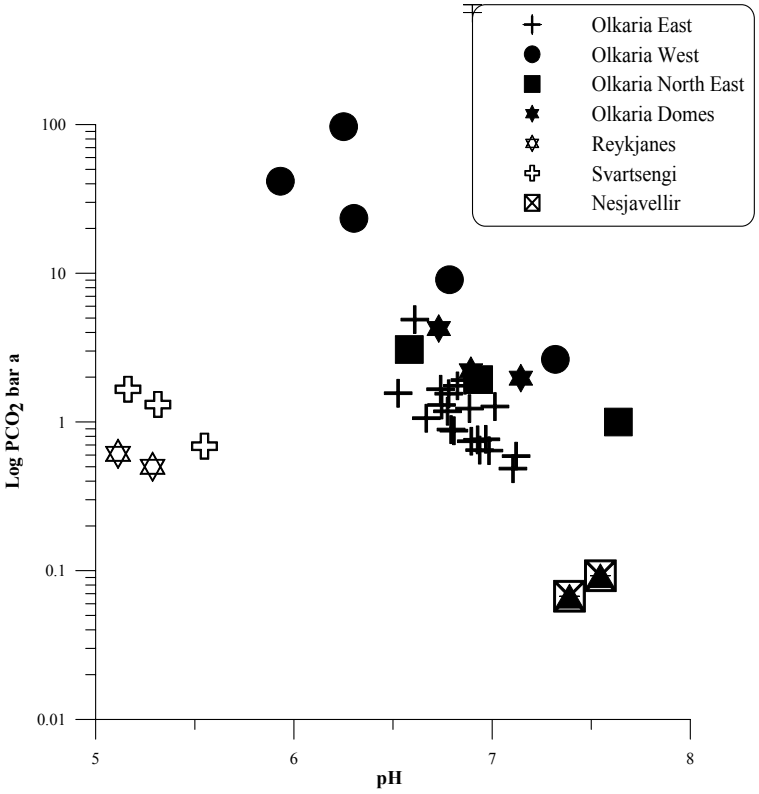

FIGURE 14: Aquifer pH vs CO_2 partial pressures in the aquifer for selected wells in the study areas

Upon condensation of separated steam, CO_2 rich condensate with a relatively low pH will form (Figure 17). The pH of condensate formed from the selected wells due to CO_2 in the Olkaria West sector is lower than that formed from the rest of the selected wells in the study areas. A complication that could arise is the influence of H_2S. The problem with CO_2 corrosion is always linked to pH and the only problem to worry about is corrosion by steam condensate. Instability of sulphide minerals rendering them less protective will contribute.

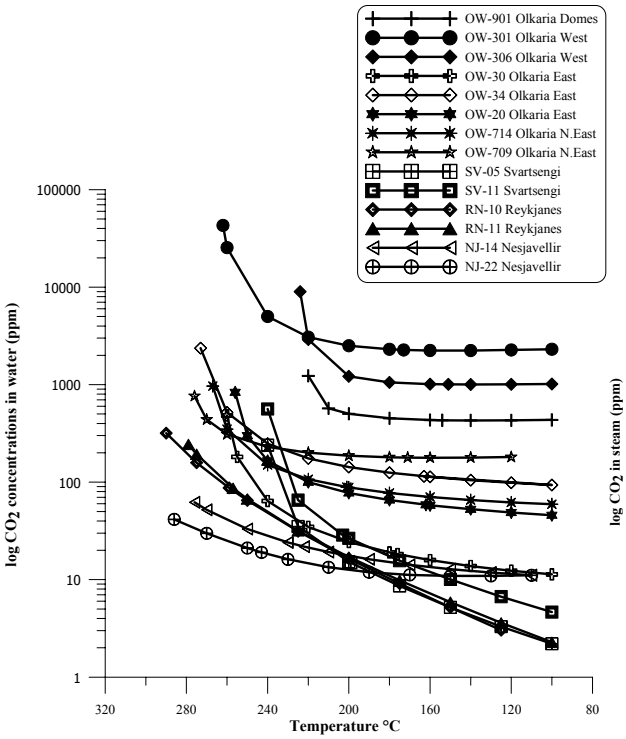

FIGURE 15: CO_2 concentrations in separated water of selected wells with several steps of single-step adiabatic steam loss

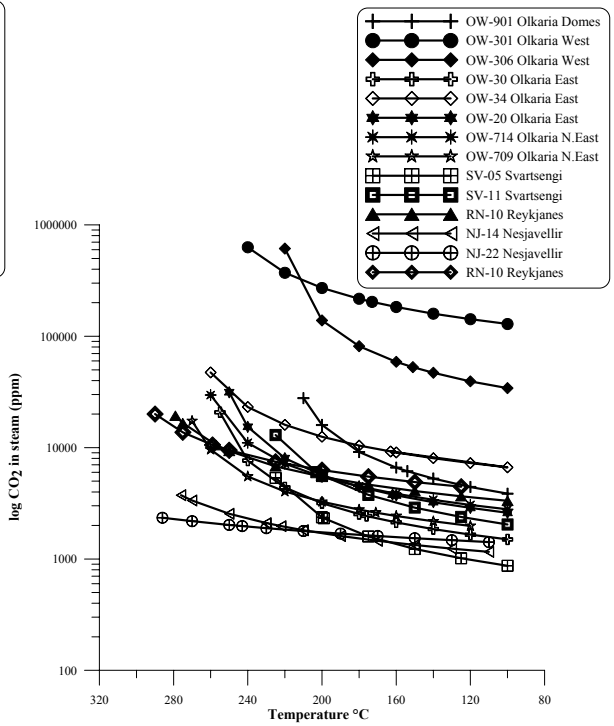

FIGURE 16: CO_2 concentrations in separated steam of selected wells with several steps of single-step adiabatic steam loss

6.2 Hydrogen chloride

Hydrogen chloride (HCl) is a component of volcanic gases and is present in steam of vapour dominated geothermal systems located in different geologic settings (Giggenbach, 1975; Truesdell et al., 1989). The acidity of Cl-SO_4 springs in some geothermal fields has been attributed to the presence of dissolved magmatic HCl (Giggenbach, 1975; Ellis and Mahon, 1977). Haizlip and Truesdell (1988) report Cl concentrations of 10-120 ppm in superheated steam in the vapour-dominated field at the Geysers in California. In Larderello, Italy, most wells produced steam with < 5 ppm Cl in the early 1960´s but later levels rose to 10-80 ppm (D´Amore et al., 1977). At Tatun, Taiwan, a dry steam well discharge contained ~3500 ppm Cl (Ellis and Mahon, 1977). In Krafla, Iceland (Truesdell et al., 1989, Truesdell, 1991) intrusion of magmatic gases into the geothermal system during the Krafla fires caused high concentrations of HCl in Krafla well KG-12. The high HCl concentrations in the superheated steam caused corrosion in this well.

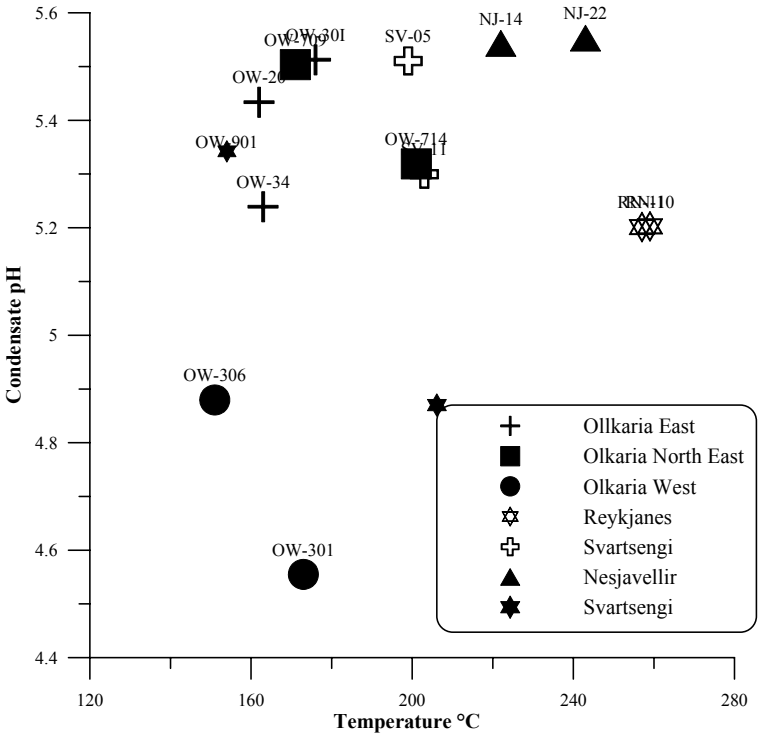

FIGURE 17: Condensate pH at separation temperatures for selected wells in the study areas

High concentrations of HCl can be generated from boiling moderate-to-high salinity brines with near neutral pH values (5-7) and with temperatures greater than about 300° C. D'Amore et al., (1990) have demonstrated a close correlation of high temperature areas of Larderello and The Geysers reservoirs with HCl in steam. Extreme boiling and drying of a reservoir originally containing a more or less concentrated brine is not limited to vapour–dominated systems, but can occur in liquid dominated reservoirs as well. Boiling in high temperature geothermal reservoirs such as Reykjanes and Svartsengi Iceland; Cerro Prieto, Mexico; Salton Sea California, could produce vapour containing HCl.

Serious corrosion has been linked with HCl in geothermal steam. Corrosion occurs when the steam condensates and the HCl dissolves in the condensate to form a strong acid, hydrochloric acid (Allegrini and Benvenuti, 1970). Hydrogen chloride is highly soluble in liquid water. For this reason HCl may be effectively removed from steam by passing it through liquid water and by minimising steam condensation along steam lines by using better insulation. This is how HCl corrosion in well KG-12 in Krafla, Iceland, was stopped (Thórhallsson et al., 1979). Injection at Larderello is known to have decreased the HCl concentration in the steam, presumably by its dissolution in the injected water. Two of the areas included in this study (Reykjanes and Svartsengi) have quite high Cl concentrations, or about 20,000 and 13,000 ppm in the reservoirs respectively. At Olkaria and Nesjavellir Cl concentrations are much lower. At Reykjanes, Nesjavellir and Olkaria, aquifer water temperatures in some wells exceed 300°C but in Svartsengi they are very constant, around 240°C. Experience has shown that corrosion is not significant at Olkaria, limited at Svartsengi but rather severe at Reykjanes. This experience stimulated a study of HCl concentrations in liquid water and steam as a function of the Cl content of the initial aquifer water and the pH and temperature of variably boiled water and associated steam.

Analysis of Cl in steam is not considered to give reliable results for HCl concentrations. Chloride analysed in condensed steam would be total chloride consisting of chlorides formed from alkali and alkali earth metals. By carrying out calculations of HCl concentrations this, gives a better estimate of chloride concentrations derived from HCl on condensation. In most cases the Cl concentrations that would be derived from HCl would not be detectable and only a very insignificant amount of carryover of liquid water would dominate the Cl in steam samples. For example at Reykjanes, 0.0005% carryover of the brine would yield 0.1 ppm Cl in the steam. For this reason, it is considered more accurate to calculate HCl in steam from experimental data on the dissociation of HCl and the distribution coefficient for HCl between liquid water and vapour. The fraction of calculated HCl concentrations are small, but when the chloride is entirely from HCl and in dry steam, even at such small concentrations this become corrosive. The chloride from the HCl becomes concentrated in dead legs and stagnant areas, which develop low pH and hence become corrosive.

The WATCH chemical speciation program (Arnórsson et al., 1982), version 2.1A (Bjarnason, 1994) was used to calculate initial aquifer water composition and the speciation distribution in this water. From the calculated activities of the H^+ and Cl^-, the concentration of the HCl_{aq} species in the water was calculated using data on the association constant for HCl_{aq} from Ruaya and Seward,(1987) assuming the the activity coefficient for this species was unity. The concentration of HCl in steam (HCl_v) was subsequently obtained from the experimental data of Simonson and Palmer (1993) for the distribution coefficient for HCl (D_{HCl}) between liquid water and steam.

According to Ruaya and Seward, (1987) the temperature dependence of the association constant for HCl_{aq} is given by:

$$-\log K_{HCl} = -2136.8898 - 1.022034 \times T + 45045 \bullet 10^{-4} \times T^2 + 50396.40/T + 901.770 \times \log T$$

where T = Temperature, in Kelvin

The distribution coefficient for HCl between vapour and liquid water ($D_{HCl,}$) is defined as:

$$D_{HCl} = \frac{[mHCl_v]}{[mHCl_l]}$$

Temperature dependence is given by (Simonson and Palmer, 1993):

$$\log D_{HCl} = -13.4944 - 934.466/T - 11.0029 \times \log\rho + 5.4847 \times \log T$$

where T = The temperature in Kelvin, as before; and
ρ = The density of solvent (g/cm^3).

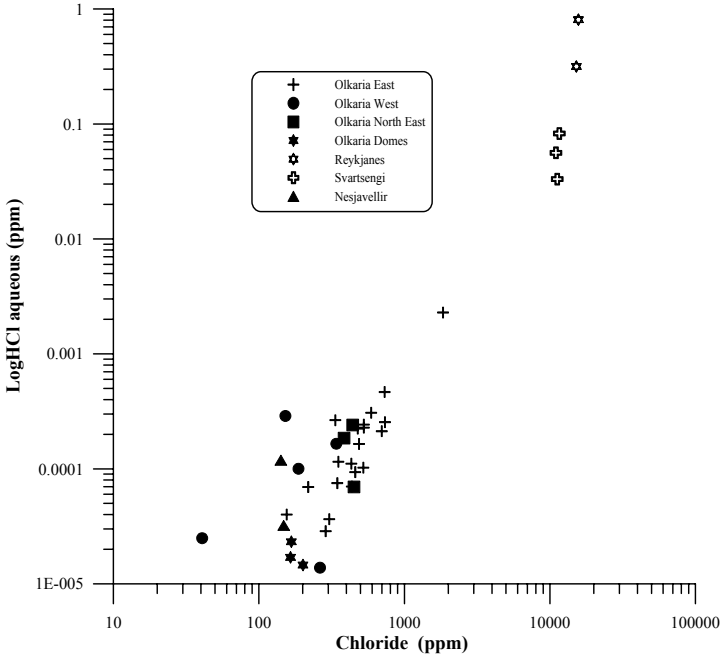

FIGURE 18: Aquifer water HCl concentrations vs. aquifer water chloride concentrations of selected wells in the study areas

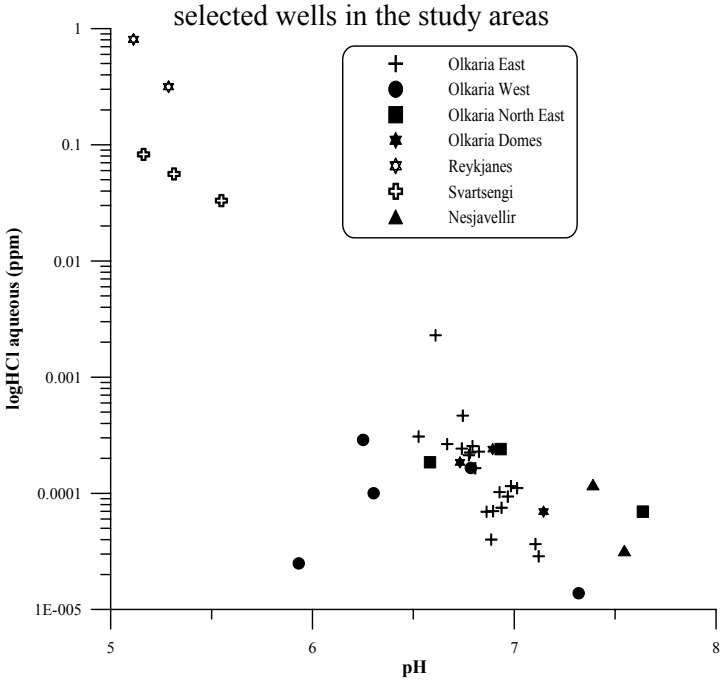

FIGURE 19: Aquifer water HCl concentrations vs. aquifer water pH of selected wells in the study areas

The density of the dilute waters from Olkaria and Nesjavellir was calculated using thermodynamic properties of water and steam given by the computer code TAFLA (Bjarnason and Björnsson, 1995). Densities for Reykjanes and Svartsengi brines were calculated using densities of saturated sodium chloride solutions provided by Potter and Brown (1977).

The calculated concentrations of HCl in the aquifer waters of the study areas are presented in Table 4 of Appendix A and depicted in Figures 18, 19, 20 respectively as a function of aquifer water chloride concentrations, pH and temperature.

The concentrations of HCl_{aq} increases with increasing aquifer water Cl concentrations, decreasing aquifer water pH and increasing aquifer temperature. The water in producing aquifers of the Olkaria wells contain HCl in the range between ~ 1×10^{-5} ppm and ~ 5×10^{-4} ppm. The aquifer water HCl concentrations in Reykjanes and Svartsengi are much higher, ranging between ~0.32 and ~ 0.81 ppm and ~3×10^{-2} and ~8×10^{-2} ppm, respectively. At Nesjavellir, the HCl in the aquifer waters is in the range ~ 3×10^{-5} - 5×10^{-5} pm for the selected wells.

There is a variation in HCl concentrations in the Olkaria well fluids of about an order of magnitude with the exception of fluid from one well, well OW-34 which has a slightly higher HCl concentration, than other Olkaria well fluids (Figure 18). At Olkaria, the variations in the HCl concentration can be attributed to the

variation in chloride concentration, pH and temperature. The chloride concentration in the aquifer waters at Olkaria varies between ~ 40 ppm and ~ 2000 ppm in the aquifer and the aquifer pH from ~ 6 to 8. Aquifer temperatures vary between ~ 200° and 300°C. The wide range in the concentrations of chloride, pH and temperatures at Olkaria contribute to the wide range of HCl_{aq} concentrations. At Nesjavellir, HCl in the aquifer fluids is very low due to the very low chloride in the aquifer water, ~ 150 ppm and a pH of the aquifer fluids of ~ 8. Aquifer temperatures at Nesjavellir range between ~ 270° and 300°C for the wells studied.

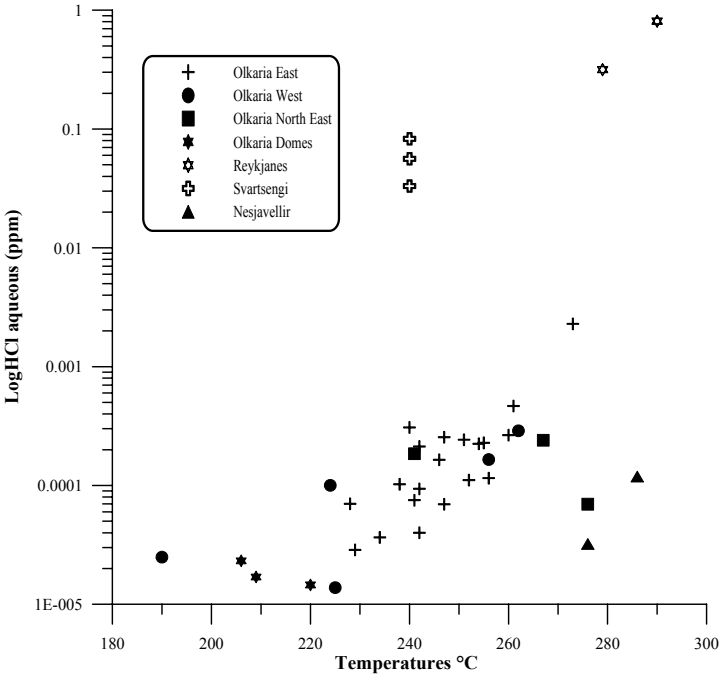

FIGURE 20: Aquifer water HCl concentrations vs. aquifer temperature (°C) of selected wells in the study areas

The high HCl concentrations in the aquifer water in Reykjanes and Svartsengi are very high compared to those of Olkaria and Nesjavellir. The high HCl concentration in the aquifer water at Reykjanes and Svartsengi is a result of high chloride concentrations and low pH in the aquifer waters of these two fields. The chloride concentrations in the waters of these two fields are ~ 20,000 ppm and ~ 13,000 respectively and the pH of the aquifer water in the range of ~ 5.1 to ~5.6. Temperatures in Reykjanes range between 250° and 320°C. At Svartsengi the temperatures are almost homogenous, being in the narrow range of 235° and 240°C.

Upon boiling the dissolved HCl is partly transferred to the steam that forms. The quantity transferred is affected by several parameters. The most important ones include changes in pH, which occur during boiling, and the temperature of the fluid mixture. Figure 21 shows how HCl concentrations in steam decrease during one step adiabatic boiling for all the wells considered in the present study.

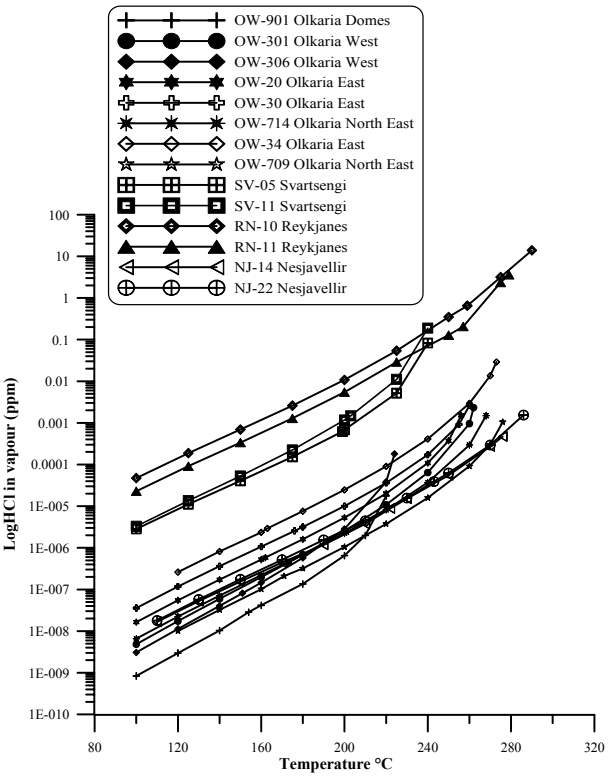

FIGURE 21: HCl in vapour formed by several steps of single-step adiabatic boiling of selected wells in the study areas

Early steam is somewhat enriched in HCl relative to the source aquifer water. Upon continued boiling the cause of the decrease is largely due to an increase in pH upon boiling and by changes in the value taken by the HCl distribution coefficient. Because it is temperature dependent the distribution coefficient, is affected by the decrease in temperature when the fluids cool by adiabatic steam loss. Changes in the Cl content of the water, which are caused by steam formation, have small effect. The HCl concentrations in steam are ~ 10^3-10^5 times more for Reykjanes

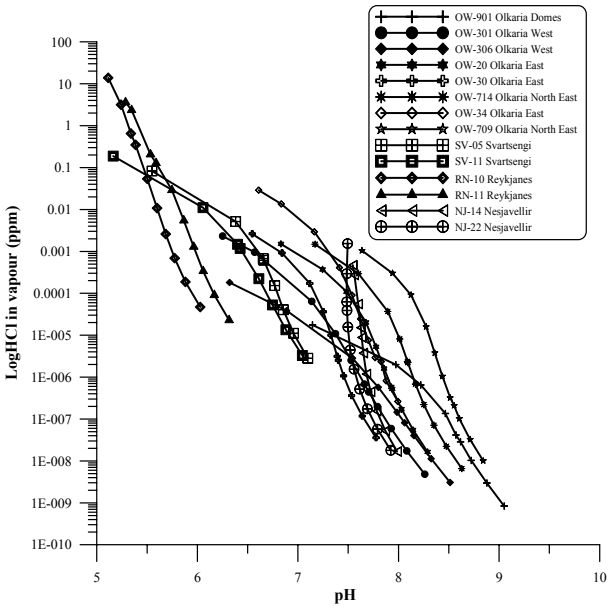

FIGURE 22: HCl in vapour with changes in pH upon several steps of single-step adiabatic boiling of selected wells in the study areas. The boiling is from the respective aquifer temperature (See Table 4 in Appendix A)

well fluids than the well fluids in Olkaria and Nesjavellir. At Svartsengi they are ~ 10^2-10^4 times higher than in the Olkaria and Nesjavellir waters.

Changes in pH are affected by the concentrations of carbon dioxide in the initial aquifer water and in the Olkaria well waters, the CO_2 concentrations are variable. The Olkaria well waters have a relatively high initial pH in the aquifer except for wells that are in the Olkaria West sector. Upon boiling by steam loss with decrease in temperature, the increase in pH is much greater for wells with a high initial concentration of CO_2 in the water in Olkaria. Figure 22 shows decrease in the HCl concentrations with increase in pH upon adiabatic boiling.

The large increase in pH in the Olkaria well waters with decrease in temperature, contributes to the low concentrations of HCl in the steam when the water boils. The Reykjanes, Svartsengi and Nesjavellir aquifer waters vary less in CO_2 gas concentration than the waters of the Olkaria. The pH of aquifer water in Reykjanes and Svartsengi are similar while at Nesjavellir the aquifer pH is higher. The relative increase in pH with decrease in temperature is gradual in Reykjanes, Svartsengi and Nesjavellir wells upon steam loss. The trends for decrease in HCl concentrations, when HCl partitions into steam, are similar to those of Olkaria aquifer fluids. As the waters cool by steam loss, HCl tends to be retained more in the liquid and less partitions the steam.

The concentrations of HCl in steam collected at the wellheads of selected Olkaria, Reykjanes, Svartsengi and Nesjavellir wells are shown in Table 5 of Appendix A. HCl concentrations in Olkaria and Nesjavellir are very low 3×10^{-8} - 3×10^{-6} ppm and 5×10^{-6} - 1×10^{-5} ppm, respectively. At Svartsengi and Reykjanes these are 6×10^{-4}-1.5×10^{-3} ppm and 2×10^{-1}-7×10^{-1} ppm, respectively. The concentrations of HCl in the separated steam conveyed to the power plant at Olkaria are very low, 10^{-8} -10^{-6} ppm. At Svartsengi they are about 5×10^{-5} - 10^{-4} ppm but as high as 0.1 ppm at Reykjanes. The high values at Reykjanes are due to the high Cl content of the aquifer water and, in particular the high pressures in the steam separators. All these concentrations are considerable lower than measured Cl concentrations in the steam of many vapour-dominated geothermal systems e.g. in dry steam from well KG-12 at Krafla, Iceland (Truesdell, 1991). Yet, corrosion at Reykjanes due to condensation of high pressure steam may be a problem. Condensation need not occur during conductive heat loss. At temperatures higher than that corresponding to maximum steam enthalpy, condensation will occur by pressure drop to the maximum enthalpy value. If the discharge is almost dry steam corrosive liquid water could be produced in this way. At Reykjanes corrosion in pipelines due to production of HCl may not occur due to formation of stable sulphide scales and the HCl could be scrubbed. The quantity of this scale is limited except from saline waters. Stable sulphide scale formation at Reykjanes has been reported by Hardardóttir et al. (2001, 2004). In steam pipelines made of carbon steel, thin coatings of stable sulphide, carbonates, silicates or metastable sulphide phases are known to form a protective coating that tends to prevent corrosion of casing and other material that would otherwise be a problem due to CO_2 and HCl. Other scales that form protective coating are carbonates. At sufficiently low pH in condensates containing HCl, phases of protective sulphides and carbonates can become unstable and dissolve and corrosion can be induced.

A 240°C a steam cap overlies the liquid-dominated reservoir in Olkaria East and a similar steam cap, also at ~240°C has formed in Svartsengi in response to pressure drawdown caused by the exploitation of the reservoir. The HCl concentrations in the steam caps of these two fields are expected to be some 10^{-3} and 10^{-1} ppm Cl in Olkaria East and Svartsengi, respectively. If all the Cl is from HCl and taking the acid to be 100 % dissociated, a concentration of 0.1 ppm Cl yields a pH of 5.5. Chloride concentrations measured in the condensate of one dry steam well at Svartsengi is about 0.6 ppm and the condensate pH of 4.3. At Svartsengi, the pipes conveying steam from one of the wells that tap dry steam from the steam cap had to be replaced due to corrosion (Thórhallsson, 2005, pers comm.). It seems unlikely that HCl is the main cause of corrosion in view of the pH value produced by 0.1 ppm HCl in the steam. CO_2 is a more likely candidate. Where severe corrosion which has been attributed to HCl has occurred, such as at Krafla, Iceland (Truesdell, 1991) the Geysers, USA (Trusedell and Haizlip, 1990) and Larderello, Italy (Allegrini et al., 1970) concentrations as high as 100 ppm in steam have been reported giving a pH of 2.5 in the steam condensate. A possible way of scrubbing out the HCl in the high pressure steam at Reykjanes and Svartsengi is to pass it through a basic solution such as a NaOH-solution.

7. SCALING IN WELLS AND SURFACE INSTALLATIONS

7.1 Theoretical aspects of calcite scale formation

Calcite is abundant as a secondary mineral in many hydrothermal systems. Many studies have indicated that >100° C waters are close to being calcite saturated (e.g. Ellis and Mahon, 1977; Arnórsson, 1978). In some exploited fields, water in producing aquifers may be calcite undersaturated. The calculated state of calcite saturation in the initial aquifer water of wells at Olkaria, Reykjanes, Svartsengi and Nesjavellir is presented in Figure 23.

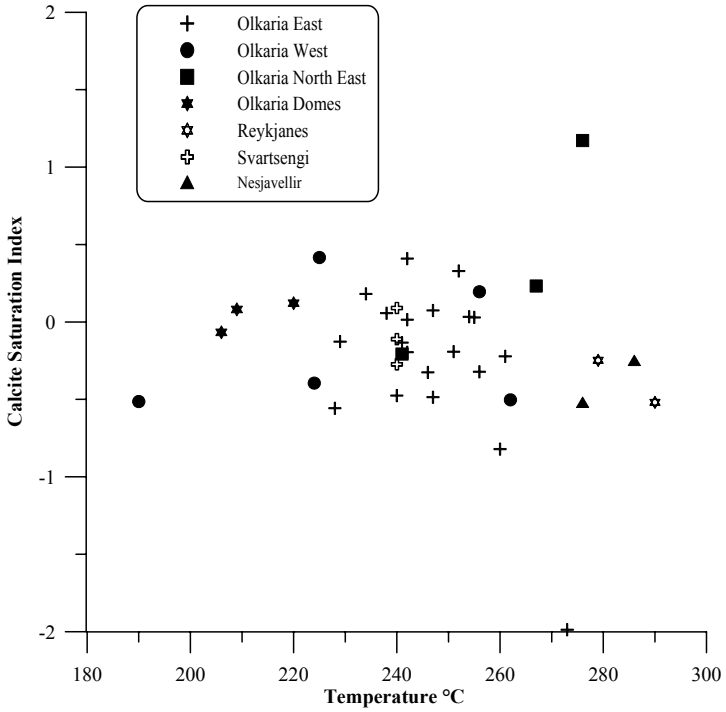

FIGURE 23: Aquifer temperature vs calcite saturation for selected wells at Olkaria, Reykjanes, Svartsengi and Nesjavellir

The data show some scatter. This is more likely due to errors in calculating the calcite activity product rather than a reflection of departure from equilibrium. In calculating the aquifer water composition with the aid of the WATCH speciation program (Arnórsson et al., 1982; Bjarnasson, 1994) Version 2.1A, it was assumed that excess well discharge enthalpy was caused by phase segregation in producing aquifers and that no equilibrium steam was present. If such steam is present in the initial aquifer fluid, the calculated aquifer water pH is too low and the aquifer water CO_2 concentration too high with the result that too low values are obtained for the calcite saturation index (SI_{cal}), i.e. calcite undersaturation, if the initial aquifer water is truly just calcite saturated. Also, some calcium may have been removed from the aquifer water upon its boiling as a consequence of calcite precipitation leading to a low calcium concentration in the water samples collected at the wellhead relative to the initial aquifer water. This effect will also tend to give low values for SI_{cal}. Removal of calcium from solution by calcite precipitation is expected to affect the calculated SI_{cal} of the dilute waters significantly at Olkaria and Nesjavellir because of their low calcium content but not the calcium-rich saline waters at Reykjanes and Svartsengi. Other errors that may contribute significantly to departure from calculated calcite equilibrium include erroneous values obtained in the measurement of pH of water samples and by contamination of these samples by condensed steam. Such contamination is particularly prone to occur when sampling water from wells with high discharge enthalpy, such as well OW-34 at Olkaria.

Figure 24 shows how the calculated saturation index for calcite varies during adiabatic boiling of aquifer water of selected wells from the study area. The shapes of the SI_{cal} curves are more accurately defined than the absolute SI_{cal} value at each temperature. The effect of depressurization boiling upon the calcite saturation state is essentially twofold. Firstly, the water is degassed with respect to CO_2, which leads to an increase in the pH of the boiling water (Figure 25) which in turn brings about an increase in the carbonate ion concentration and hence in the $[Ca^{+2}][CO_3^{-2}]$ solubility product.

Secondly, depressurization boiling causes cooling of the water. The solubility constant for calcite increases with decreasing temperature. Degassing by pressurization boiling causes an initially calcite saturated solution to become supersaturated whereas the cooling by this boiling has the opposite effect.

The solubility of CO_2 in water changes with temperature, being at minimum around 200°C. Degassing during the early stages of boiling is accordingly most effective for aquifer waters with temperatures around 200°C. For aquifer waters with temperatures around 300˚C, or higher, early degassing with respect to CO_2 is slow due to its relatively high solubility in water at these high temperatures.

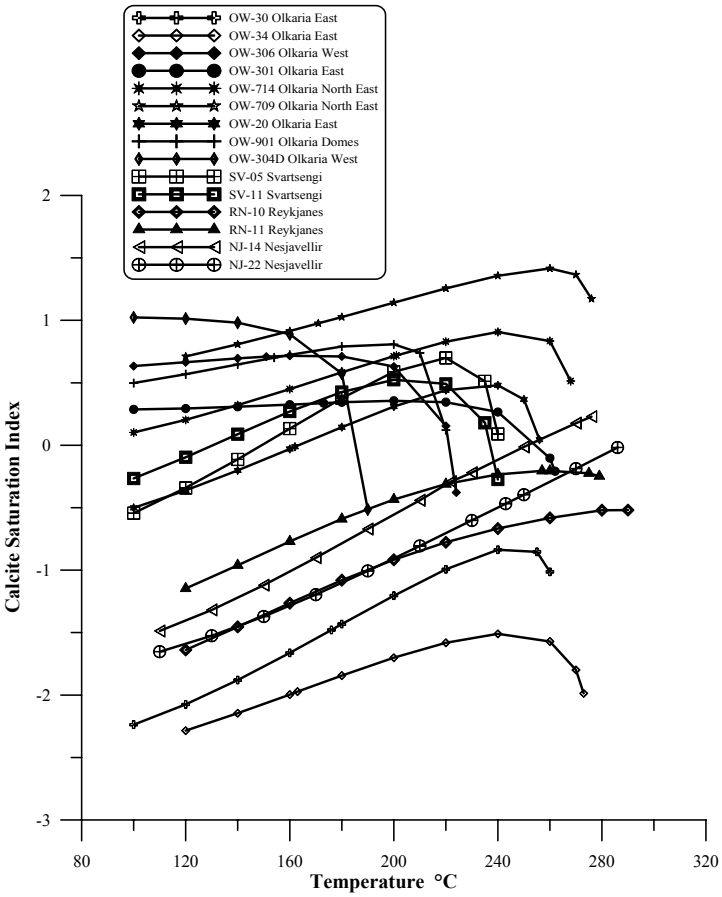

FIGURE 24: Changes in calcite saturation produced by several steps of single-step adiabatic steam loss for selected well fluids at Olkaria, Reykjanes, Svartsengi and Nesjavellir

The shape of the curves in Figure 24 can essentially be explained by a combination of three factors, (1) CO_2 degassing during boiling, (2) the solubility of CO_2 in water as a function of temperature and (3) the retrograde solubility of calcite with respect to temperature. The concentration of CO_2 in the initial aquifer fluid also has an influence. Aquifer waters with temperatures below about 280˚ C show an increase in the value of SI_{cal} during the early stages of boiling and greater the lower the aquifer temperature. Such an increase is not observed for the ~300˚ C aquifer waters at Nesjavellir. Maximum SI_{cal} values are attained some 20-40 °C below the initial aquifer temperature. At maximum the waters have largely been degassed and at temperatures below the maximum, SI_{cal} values become successively lower due to increasing calcite solubility with decreasing temperature. For the relatively hot aquifer waters at Nesjavellir, SI_{cal} values decrease progressively with decreasing temperature due to the combined effects of increasing calcite solubility, limited CO_2 degassing during the early stages of boiling due to the relatively high CO_2 solubility in water at the high temperatures and relatively low CO_2 concentrations in the initial aquifer waters. Continued high SI_{cal} values for wells OW-301 and OW-304 during boiling all the way down to atmospheric pressure is due to the high CO_2 content of the initial aquifer fluid which requires extensive steam formation for extensive degassing of the aquifer water.

The results discussed above and presented in Figures 23 to 25 assume adiabatic boiling and the equilibrium distribution with respect to CO_2 is attained between the liquid water and steam phases. Such equilibrium may not be attained due to rapid steam formation and insufficient time for the CO_2 to be transferred from the boiling water to the forming steam which is required for attainment of CO_2 distribution equilibrium between the fluid phases. Incomplete CO_2 transfer would change the shape of the curves in Figure 24 in such a way that the maximum would be depressed and the overall change in SI_{cal} would decrease more gradually with decreasing temperature.

Calcite scale formation is not expected to be a problem at Nesjavellir and Olkaria East, Olkaria, the reason being the dilute nature of the waters and the high temperatures at Nesjavellir. However, in Olkaria West calcite scale formation in wells may be a problem, depending on the depth level of first boiling. If it is within the well it may be relatively severe but not so if extensive boiling starts in

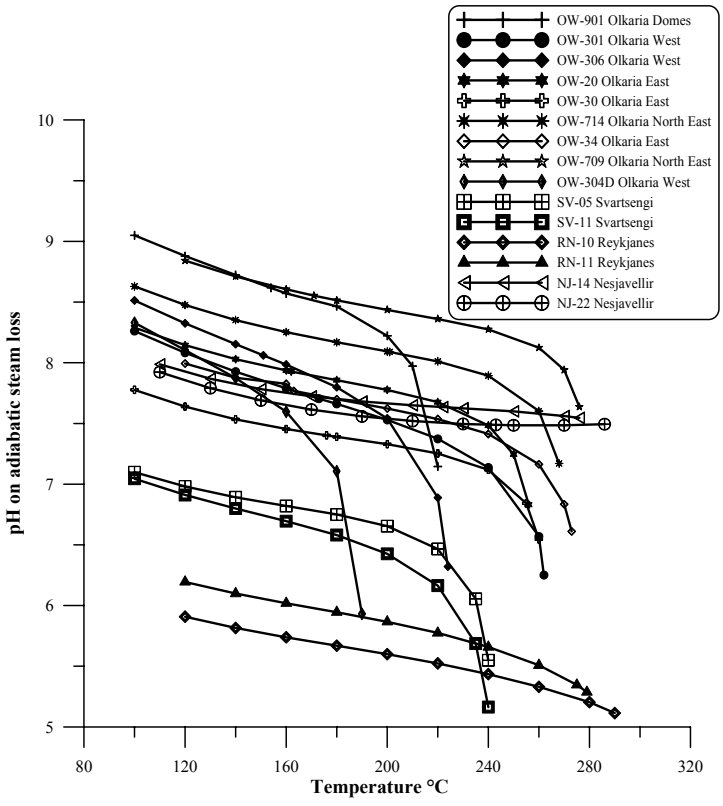

FIGURE 25: Calculated aquifer water pH for selected Olkaria, Reykjanes, Svartsengi and Nesjavellir wells and changes in pH during several steps of single-step adiabatic steam loss

producing aquifers because the pore spaces in the rock are expected to be able to cope much longer with calcite precipitation than the wellbore (see Arnórsson, 1978). The extent of CO_2 degassing is also important it is anticipated that calcite scaling will be less for good producers than for poor wells.

At Svartsengi calcite scaling was troublesome in shallow wells during the early years of production when the first level of boiling occurred within the producing wells. Pressure drawdown in the reservoir by exploitation caused extensive boiling in producing aquifers of these shallow wells with the result that calcite scale formation was no longer observed. It is that Calcite is still considered to be deposited but in the aquifer outside the wells. At Reykjanes calcite scaling has not been observed as a problem. The cause is considered to be high reservoir temperatures and high yield of wells which tends to cause incomplete CO_2 degassing during boiling.

7.2 Scaling tests at Nesjavellir

It is common practice in the geothermal industry to carry out scaling and corrosion tests to aid material selection and quantify the rate of scale deposition which is not possible theoretically. This involves insertion of plates into the stream of the geothermal fluids and the study of their corrosive nature and any deposits that may form on the plates. The present scaling study at Nesjavellir involved the insertion of stainless steel coupons into the two phase flow pipelines at two wellheads and into the stream of separated water upstream and downstream of a retention tank. This water is significantly supersaturated with respect to monomeric silica (i.e. it is present mostly as single SiO_2 molecules). Monomeric silica grows on surfaces which act as active sites as mechanism of silica deposition. Downstream of the retention tank, the water is diposed of into an injection well. In the tank most of the silica in excess of amorphous silica solubility polymerizes. Polymeristion goes through a stage process i.e. monomer $\rightarrow$ dimers $\rightarrow$ trimers $\rightarrow$ tetramers $\rightarrow$ polymers $\rightarrow$ gel etc. Polymerisation continues until silica saturation is reached. It is known that (Yanagase et al., 1970; Rothbaum et al., 1979) fully polymerized silica precipitates much more slowly from solution than monomeric silica, at least from dilute water as such that at Nesjavellir. The purpose of the retention tank is thus to reduce amorphous silica deposition in the injection well and the receiving aquifers. The purpose of the scaling tests up and downstream from the retention tank was thus to observe the extent to which silica polymerisation reduced the rate of amorphous silica precipitation. The purpose of the tests at the wellheads was principally to observe the rate and nature of sulphide scale formation and to identify whether phases other than sulphides formed in significant amounts.

A simplified process flow diagram for the Nesjavellir co-generation power plant is shown in Figure 26. The diagram shows the process flow from the geothermal wells being separated into steam and water at ~ 14 bar absolute pressure in a central separation station. The steam is piped to power plant

where it passes through mist eliminators. The exhaust steam from the turbines is used to preheat fresh water while the water from the steam separators heats the preheated water to the temperature required for the district heating system.

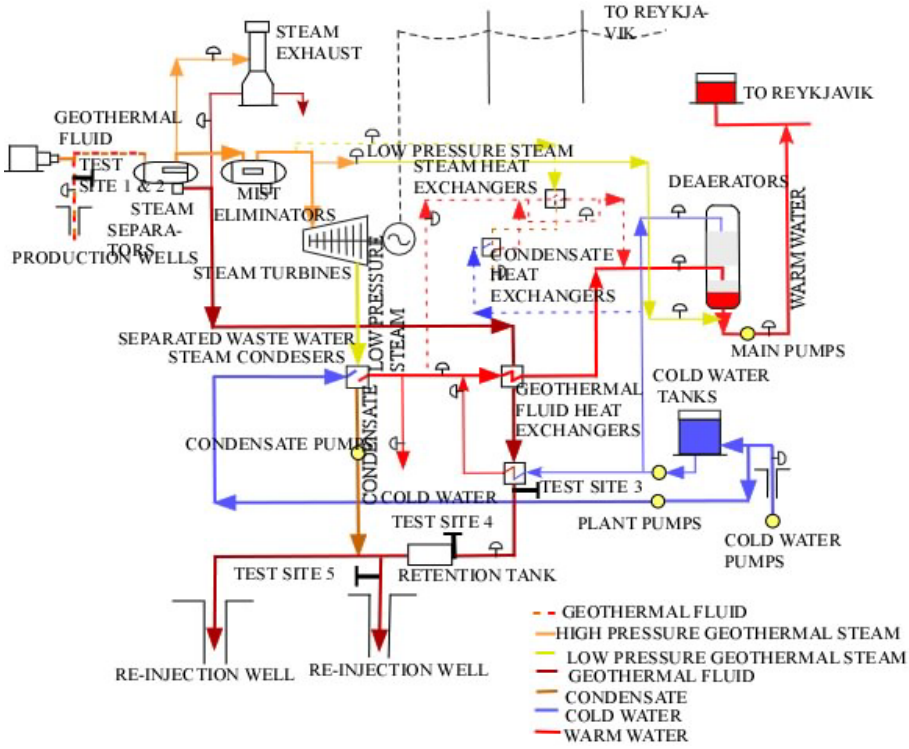

FIGURE 26: Simplified process diagram of the Nesjavellir co-generation power plant

As the cold ground water is saturated with dissolved oxygen and becomes corrosive when heated, the heated water is de-aerated before leaving the plant. De-aeration is achieved by boiling under vaccum and by injecting small amounts of geothermal steam, which contains H_2S, as shown in Figure 26 and described in more detail by Gunnarsson et al., (1992).

Demand for space heating varies over the year while generation of electricity is run as a base load. The output of the wells is regulated accordingly to the energy demand and thus, the steam and the geothermal water are utilised in the most efficient way possible for co-generation of electrical and thermal power.

7.2.1 Test coupons

Scaling tests were conducted on fifteen coupons of stainless steel 304 (Figure 27). At the end of the test only nine coupons were used in all, as six coupons were lost during the test. The specimens were labelled by imprinting the designation codes into the metal surface using hardened steel stencil stamps hit with a hammer. These codes were numbered in a sequence as shown in Figure 27.

FIGURE 27: Prepared test coupons with imprinted identification number codes

The arrangement consists of a nozzle that is fitted with a fully open gate or plug valve. The rod shaped specimen holder is contained in a retraction chamber which is flanged to the valve, and is fitted additionally with a drain valve. The other end of the retraction chamber contains a packing gland through which the specimen holder passes. The test specimens are mounted on the rods in the extended position and are then drawn into the retraction chamber. The chamber is bolted to the gate or plug valve, which is then opened up to allow the specimens to be moved into the operating environment. The sequence is reversed to remove the specimens. The type of the retractable specimen holders used in this work is

FIGURE 28: Retractable coupon holders, a) Used for high pressure points e.g. at the wellheads; and b) For low pressure points e.g. on the separated water line at the re-injection well

shown in Figures 28 a and b. In Figure 28 a a test holder for high pressure applications is shown and this was used for test coupons at the wellheads. In Figure 28 b is shown coupon test holders for low pressure applications as one that was used on the waste water line at the re-injection well. These have test coupons attached to them.

The coupons were cleaned, dried and their weights taken before they were introduced into the test environment. The coupons were mounted on retractable "slip in" specimen holders. These have the advantage of being inserted into plant test environment without the need to shut down. The coupons were first abrased with a soft sand paper then cleaned in hot distilled water before being degreased in isopropyl alcohol. The method for cleaning and preparing the coupons is detailed in Appendix B.

7.2.2 Test procedures and selection of test sites for the study

The retractable specimen holders with the cleaned dried and weighed stainless coupons screwed onto them were inserted in different fluid environments. During the tests the pressure at the wellhead of one of the wells (NJ-14) was 25 bar and that of the other (NJ-22) was 34 bar. The discharge enthalpies of NJ-14 and NJ-22 are 1400 kJ/kg and 1800 kJ/kg, respectively. Coupons were inserted at the wellheads of each of these two wells. A third site was chosen just downstream of the heat exchangers inside the plant which recieve separated water at about 188°C. At this study point the separated waste water extruding from the heat exchangers has cooled to 60-95°C depending on the demand for hot water in Reykjavik. The fourth site was at the point of entry to the retention tank and the fifth where waste water flows into the injection well. The last two sites were chosen to investigate the effect of silica polymerisation in the retention tank on the rate of amorphous silica deposition. The different types of selected test sites are shown in Figures 29, 30 and 31 respectively.

The test coupons were introduced the test sites on 06 July 2005 at the retention tank and re-injection well site and on 14 July 2005 at the wellheads of NJ-14 and NJ-22 and after the waste water leaves the heat exchangers. The coupons were inspected after ~ 13 weeks on 14 October 2005 to check on any signs of scale deposition. On this date one coupon was extracted from each test site and replaced with a new set of cleaned and weighed test coupons. These new test coupons, together with the ones that had been left intact 13 weeks were kept in place for an additional ~ 16 weeks to monitor the deposition rates from fluids at all the sites. In all, the test thus lasted for ~ 29 weeks. The test specimens were removed from the test sites on 30th January 2006. Incidentally, when we went to take out the test coupons from all the sites on this date, it was realised that the coupons in the sites at wells NJ-14, NJ-22 and the site after the heat exchangers were missing from the holders. It was hard to establish what caused their removal but it could have been due to unexplained changes in the flow patterns of the well fluids and the separated water downstream of the heat exchangers that could have

FIGURE 29: Coupons at the wellhead of well NJ-14

loosened the screws and nuts on the holders and blown the coupons into the flow line. The loss of these coupons was rather unexpected. On 30 January, 2006 all the test coupons were removed from the test sites. At the test sites at the entry of the retention tank and the injection well, coupons that had been replaced and those that lasted for 29 weeks in the test environment were both recovered. The thickness of the scale deposited on the test coupons was measured with a micrometer screw gauge. After drying the test coupons, these were stored in a dessicator to remove moisture and their weights determined.

FIGURE 30: Coupons at entry to the retention tank

7.3 Analysis of scales

Scales that formed on the coupons were studied by different analytical tools. They included binocular microscope examination, Fourier transform infrared spectroscopy, (FTIR) scanning electron microscopy (SEM- EDS), X-Ray powder diffraction (XRD) and chemical analysis by inductively coupled plasma emission spectroscopy (ICP-AES). UV spectrophotometry was used to determine silica in the scales. Brief descriptions of each technique are given in Appendix B.

FIGURE 31: Coupons at the re-injection well

The nature of the scale forming environment and type of scale formed is conveniently divided into two groups: Scales forming from two-phase fluid at wellheads and scales forming from separated water after the heat exchangers, at the entry to the retention tank and just upstream of the re-injection well. Scales forming from separated water are dominantly amorphous to X-rays and the most abundant phase is amorphous silica. The scales forming at the wellhead are of different a nature, being mostly sulphides in the case of well NJ-14 but oxides of iron in well NJ-22.

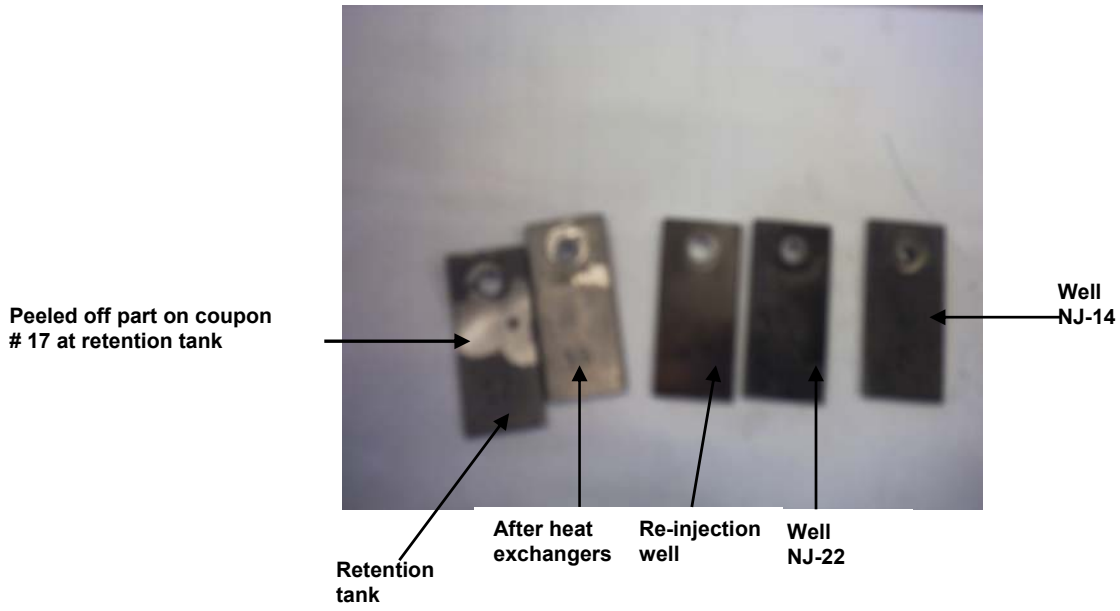

FIGURE 32: Photograph of coupons after a 13 week test period

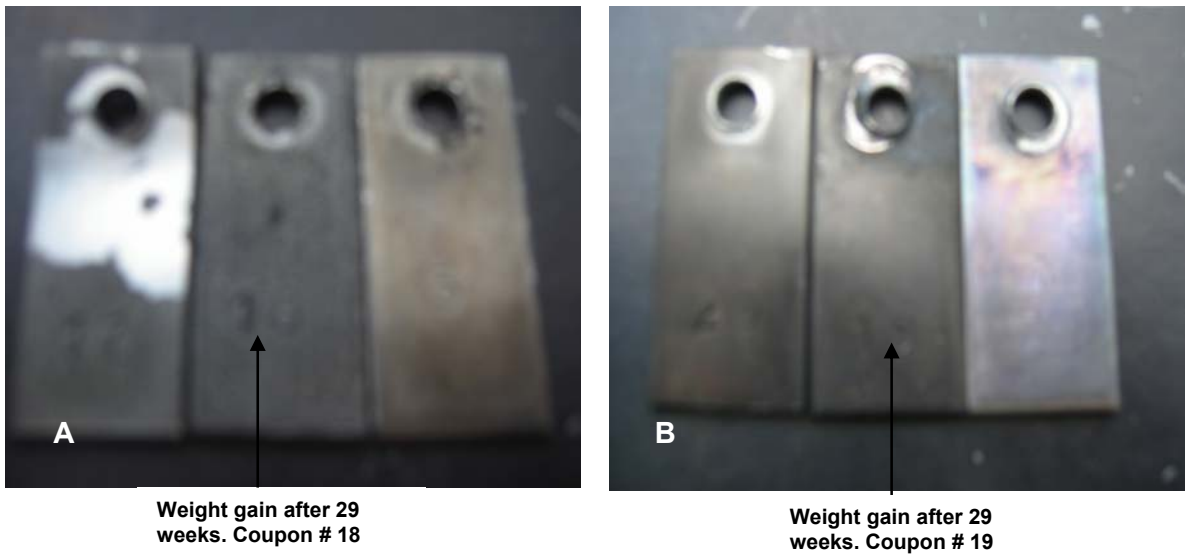

FIGURE 33: Photos showing deposition of scale on test coupons at, a) The retention tank; and b) The injection well

Of coupons removed from the retention tank and heat exchangers after 13 weeks, there was some scale on one coupon that peeled off slightly while it was being removed so that the measured weight gain is low for this coupon. The coupons after 13 weeks in the test environment are shown in Figure 32. In Figures 33 there are shown photographs of test coupons at the entry to the retention tank and at the injection well, respectively.

7.3.1 Binocular microscope descriptions

Coupon # 16 (After heat exchangers): Fine grained dark grayish deposits observed on the coupon. The deposit formed thin sheets that indicated signs of peeling off. Dark grey deposits on the edges. There appeared to flow banding on the edges.

Coupon # 20 (Re-injection well): A very dark grey deposit on the test plate. The deposit is very fine grained and does not show any flow banding. It is adherent to the coupon plate. The coupon is fully covered with fine white grained deposit.

Coupon # 10 (Well NJ-14): The coupon was completely covered with dark grey fine and coarse deposits. The coarse deposits flake off slightly but the fine deposit is very adherent to the coupon. The flakes are fine grained and dark grey in colour. Sulphide crystals are abundant.

Coupon # 25 (Well NJ-22): Dark grey to black deposits formed on the plate. On some parts of the plate the deposits are rather thick. The thickness was not uniform. Occasionally the deposit flakes off though in most instances it is adherent onto the plate. Sulphide crystals not nearly as abundant as in scale from NJ-14. Very fine grained.

Coupon # 17 (At entry to re-injection well): A very fine thin sheet of deposit on the plate. The deposit was light grey in colour, had partly peeled off from the plate when the coupon holder was being removed from the insertion point at the delay tank. No signs of flaking. White to brown coloured crystals.

Coupon # 18 (At entry to re-injection well): Dark grey and white crystals were distributed on the plate: The white crystals have different shapes and sizes and are widespread on the coupon plate. Some crystals are glass like, some are white but not shiny, occasional brown crystals probably silica or pyrite in the scale. Some reddish crystals were present in this coupon scale probably haematite. Some white crystals embedded in the background.

Coupon # 5 (At entry to re-injection well): The deposit was dark grey and non-uniform white-brownish crystals were widely embedded in a finer background. Some crystals look glass like.

Coupon # 19 (At re-injection well): A very thin layer of fine dark grey to black evenly distributed deposit on the coupon.

7.3.2 Fourier transform infrared measurement

IR spectra of scales formed at the wellheads of wells NJ-14, well NJ-22, separated water after the heat exchangers, at entry to the retention tank and just upstream of the injection well are shown in Figure 34. The spectra of the samples from the wellheads show strong similarities. So do samples of scales formed from separated water. There is, however, a considerable difference between the two groups of samples. The IR spectra largely reflect Si-O bonding and do not provide information on the presence or absence of sulphide phases.

Molecular water is present in all the scales as indicated by vibrational bands at 1630-1641 and 1410-1443 cm^{-1}. In the region 2923-2842 cm^{-1} the wavelength band could be associated with C-H groups and this could be due to oil or grease and indicate contamination. The band in the region 3533-3541 cm^{-1} is caused by OH-groups in the crystal lattice of bonded H_2O. Wavelength and in scale samples from separated water at 1100 cm^{-1} with shoulders on both the low energy sides reflect a Si-O-Si structure characteristic of amorphous silica. In the scale samples from the wellheads, these bands are shifted to about 1030 cm^{-1} due to the presence other silicon compounds, e.g. silicates. They resemble those of the analcime-leucite group Na, K and Mg may have entered the structure. Medium strength peaks at 442-465 cm^{-1} are presented in all scale samples. They are caused by bending vibrations of an O-Si-O structure. In the scale samples from the wellheads, the wavelength bands at 723-790 cm^{-1} are probably due to symmetrical stretching of tetrahedrally co-ordinated Si and Al.

7.3.3 X-ray diffraction measurements

X-ray diffraction patterns revealed by all the scale samples except from the re-injection well are shown in Figure 35.

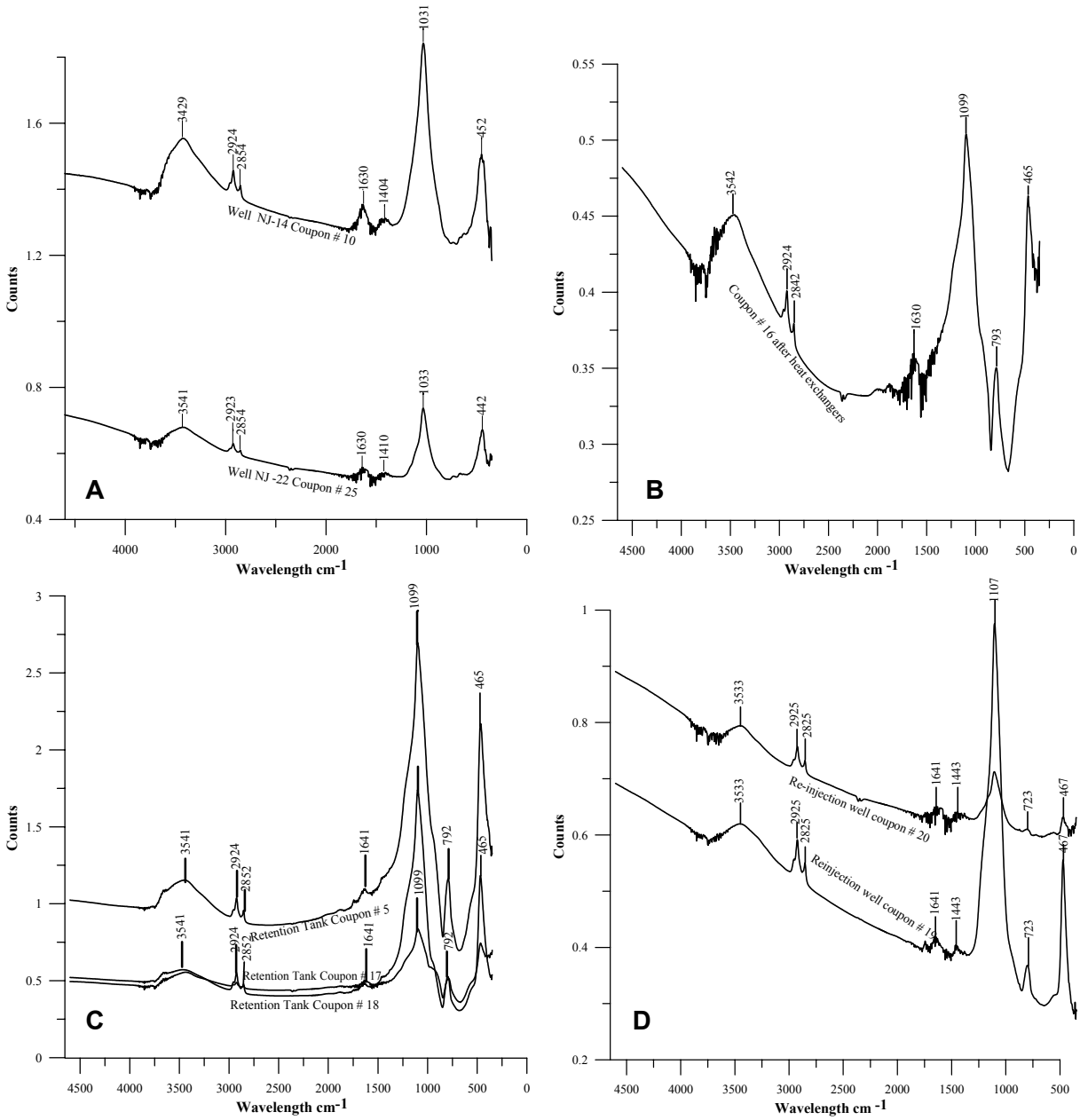

FIGURE 34: IR spectra of scales deposited on coupons at, a) The wellheads of NJ-14 and NJ-22, b) After the heat exchangers, c) At the entry to the retention tank, d) At the re-injection well

No clear diffraction peaks could be observed in the scale of the coupons from the wellheads of NJ-14 and NJ-22 except for a small peak at ~ 7 ˚ 2θ for the sample from NJ-22 which indicates some clay and a peak at ~ 29.5˚ 2θ in the sample from NJ-14 which could be due to chalcopyrite.

The X-ray diffraction patterns for the scales forming from separated water after the heat exchangers and before the retention tank are very similar. This is shown in Figure 33. The scale formed on the coupon at the injection well was too small for X-Ray examination. The most prominent feature in the scales is a broad peak at ~ 23˚ 2θ which is characteristic of amorphous or opaline silica. Small peaks at ~ 7 ˚ 2θ and ~ 12.5 ˚ 2θ were identified in two samples before the retention tank. These reflect the presence of clay minerals. Minor peaks at ~ 29.5˚ 2θ, ~31.5˚ 2θ and ~ 45.5˚ 2θ were also observed. These reflect the presence of chalcopyrite, halite (NaCl) and sylvite (KCl). In these samples the presence of chalcopyrite considered could indicate some minor crystalline phases in the scale. Halite (NaCl) and sylvite (KCl) will have formed by evaporation of geothermal water on the coupons when dried and do not represent a part of the scale. They are easy to detect in the X-ray diffraction because of their cubic structure.

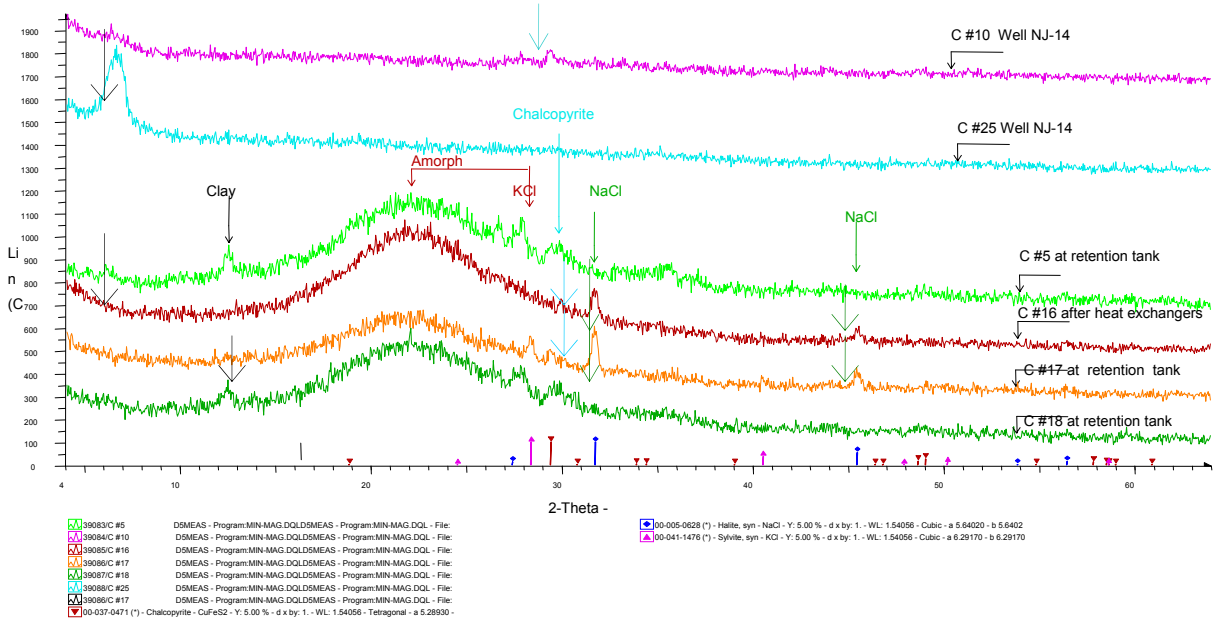

FIGURE 35: XRD spectra of scales formed at the wellheads of wells NJ-14 and NJ-22, after the heat exchangers and at the entry to the retention tank

7.3.4 Chemical analysis by Scanning Electron Microscopy – Electron Dispersive Spectroscopy (SEM-EDS)

SEM-EDS chemical analyses of all the scale samples are presented in Table 1 of Appendix C. They provide a semi-quantitative chemical composition of the scales. These are shown together with the spectra of spot analysis and the scanned electron micrographs in Appendix C. Chemical analysis can be intepreted with respect to the test sites where the scale formed. A summary of the calculated composition of the elements as oxides and sulphides are presented together with the chemical analysis of the scales in Tables 2 and 3 in Appendix C.

Scales formed from the wellhead of NJ-14 are largely composed of a high percentage of sulphur (S) and iron (Fe) and a low percentage of silicon (Si) and oxygen (O). Major elements such as sodium (Na), potassium (K), calcium (Ca), magnesium (Mg), are detected at trace levels but these may not constitute the scale but could be derived from the water that was dried on the surface of the coupons. Low concentrations of elements e.g. aluminium (Al), copper(Cu), vanadium (V), zinc (Zn), silver (Ag), manganese (Mn), nickel (Ni) are detected in this scale.

The large amounts of sulphur and iron in the scale suggest the scale is largely iron sulphide ~ 96 percent as sulphides indicated in Table 2 in Appendix C. Other sulphides of the elements such as Cu, V, Zn, Ag, Mn, Ni are present in trace amounts. The analysis reveals cubic crystals in this scale. A representative Scanning Electron Micrograph of the crystaline sulphide phases is shown in Figure 36.

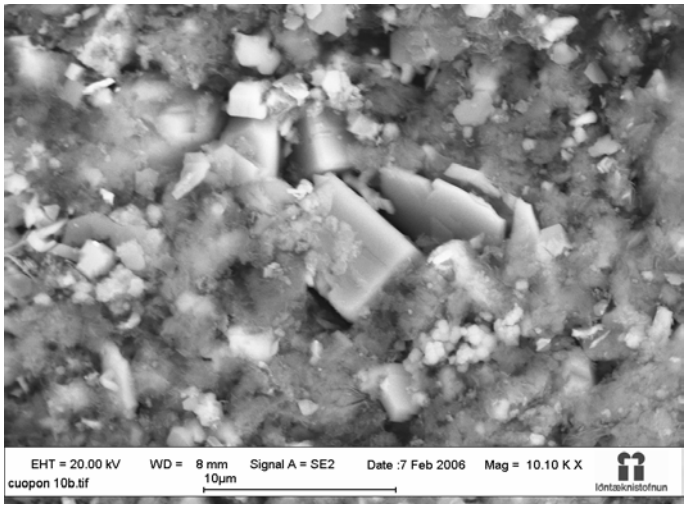

FIGURE 36: Scanning Electron Micrograph showing crystals of sulphides from scale on test coupons inserted at the wellhead of Well NJ-14

Scales formed at the wellhead of well NJ-22 consist of a high percentage of oxygen and iron with trace amounts of the major elements i.e Na, K, Ca, and Mg, and traces of the elements V, Cr, Mn, Ni, Cu, Zn and S. The major elements detected may have formed on the scale during drying of coupons. Slightly large amounts of Al and Si were observed in this scale. The major component of the scales constitutes mostly oxides of iron (42 %) mixed with silica (38 %) (Table 2 in Appendix C). This suggests that the scale formed at this well is probably a mixed scale of oxides and sulphides.

Scales formed after the heat exchanger, at the entry to the retention tank and at injection well were formed from separated water. This separated water is relatively cool, between 60 ° and 95 ° C depending on the load for hot water in Reykjavík. Chemical analysis of the scales using the SEM indicates that the major components of the scale are silicon (Si) and oxygen (O). Traces of other elements such as sodium (Na), potassium (K), chloride (Cl), are found in the scale samples. They are likely derived from the water that has dried on the surface of the coupons. Other elements detected in the scale samples were Al., Fe, Cu and S. The presence of these elements is indicative of some sulphides. Small concentrations of Mn, Fe, Ni and Cr in these samples are likely to originate the steel in the coupons. The composition of the scales indicates that it is mainly silica. The presence of Al indicates that the silica phase contains some impurity including this element.

7.3.5 Chemical analysis of scales by the Inductively Coupled Plasma – Atomic Emission Spectra (ICP-AES)

Weighed scale samples from two test sites, after the heat exchangers and at the entry to the retention tank were leached in 20 ml of 0.16N HNO_3 (Table 6 of Appendix A). These sites accumulated sufficient scale to scrape it off. Solutions of these scales were analysed by ICP-AES (Table 6 of Appendix A).

The major elements Na, K, Ca, Mg and Si are present in trace amounts in all the leached solutions of the scales. Iron and Al are detectable. Significant Ni was present. It seems possible that Ni comes from the coupon steel scraped with the scale from the coupon and leached into solution. The analyses indicate a slightly higher silicon content of scales formed at the retention tank than those formed after the heat exchangers.

7.3.6 Analysis of scales in the UV spectroscopy

Weighed samples of scales were taken and dissolved in 0.5 ml of cold hydrofluoric acid + 4.5 ml distilled water. This was diluted to 100 ml for spectrophotometric analysis to determine the amount of silica in the scales. There may have been limitations here, as the dissolution of the scales was incomplete and is equally dependent on the weight of scale sample taken. Some of the silica could have been leached into the 20 ml of 0.16 N HNO_3 used to leach ions from the scale for the ICP-AES analysis. This was calculated and added to the percent silica determined spectrophotometrically. The percent silica seems to be related to the weight of scale sample taken. The silica concentration as a percent varies between 26 -53 percent for the scales from the two test sites, after the heat exchangers and at the retention tank entry. Percent silica analysed spectrophotometrically decreases progressively with respect to the weight of the scale sample. Silica constitutes a higher percentage of the scales formed at the test site after the heat exchangers and the retention tanks. The other elements analysed in solution using ICP-AES and calculated as oxides are at low levels. The results of analysis by UV spectrophotometry and subsequent calculation are shown in Table 7 of Appendix A.

7.3.7 Quantity of scale

Weight gain and thickness on the nine test coupons were determined after removal of the coupons from the test sites. The results are shown in Table 8a in Appendix A. A different balance was used to measure the weights before and after the test. This required calibration using a set of prepared test coupons on both balances. The calibration results are shown in Table 8b in Appendix A.

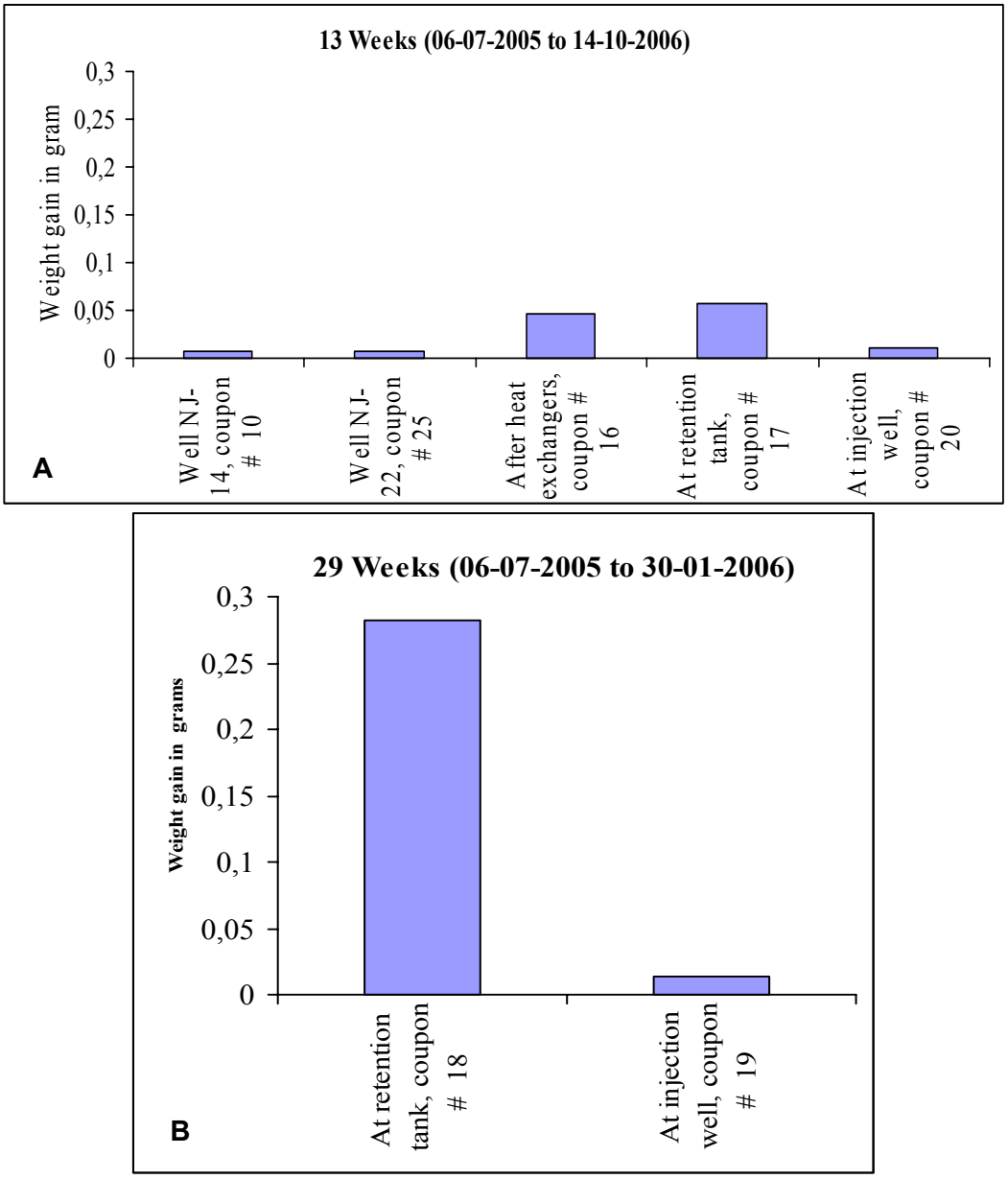

FIGURE 37: Weight gain of scale at various test sites for, a) 13 weeks test, and b) 29 weeks test

The greatest weight gain and scale thickness are observed at the test site just upstream of the retention tank. Weight gain and scale thickness at the various test sites are shown in Figures 37 and 38, respectively.

The smallest weight gain was measured at the wellheads of NJ-14 and NJ-22. The fluid at the wellheads is two phase and very fast flowing. This may affect the amount of scale deposited on the coupons. At the wellheads, the two phase fluid is at high temperature and is amorphous silica undersaturated. Therefore amorphous silica is not expected to form at the respective wellheads. By contrast the separated water studied for scale formation is at 60-90˚ C and amorphous silica supersaturated. The weight gain of the coupons after the heat exchangers and the retention tank entry is significantly higher than at the injection well. The difference is a measure of the success of the polymerization in the retention tank to slow down amorphous silica deposition. The weight gain of 280 mg after 29 weeks was measured at the retention tank entry and a scale thickness of 0.146 mm. This translates to a deposition rate of 0.26 mm/yr. At the injection well weight gain on the coupons was 14.1 mg and the scale thickness 0.0094 mm. This translates to a deposition rate of ~0.017 mm/yr or 20 times less.

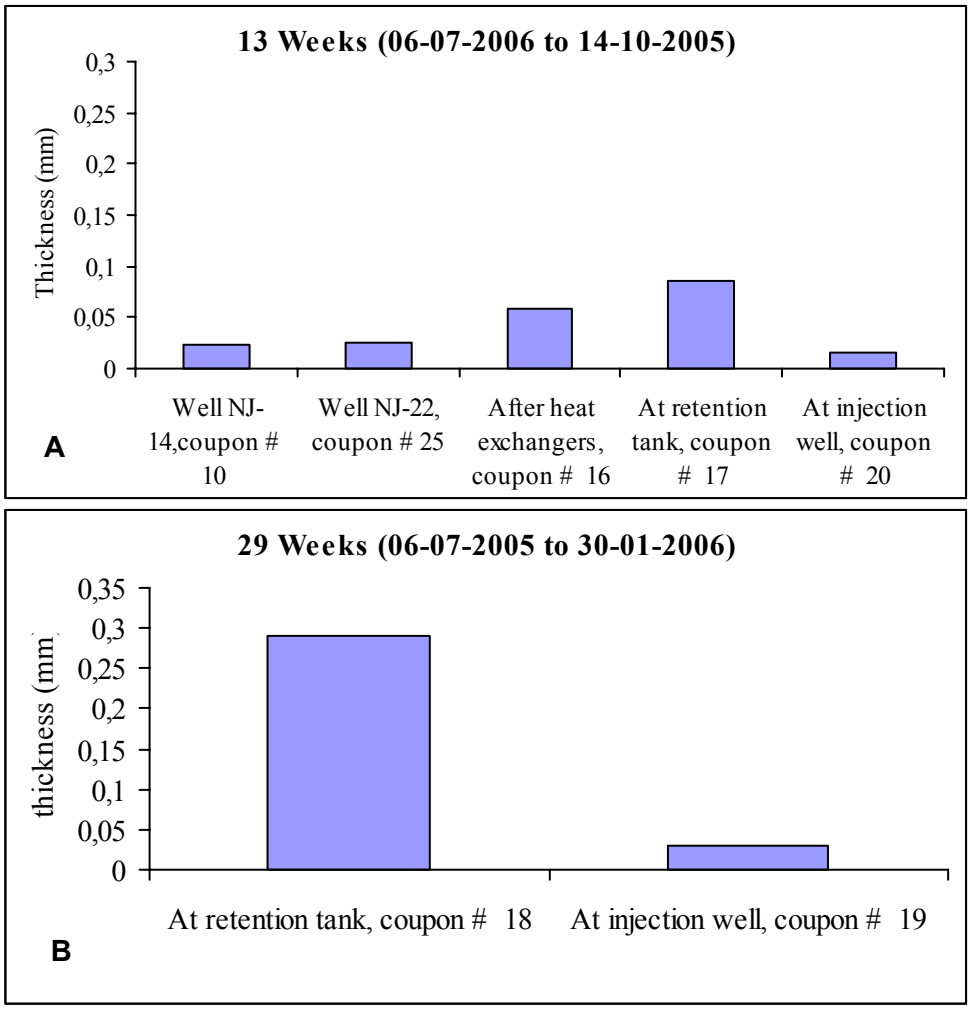

FIGURE 38: Scale thickness at the various test sites for, a) 13 weeks test, and b) 29 weeks test

8. EVALUATION OF SCALES DEPOSITED AT OLKARIA WELL OW-34, KENYA

Olkaria well OW-34 was drilled as a make up well together with wells OW-33, OW-32, OW-31, OW30 and OW-29 after steam decline was experienced in the Olkaria East Production Field during the first five years of production. Well OW-34 was connected to the steam gathering system in March, 2001 and was disconnected in September, 2002 after its output, as measured by the pressure drop across the orifice plate, indicated a substantial drop. On dismantling the flow pipes and wellhead equipment, a thick deposit of scale which was intense, almost 1 inch thick, was found inside the two phase pipe line. The scale also formed in the wellhead separator and in the separated water flowline. Since the commissioning of the Olkaria I plant and production from the Olkaria East Production Field, until 2002 no other well had experienced this kind of intense scale deposition. Well OW-34 is anomalous. The concentration of chloride in the water is high because of its discharge enthalpy. This was unusual and what caused the scale to form was not known. The general location of wells in Olkaria East Production Field with well OW-34 is shown in Figure 39.

8.1 Output characteristics of well OW-34

Three flow tests have been conducted on this well, in 1993, 1996 and 2003. The first flow test was carried out upon completion of drilling, the second to monitor tracer tests and the effect of cold water injection in well OW-R3 and the third to investigate the causes of decline in steam output. The well was discharged under different throttle conditions using different "lip pressure" pipe sizes i.e. 8", 6", 5", 4" and 3". During the first test enthalpy varied between 2640 kJ/kg and 2680 kJ/kg and the water flow rate between 0.85 and 1.55 t/hr. In the second test, the discharge enthalpy was about 2650 kJ/kg and water flow rate between 2.2 and 3.3 t/hr, while in the third test enthalpy ranged from 2670 kJ/kg to 2675 kJ/kg and water flow rate from 1.5 t/hr to 2.1 t/hr. A summary of these tests is shown in Table 9a, in Appendix A (Opondo and Ofwona, 2003).

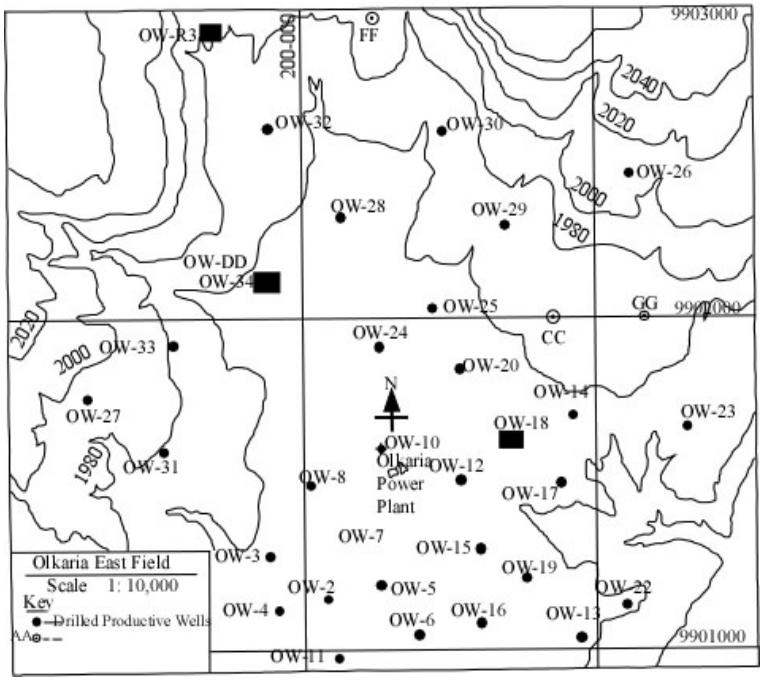

FIGURE 39: Location of wells in Olkaria East production field

When the well was connected to the production system, steam output well declined from ~42.8 t/h (Kariuki and Opondo 2001) in June 2001 to 7.2 t/h in March 2002. The output of well OW-34 with time when it was connected to the production system is shown in Table 9 b, in Appendix A.

While the enthalpy differences may appear small, at such high enthalpies close to the enthalpy of dry steam these small differences have tremendous effects on the solute content of the water discharged at atmospheric pressure. Over all the discharge tests, the discharge enthalpy varied between 2640 kJ/kg and 2680 kJ/kg at the throttle conditions and the steam fractions calculated at atmospheric pressure (X_s) are high, or between 0.9973 and 0.9996.

8.2 Water composition of well OW-34

Well OW-34 is water composition is shown in Table 10 of Appendix A together with that of a selected few make up wells, i.e. wells OW-33 and OW-32 and some wells where discharge enthalpy is very high, or wells OW-10 and OW-18 which have been under exploitation for long. Well OW-18 has water flowrates and discharge enthalpy trends that resemble those of Olkaria well OW-34. The concentration of the solute constituents Cl, F, K and Na are much higher in the separated water of well OW-34 than that of well OW-18. The silica concentration is relatively high in this well water, higher than in most separated waters of the other wells. The Cl^- concentration in the separated water at atmospheric pressure in well OW-34 is ~ 4000 ppm and Na ~ 2400 ppm. The silica concentration is relatively high, ~ 900 ppm SiO_2.

8.3 Chloride concentration as a function of vapour pressure at selected discharge enthalpies

Chloride concentration was modelled as a function of selected discharge enthalpies and vapour pressures. Discharge enthalpies selected were 2450, 2500, 2550, 2600, 2650 and 2675 kJ/kg and the vapour pressures ranged from 25 bars to 0.8 bar absolute. An initial chloride concentration of 100 ppm at a vapour pressure of 25 bars was selected.

Calculation of any solute constituent concentration e.g. chloride (Cl) in water at any pressure given the initial concentration in the fluid is based on the following equation:

$$Cl_s = Cl_{in}\frac{1-X_{in}}{1-X_s} \qquad 8.3.0$$

where X_s and X_{in} represent the steam fraction at any vapour pressure and 25 bar-abs, respectively. Cl_s and Cl_{in} represent the Cl concentrations in water at vapour pressure P_s and 25 bars, and:

$$X_s = \frac{h_t - h_s}{L_s} \qquad 8.3.1$$

$$X_{in} = \frac{h_t - h_{in}}{L_{in}} \qquad 8.3.2$$

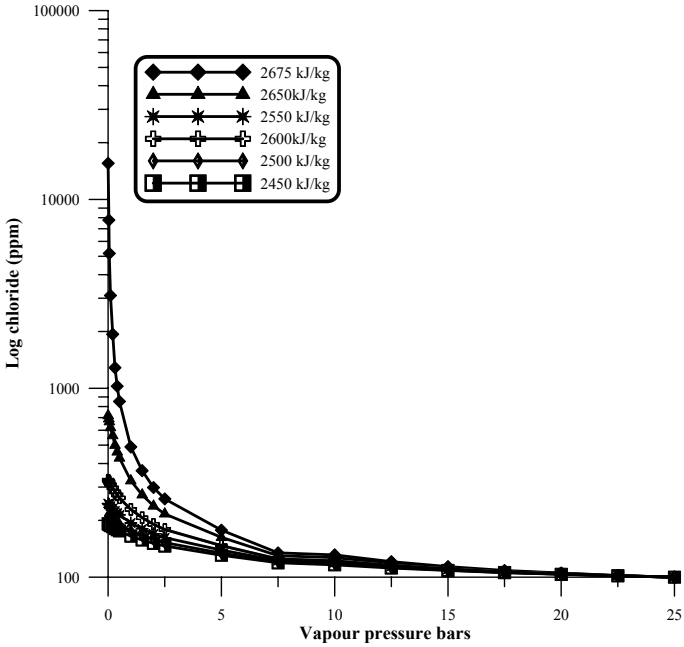

FIGURE 40: Modelled chloride concentrations at selected enthalpies with variations in vapour pressure

h_t represent the selected discharge enthalpy and h_{in} and h_s denote the enthalpy of steam saturated water at vapour pressures of 25 bar-abs, respectively. L_{in} and L_s represent the latent heat of vaporisation at 25 bar-abs vapour pressure.

Calculated Cl concentrations as a function of vapour pressure at the selected enthalpies are shown in Figure 40. At high enthalpies, especially enthalpies close to those of dry steam i.e 2675 kJ/kg and at low vapour pressures close to atmospheric pressure the chloride concentration increase exponentially and by more than 2 orders of magnitude. By lowering the enthalpy of the well by 25 - 2650 kJ/kg the chloride concentrations at the low vapour pressures drops drastically. It drops by almost 2 orders of magnitude at vapour pressures close to

atmospheric pressure. The results demonstrate that at discharge enthalpy close to that of dry steam and at low vapour pressures close to atmospheric pressure, most of the liquid is evaporated and the solutes become highly concentrated in the residual water.

8.4 Scales deposited at well OW-34

Scales formed from Olkaria well OW-34 fluids during production were in the two phase line, inside the separator and in the separated water line. The wellhead pressure in well OW-34 during the time the well was in production was ~ 6 bar g. The fluids are separated at 6 bar g in the wellhead separator. The separated water line is exposed to the atmosphere at the atmospheric silencer. Atmospheric pressure at Olkaria is ~ 0.8 bars. The layout of the flowline and wellhead equipment where the scale samples were collected is shown in Figure 41.

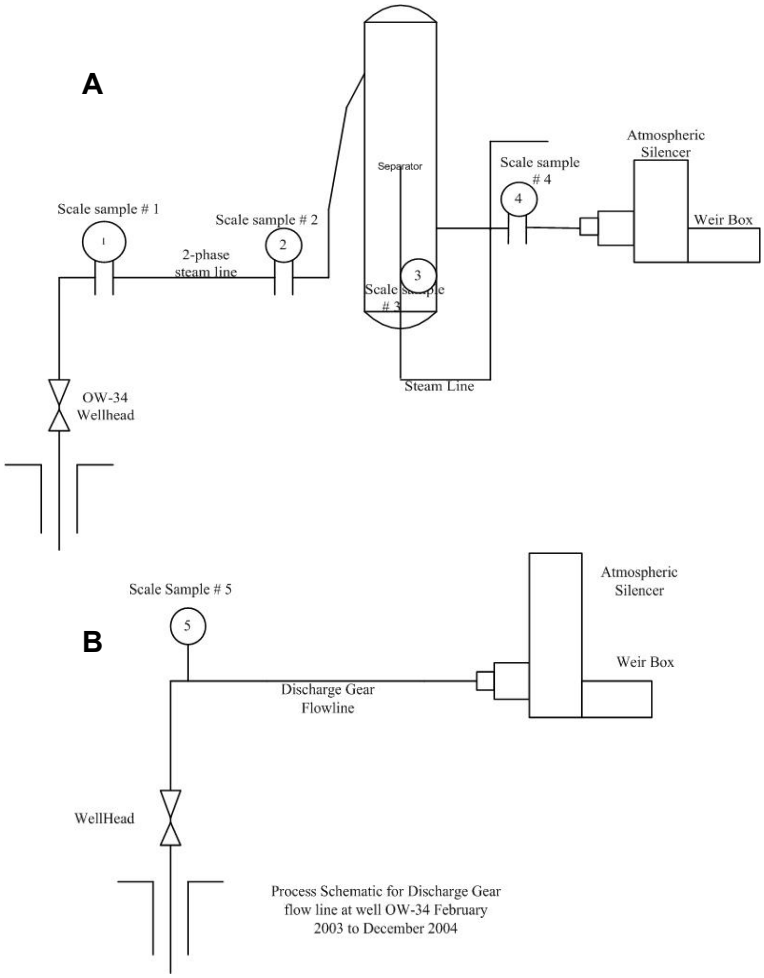

FIGURE 41: a) Layout of wellhead for well OW-34 fluids showing where the scale that formed during production from March 2001 to September 2002 was collected; b) Layout of wellhead during discharge tests in which scale samples were collected

In February to March 2003 a discharge flow test was conducted and the discharge gear left on the well pad after the tests until December 2004. The master valve of this well was leaking and in the process formed a scale in the two phase flow line. This scale was ~ 1 inch thick at the Tee connection. The layout of the discharge test gear and the location where the scale sample was collected are shown in Figure 41 b.

During production of the well in 2001-2002 the heaviest scale formed in the two phase pipeline at a sharp bend that lead to the steam separator station. The thickness of this scale was about 1 inch after about 18 months of the well being connected to the steam gathering system. The scale constricted the two-phase pipeline and drastically reduced the amount of fluid that flowed in the pipe and the total steam output of the well. The scale in the two phase line at location 2 (see Figure 41 a) is shown in Figure 42. Scale sample # 3 was collected from inside the separator vessel, as shown in Figure 43.

Other scale samples were collected from the wellhead Tee connection after the master valve (Figure 44). The texture of the scale deposited at the well head Tee connection was similar to those deposited in the two phase pipeline, though the thickness of the scales varied. About ½ inch of scale was deposited and was hard. The fourth scale sample was collected from the separated waste water line. This scale was mainly white in colour, with a little brown tinge. The deposit formed globules and ripples and was about ½ inch in thickness. The scale deposited from the waste water line is shown in Figure 45.

FIGURE 42. Scale deposited on the two phase line (scale # 2)

FIGURE 43: Scale sample from inside the separator of well OW-34 (scale # 3)

FIGURE 44: Scale formed at the Tee connection on well OW-34 master valve (scale # 1)

FIGURE 45: Scale deposit in the waste water line of well OW-34 (scale # 4)

A fifth scale was collected from the Tee connection of the dismantled well discharge test gear. The scale was layered and the top layer was black and brittle while the layer below was slightly brown to white. The thickness of scale deposit was close to 1 inch, formed between March 2003 and December 2004. The leakage could have contributed to further cooling of the fluid under flow conditions that are not typical when the well is free flowing. The scale deposit is shown in Figure 46.

FIGURE 46: Deposit of scale formed when well OW-34 master valve was leaking (scale # 5 December 2004)

8.5 Analysis of scales from well OW-34

Techniques for the analysis of scales from Olkaria well OW-34 were similar to those applied in the analysis of scales deposited on coupons at Nesjavellir described in section 7.3. Infrared analysis of the scale samples from the process flow from sample # 1 to # 5 are shown in Figure 47.

The IR spectra of scale samples #1 to # 5 all have IR features similar to those of precipitated silica gel or amorphous silica. A broad asymmetric stretching band is observed in all the spectra between 3200 cm^{-1} and 3600 cm^{-1}. In all the scales the spectra bands at ~ 3469 to 3554 cm^{-1} are associated with the hydroxyl group (OH) of the bound water in the crystal lattice. Weak symmetric stretching vibration bands are observed at ~ 2852 cm^{-1} and 2848 cm^{-1} and these represent C-H groups that could be due to contamination by grease or oil. Molecular water (H_2O) is present in these scales represented by the spectra band at 1641 cm^{-1}. In all the scales there is a strong peak in the range ~1099 - ~1033 cm^{-1} from bending O-Si-O vibrations due to antisymmetric Si-O-Si stretches. The second strongest peak between ~ 469 and 465 cm^{-1} is due to O-Si-O bending vibrations and a weaker band near 793-795 cm^{-1} is evaluated as due to symmetrical stretching of tetrahedrally co-ordinated Si and Al. The 1099-1033 cm^{-1} band has shoulders at ~1200 cm^{-1} on the low energy side and ~ 950-970 cm^{-1} on the high energy side. The 950-970 cm^{-1} peak is particularly characteristic of amorphous silica.

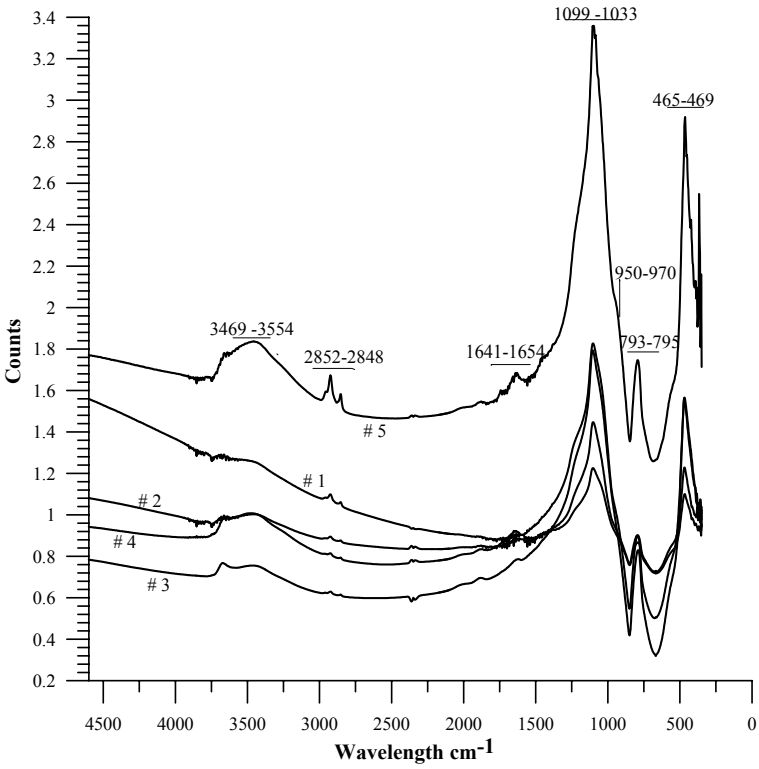

FIGURE 47: Infrared spectra of scale samples #1 - # 5 collected from Olkaria well OW-34

Scanned Electron Micrographs of the scale samples from well OW-34 fluids are presented in Appendix C together with chemical analysis, shown in Table 2 and a summary of elements calculated as oxides is presented in Table 3 of Appendix C.

All the scale samples # 1 to # 5 are predominantly composed of Silicon (Si) and Oxygen (O). The percent silicon composition in the scale samples # 1 to # 3 suggest that silicon composition (Si) ranged between ~58 and ~37% and that of oxygen (O) varied between 61 and 39%. These samples did not show any trace amounts of other elements in them. They could represent almost pure amorphous silica phases (Appendix C). Scale samples # 4 and # 5, though largely silica rich had a higher iron and aluminium content. Trace concentrations of iron in scale # 4 could have its origin in the pipework or probably the walls of the separator while that of scale # 5 could have its origin from the pipework in the discharge flow line.

X-ray diffraction patterns for the scales formed from Olkaria well OW-34 are shown in Figure 48. All the scales of samples # 1 to # 5 are largely amorphous to X rays. They all depict a broad peak at ~ 23˚ 2θ, characteristic of amorphous silica or opaline silicates. Scale sample # 5 has a small diffraction peak centred at ~ 27˚ 2θ alongwith the broad spectra band at ~ 23˚ 2θ for amorphous silica phases. The diffraction peak at ~ 27 ˚ 2θ could be due to quartz in the scale sample.

Results of chemical analysis of the scales by ICP are shown in Table 6 of Appendix A together with analysis of scales formed on coupons at Nesjavellir. Scales # 1 to # 4 have trace amounts of the major aqueous cations except for calcium which is present in high concentrations in scale # 3 Zinc is abundant in scale # 1. The source of high calcium (Ca) and zinc (Zn) concentrations in these scales is hard to establish but could be due to contamination. The calcium may also reflect the presence of a

calcium silicate or calcium carbonate. Concentrations of the major elements, sodium, potassium, calcium are relatively high in scale sample # 5 has and also those of the transition elements relative to the other scale samples. The high concentrations of the major elements could be due to incorporation of brine into the scale. The iron (Fe) and aluminium (Al) contents in this scale sample are relatively high. It is probable that the Fe was dissolved from the flowpipe. Iron content is also relatively high in scales #1 and #2 and it is likely that the source of this relatively high iron is the two phase pipeline and that it is dissolved from the pipeline. The high contents of Al in scale #5 could be indicative of some clays in the scale or Al in the amorphous silica phase.

Silica content of scale samples # 1 to # 5 as also analysed spectrophotometrically. The percentage of silica in all scales was above ~ 40 percent. In scale # 3 the percentage of silica is close to 90 percent. The percentage of silica in the scales could vary during dissolution. It is probable that all or most of the silica did not dissolve during dissolution. Silica constitutes a major component of these scales as determined by the UV spectrophotometry. The total silica composition determined by UV spectrophotometry plus that obtained from the analysis by ICP totalled ~ 45 percent for the scale with the lowest silica concentration and ~ 100 percent for the scale with highest silica concentration. The results of analysis by UV spectrophotometry and subsequent calculation are shown in Table 7 of Appendix A.

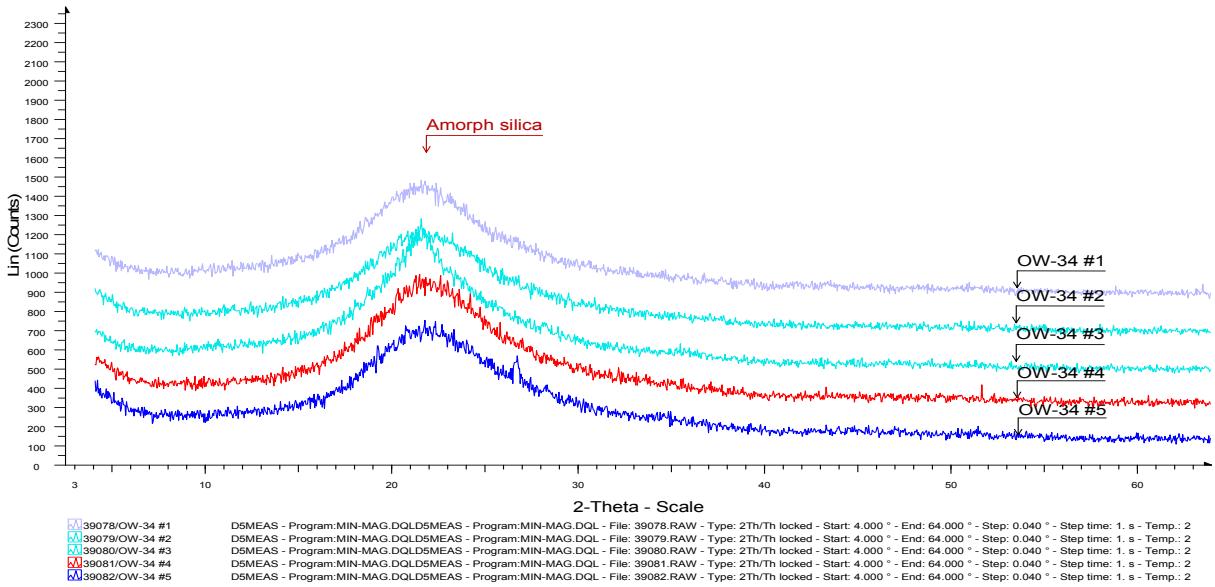

FIGURE 48: X-Ray diffraction analysis of scale samples # 1 - # 5 from Olkaria well OW-34

9. CONCLUSIONS

Olkaria well fluids generally exhibit a discharge enthalpy that ranges from slightly less than 1000 kJ/kg to a saturated steam enthalpy of about 2700 kJ/kg. Most wells have "excess enthalpy". Enthalpy for selected wells from Svartsengi, Reykjanes, and Nesjavellir is variable. In Svartsengi the enthalpy of the fluids is fairly homogenous and apart from wells that tap into the shallow steam cap, average enthalpy for the fluids is ~ 1030 kJ/kg. Enthalpy of well fluids in Reykjanes is slightly higher, between 1300 kJ/kg and 1400 kJ/kg for the selected wells. At Nesjavellir the discharge enthalpies of the wells are high and most wells have enthalpy >1600 kJ/kg. For the selected wells, the enthalpy varied between ~ 1400 kJ/kg and ~ 1800 kJ/kg. "Excess enthalpy" in all wells considered for the present study is adequately explained by phase segregation in producing aquifers.

The average of tqtz and tNa/K for the wells studied in Olkaria and Nesjavellir were taken to represent the aquifer temperatures. Quartz equilibrium temperatures were calculated using the phase segregation model. Large differences are observed between tqtz and tNaK for some wells in Olkaria. These wells have discharge enthalpy close to that of steam saturated water at aquifer temperature so aquifer water composition is not the source of error. Measured downhole aquifer temperatures in thermally stabilised wells were used for Reykjanes and Svartsengi.

The phase segregation model does not take into account changes in composition of the flowing fluid between the wellhead and initial conditions by precipitation or dissolution of minerals. When geothermal water degasses by boiling, many reactions tend to occur. Changes in temperature occur as a consequence of depressurisation boiling and may cause changes in saturation with respect to many minerals. Speciation calculations may thus indicate significant departures from equilibrium between minerals and the water in the aquifer beyond the depressurisation zone, even when such equilibrium is closely approached in the initial fluid. Large errors in SI values can arise when potential mineral and precipitation reactions are ignored, especially for minerals which contain chemical components present in low concentrations in the initial water. The effect is much smaller for components, which are abundant in the fluid such as reactive gases (CO_2, H_2S and H_2)

The concentration of CO_2 in the aquifer water of Olkaria, Reykjanes, Svartsengi and Nesjavellir is generally in the range of 60-5000 ppm except in Olkaria West where it is as high as 43,026 ppm. In Olkaria West the aquifer fluid CO_2 concentrations are considered to be much affected by its rate of supply from the magmatic heat source where in other parts of Olkaria and the other study areas aquifer water CO_2 is fixed by equilibration with a specific mineral buffer. The CO_2-rich waters in Olkaria west could cause corrosion on the outside of well casing. This should be investigated. Condensates that form due to dissolution of CO_2 would be lower for Olkaria West than in the rest of the study areas. The relatively low concentrations of CO_2 in the other sectors of Olkaria, as well as Reykjanes, Svartsengi and Nesjavellir do pose a low risk in developing CO_2 rich water that would be corrosive.

HCl concentrations in the aquifer waters and steam are controlled by pH, temperature and chloride concentrations. The Olkaria and Nesjavellir aquifer waters contain very low HCl concentrations (1.65×10^{-5} and 2×10^{-3} ppm in Olkaria and 1×10^{-5} ppm in Nesjavellir). In Reykjanes and Svartsengi, the HCl concentration is higher (0.32 and 0.81 ppm and 0.056 and 0.083 ppm, respectively) due to a lower pH and higher chloride concentrations in the fluids. Much higher HCl concentrations are present in the steam at the wellheads at Reykjanes (0.65 ppm) than at Svartsengi due to high steam separation pressures. The HCl in the steam at Reykjanes would produce a pH of about 5.5 in a condensate. It is accordingly concluded that HCl in steam (0.65 ppm) at the wellheads at Reykjanes is an unlikely corrosion candidate and even much less likely in the other study areas.

The undisturbed aquifer waters in all the study areas are expected to be close to equilibrium with calcite. Calculated saturation indices for calcite show, however, considerable scatter. The cause of this scatter is partly considered to be analytical imprecision, particularly with respect to pH but also removal of calcium from solution between initial aquifer conditions and wellhead by calcite precipitation. Further the quality of the thermodynamic data used to calculate the calcite activity

product may contribute as well as the presence of equilibrium steam in the aquifer. In calculating aqueous species distribution in the aquifer water such equilibrium steam was assumed not to be present. Calculated variation in the calcite saturation state upon adiabatic boiling is considerably more accurate than calculation of the absolute saturation state. Upon boiling degassing of the water with respect to CO_2 generally causes an initially calcite saturated water to become supersaturated. This is particularly the case with waters high in CO_2 such as in Olkaria West and where aquifer temperatures are around 200°C but CO_2 solubility in water at minimum around 200°C. In relatively high temperature and low CO_2 waters, such as at Nesjavellir, early boiling may only cause limited degassing and not calcite supersaturation. Prolonged depressurization boiling, which leads to a decrease in fluid temperature, decreases the calcite saturation index due to the retrograde solubility of calcite with respect to temperature. This often causes boiled geothermal waters to be calcite undersaturated. Calcite scaling is not expected to be a problem at Olkaria and Nesjavellir and neither at Svartsengi and Reykjanes if the first depth level of boiling is outside wells i.e. in the producing aquifers.

Scaling tests at Nesjavellir showed that at high temperatures of the wellheads of wells NJ-14 and NJ-22, the two phase fluids deposited scales that were dominantly sulphide phases in well NJ-14 fluids and mixed sulphides and oxides in the case of well NJ-22. The scales were essentially amorphous to X-rays. There were however, some indications of some mineral phases in the scales such as chalcopyrite and clayey material. Separated waters after the heat exchangers, entry to the retention tank and at the injection well deposited mainly amorphous silica but there are also some indications of the presence of clays in the scales. The rate of deposition of ~0.261 mm/yr was highest at the entry to the retention tank and much lower of ~ 0.0168 mm/yr at the injection well. Silica polymerisation occurs in the retention tank and this reduces the rate of silica deposition at the injection well. At entry to the retention tank, the high rate of deposition could be due to supersaturation by monomeric silica which causes a higher rate of precipitation (Yanagase et al., 1970; Rothbaum, 1979). An intermediate test site between the steam separators and the wellheads could be chosen to investigate the type of scales that would form.

The solute content of the water discharged from the atmospheric silencer of Olkaria well OW-34 is high The discharge enthalpy of the well fluids is close to that of dry steam leading to extensive evaporation of the water fraction in the discharge by depressurization boiling to a low pressure. This extensive evaporation is thought to be the cause of the high salt content of the water discharged at atmospheric pressure as well as the extensive amorphous silica scale formation.

A solution to this scaling problem involves mixing of the discharge of well OW-34 with separated brine or condensate from another well e.g. well R-3 where separated brines from the Olkaria II plant are being re-injected to lower the discharge enthalpy of OW-34. This will reduce the amount of evaporation of water in well OW-34. Theoretical calculations based on mass balance equations, chloride concentration of spent brine being re-injected in well R-3 and that of well OW-34 for purposes of diluting the water have been tried. In this way aqueous silica concentrations will not build up to the same extent and amorphous silica deposition will be reduced or inhibited.

REFERENCES

Allegrini, G., and Benvenuti, G., 1970: Corrosion characteristics and geothermal power plant protection (Collateral processes of abrasion, erosion and scaling) *U.N. Symposium on the development and utilisation of geothermal resources, Pisa, Geothermics,* 865-881.

Ármannsson, H., 1989: Predicting calcite deposition in Krafla boreholes. *Geothermics, 18,* 25-32.

Ármannsson, H., 2003: CO_2 emissions from geothermal plants. *Proc. of the International Geothermal Conference IC2003, Reykjavik,* 56-62.

Ármannsson, H., Gíslason, G., and Haukson, T., 1982: Magmatic gases in well fluids aid the mapping of the flow of pattern in a geothermal system. *Geochim. Cosmochim. Acta, 46,* 167-177

Arnórsson, S., 1978: Precipitation of calcite from flashed geothermal waters in Iceland. *Contrib. Mineral. Petrol., 66,* 21-28.

Arnórsson, S., 1981: Mineral deposition from Icelandic geothermal waters, environmental and utilisation problems. *J. Petr. Techn., 33,* 181-187.

Arnórsson, S., 1989: Deposition of calcium carbonate from geothermal waters – theoretical considerations. *Geothermics, 18,* 33-89.

Arnórsson, S., 1995: Scaling problems and treatment of separated water before injection. In: Rivera, J. (ed), *Injection technology.* World Geothermal Congress 1995; IGA pre-congress course, Pisa, Italy, May 1995, 65-111.

Arnórsson, S., 2000a: The quartz and Na/K geothermeters. I. New thermodynamic caliberation. *Proc. of World Geothermal Congress 2000, Kyushu- Tohuku, Japan,* 929-933.

Arnórsson, S., 2000b: Injection of waste geothermal fluids: Chemical aspects. *Proc. of the World Geothermal Congres 2000, Kyushu- Tohuku, Japan,* 3021-3025.

Arnórsson, S., and Stefánsson, A., 2005: Wet steam well discharges.I. Sampling and calculation of total discharge compositions. *Proc. of World Geothermal Congress 2005, Antalya, Turkey,*

Arnórsson, S., D'Amore, F., and Gerardo-Abaya, J., 2000: Isotopic and chemical techniques in geothermal exploration, development and use. In: Arnórsson, S. (ed.), *Isotopic and chemical techniques in geothermal exploration, development and use. Sampling methods, data handling, interpretation*. International Atomic Energy Agency, Vienna.

Arnórsson, S., Geirsson, K., Andrésdóttir, A., and Sigurdsson, S., 1996: *Compilation and evaluation of thermodynamic data on aqueous species and dissociational equilibria in aqueous solution I. The solubility of CO_2, H_2S, H_2, N_2, O_2 and Ar in pure water.* University of Iceland, Science Institute, report No. RH-17-96, 74 pp.

Arnórsson, S., Sigurdsson, S., and Svavarsson, H., 1982: The chemistry of geothermal waters in Iceland I. Calculation of aqueous speciation from 0°C to 370°C. *Geochim. Cosmochim. Acta, 46,* 1513-1532.

Benoit, W., 1989: Carbonate scaling characteristics in Dixie Valley, Nevada geothermal wellbores. *Geothermics, 18,* 41-48.

Bertini, R., 2005: World geothermal power generation in the period 2001-2005. *Geothermics, 34,* 651-690.

Bjarnasson, J.Ö., 1984: *Chemical composition of geothermal brine and steam in well 9 in Reykjanes.* Orkustofnun, Reykjavík, report OS-84049/JHDY3B (in Icelandic).

Bjarnasson, J.Ö., 1994: *Computer code WATCH, version 2.1.* Orkustofnun, Reykjavík, 56 pp.

Bjarnasson, J.Ö., and Björnsson, G., 1995: *Computer Code TAFLA, version 2.0.* Orkustofnun, Reykjavík, 56 pp.

Björnsson, G., 1999: Predicting future performance of a shallow steam zone in the Svartsengi geothermal field, Iceland. *Proc. of 24th Workshop on Geothermal Reservoir Engineering, Stanford University, Stanford, California.*

Björnsson, G., and Steingrímsson, B., 1992: "Fifteen years of pressure and temperature monitoring in the Svartsengi geothermal field, Iceland". *GRC, Transactions, 16,* 627-632.

Björnsson, S., Arnórsson, S. and Tómasson, J., 1972: Economic evaluation of Reykjanes thermal brine area. *Am. Ass. of Petrol. Geol. Bull. 56 (12),* 238-239.

Bodvarsson, G. S., and Pruess, K., 1987: *Numerical simulation studies of the Olkaria geothermal field.* Kenya Power Company Co. Ltd, unpublished internal report.

Boulton, L.H., and Wright, G.A., 1983: *Fundamentals of metallic corrosion and its prevention.* Australasian Corrosion Association, New Zealand Branch Inc., Auckland, New Zealand, 40 pp.

Browne, P.R.L., 1984: Subsurface stratigraphy and alteration of the eastern section of Olkaria geothermal field, Kenya. *Proc of 6th New Zealand Geothermal Workshop, Geothermal Institute, Auckland,* 33-42.

Busenberg, E., and Plummer, L.N., 1986: A comparative study of the dissolution and crystal growth kinetics of calcite and aragonite. *USGS Bull. 1578, 139-168.*

Candelaria, M.R., Cabel Jr., A.C., Buning, B.C., and Noriega Jr., M.T., 2000: Calcite inhibition field trials at the Mindanao geothermal production field (MGPH), Philippines. *Proc.of World Geothermal Congress, Kyushu-Tohuku, Japan,* 2171-2176.

Chen, C.T., and Marshall, W.L., 1982: Amorphous silica solubilities IV: Behaviour in pure water and aqueous sodium chloride, sodium sulphate, magnesium chloride and magnesium sulphate solutions upto 350°C. *Geochim. Cosmochim. Acta, 46,* 279-28.

Clarke, M.C.G., Woodhall, D.G., Allen, D., and Darling, G., 1990: *Geological, volcanological and hydrological controls on the occurrence of geothermal activity in the area surrounding Lake Naivasha, Kenya, with coloured 1:100,000 geological maps.* Ministry of Energy, Nairobi, 138 pp.

Conover, M., Ellis, P., and Curzon, A., 1979: Material selection guidelines for geothermal power systems – An overview. In: Casper, L.A., and Pinchback, T.R., (eds)*, Geothermal scaling and corrosion.* ASTM, STP 717, 17 pp.

Corsi, R., 1986; Corrosion and scaling in geothermal fluids. *Geothermics, 15,* 94 -96.

D'Amore, F., Celati, R., Ferrara, G.C., and Panichi, C., 1977: Secondary changes in chemical and isotopic composition of the geothermal fluids in Larderallo. *Geothermics, 5,* 153-163.

D'Amore, F., Giusti, D., Abdallah, A., 1998: Geochemistry of high-salinity geothermal field of Asal., Republic of Djibouti, Africa. *Geothermics, 27,* 197-210.

D'Amore, F., Truesdell, A.H., and Haizlip, R.J., 1990: Production of HCl by mineral reactions in high-temperature geothermal systems. *Proc. of 15th Workshop on Geothermal Reservoir Engineering, Stanford, Stanford University, Ca.,* 199-210.

Dominguiz, A., 1980: Well completion and development at Cerro Prieto. *Geothermics, 9, 101-131.*

Durak, S., Erkan, B., Askoy,N., 1993: Calcite removal from the wellbores of Kizildere geothermal field, Turkey. *Proc. of the 15th New Zealand Geothermal Workshop, Auckland, NZ,* 5-10.

Ellis, A.J., and Mahon, W.A.J., 1977: *Chemistry and geothermal systems.* Academic Press, New York, 392 pp.

Franzson, H., 1983: The Svartsengi high-temperature field, Iceland. *GRC, Transactions, 7,* 627-633.

Franzson, H., 1995: Geological aspects of the Svartsengi high-T field Reykjanes peninsula, Iceland. *Proc. of the 8th International Symposium on Water-Rock Interaction - WRI-8,* 497-500.

Fournier, R.O., 1973: Silica in thermal waters: Laboratory and field investigations. In: *Proc. Int. Symp. on Hydrogeochemistry and Biochemistry, Tokyo, 1970, I - Hydrochemistry.* Clark, Washington, D.C., 122-139.

Fournier, R.O., 1983: A method of calculating quartz solubilities in aqueous sodium chloride solutions. *Geochim. Cosmochim Acta, 47,* 579-586.

Fournier, R.O., 1985: The behaviour of silica in hydrothermal solutions. In: Berger, B.R., and Bethte, P.M. (eds.), *Geology and geochemistry of epithermal systems. Society of Economic Geologists,* 45-61.

Fournier, R.O., and Marshall., 1983: Calculation of amorphous silica solubilities at 25˚ C to 300˚ C and apparent cation hydration numbers in aqueous salt solutions using the concept of effective density of water. *Geochim. Cosmochim Acta, 47,* 587-596.

Fournier, R.O., and Potter, R.W., 1982: The solubility of quartz from 25˚C to 900˚C at pressures upto 10,000 bars. *Geochim. Cosmochim. Acta, 46,* 1969-1973.

Fournier, R.O., and Rowe, J.J., 1966: Estimation of underground temperatures from the silica contents of water from hot springs and wet steam wells. *Am. J. Sci., 264,* 685-697.

Fournier, R.O., and Rowe, J.J., 1977: The solubility of amorphous silica in water at high temperatures and pressures. *Am. Min. Sci., 62,* 1052-1056.

Fridriksson, T., Kristjánson, B.R., Ármannsson, H., Margétardóttir, E., Ólafsdóttir, E., and Chiodini, G., 2006: CO_2 emissions and heat flow through soil, fumaroles and steam heated mud pools at Reykjanes geothermal area, SW Iceland. *Applied Geochemistry, 21,* 151-1569.

Gallup, D.L., 1989: Iron silicate scale formation and inhibition at the Salton Sea geothermal field. *Geothermics, 18,* 97-103.

Gallup, D.L., 1993: The influence of iron on the solubility of amorphous silica on hypersaline geothermal brines. *Proc. of 1991 Symposium on Chemistry in High Temperature Aqueous Solutions, Provo, UT F6f,* 1-16.

Gallup, D.L., 1998: Aluminium silicate scale formation and inhibition (2): Scale solubilities and laboratory and field inhibition tests. *Geothermics, 27,* 485-501.

Gallup, D.L., Andersen, G.R. and Holligan, D., 1990: Metal sulphide scaling in production well at Salton Sea geothermal field. *GRC Transactions, 14,* 1583-1590.

Garcia, S.E., Candelaria, M.N.R., Baltazar, A.D.Jr. Solis, R.P., Cabel, A.C.Jr., Nogara, J.B., and Jordan, O.T., 1996: Methods of coping with silica deposition, the PNOC-experience. *Proc. of 17th Annual PNOC-EDC Geothermal Conference, Manila,* 93-109.

Giggenbach,W.F., 1975: Variations in the carbon, sulphur and chlorine contents of volcanic gas discharges from White Island, New Zealand. *Bull. Volcanol., 39,* 15-27.

Giroud, N.R., 2006: *Personal communication*

Gíslason, G., and Gunnlaugsson, E., 1994-1995: *Research on silica polymerisation in heat exchangers* (in Icelandic). Hitaveita Reykjavikur, Reykjavík, three reports, 9 pp.

Gíslason, S.R., Heaney, P.J., Oelkers, H.E., and Schott, J., 1997: Kinetic and thermodynamic properties of moganite, a novel silica polymorph. *Geochim. Cosmochim. Acta, 61,* 1193-1204.

Gunnarsson, Á., Steingrímsson, B.S., Gunnlaugsson, E., Magnússon, J., and Maack, R., 1992: Nesjavellir geothermal co-generation power plant. *Geothermics, 21,* 673-681.

Gunnarsson, I., and Arnórsson, S., 2000; Amorphous silica solubility and the thermodynamic properties of $H_4SiO°_4$ in the range of 0° to 350°C at P sat. *Geochim. Cosmochim. Acta, 64,* 2295-2307.

Gunnarsson, I., and Arnórsson, S., 2005: Impact of silica scaling on the efficiency of heat extraction from high-temperature geothermal fluids, *Geothermics, 34,* 320-329.

Haizlip, J.R., and Truesdell, A.H., 1988: Hydrogen Chloride in superheated steam and chloride in deep brine at the Geysers geothermal field, California. *Proc. of 13th Workshop on Geothermal Reservoir Engineering, Stanford, California, SGP-TR,* 93-99.

Hardardóttir, V., Ármannsson, H., Thórhallsson, S., 2004: Scaling studies on brine from wells 9 and 11, in the Reykjanes high temperature area, Iceland. *13th Scandinavian Corrosion Congress (Nordisk Korrosionsmöte) NKM 13, Reykjavik, Iceland,* 14 pp.

Hardardóttir, V., Ármannsson, H., and Thórhallson, S., 2005: Characterisation of sulphide-rich scales in brine at Reykjanes. *Proc. World Geothermal Congress 2005, Antalya, Turkey.*

Hardardóttir, V., Kristmannsdóttir, H., and Ármannson, H., 2001: Scale formation in wells RN-09 and RN-08 in the Reykjanes geothermal field, Iceland. *Proc of the 10th Inter. Symp. on Water-Rock Interaction, Villasimius, Italy, Balkema. Rotterdam,* 851-854.

Hauksson, T., 1996: *Silica polymerisation in high temperature geothermal water – Exploration on rate of silica polymerisation in turbulence flow* (in Icelandic). Report for Hitaveita Reykjavíkur, Reykjavik, 138 pp.

Hedenquist, J.W., and Stewart, M.K., 1985: Natural CO_2-rich steam- heated waters in the Broadlands-Ohaaki geothermal system, New Zealand: Their chemistry, distribution and corrosive nature. *GRC, Transactions*, *9*, 245-250.

Henley, R.W., 1983: pH and silica scaling control in geothermal field development. *Geothermics, 12,* 307-321.

Henley, R.W., Truesdell, A.H., and Barton, P.B., 1984: Fluid-mineral equilibria in hydrothermal systems. *Reviews in Economic Geology, 1,* 267 pp.

Horne, R.N., Satik, C., Mahiya, G., Li, K., Ambusso, W., Tovar, R., Wang, C., Nassori, H., 2000: Steam-water relative permeability. *Proc. World Geothermal Congress 2000, Kyushu-Tohoku, Japan, 2609-2615.*

Hurtado, R., Andritsos, N., Mouza, A., Mitrakas, M., Vrouzi, F., and Christanis, K., 1989: Characteristics of scales from Milos geothermal plant. *Geothermics, 18,* 169-174.

Itoi, R., Fukuda, M., Jinno, K., Hirowatari, H., Shinohara, N., Tomita, T., 1989: Longterm experiments of waste water re-injection in the Otake geothermal field, Japan. *Geothermics, 18,* 153-160.

Jones, D.A., 1996*: Principles and prevention of corrosion* (2nd edition). Prentice Hall, Upper Saddle River, NJ, 572 pp.

Karabelas, A.J., Andristsos, N., Mouza, A., Mitrakas, M., Vrouzi, F., Christanis, K., 1989: Characteristics of scales from the Milos geothermal plant. *Geothermics, 18, 169-175.*

Kariuki, M.N., and Opondo, K.M., 2001: *Status report on steam production assessment of reservoir and steam status in Olkaria East Field, 1st half 2001*. KenGen, Nairobi, unpublished internal report.

Karlsdóttir, R., 1997: *TEM resistivity survey on the outer Reykjanes Peninsula*. Orkustofnun, report OS-9700 (in Icelandic,) 63 pp.

Karingithi, C.W., Arnórsson, S, Opondo, K.M., and Grönvold, K., 2006: Hydrothermal mineral buffers controlling reactive gas concentrations in Olkaria geothermal system, Kenya. *Geochim. Cosmochim. Acta, submitted.*

Kato, K., Ueda, A., Mogi, K., Nakazawa, H., Shimizu, K., 2003: Silica recovery from Sumikawa and Onuma geothermal brines (Japan) by addition of CaO and cationic precipitants in a newly deviced seed circulation device. *Geothermics, 32,* 239-274.

Kiyota, Y., Hirowatari, K., Tokita, H., Haruguchi, K., Uogata, K., 2000: Evaluation on geothermal injection treatment by pH modification. *Proc. of the World Geothermal Congress 2000, Khushu-Tohuku, Japan,* 3077-3082.

Kjartansson, G., 1996: *Nesjavellir - Experimental test on geothermal brine heat exchanger in pilot plant and power plant 1985-1996* (in Icelandic). Report from Hitaveita Reykjavíkur, Reykjavik, Iceland, 102 pp.

Li, K., Horne, R.N., 2004: Universal capillary pressure and relative permeability model from fractal characterisation of rock. *Proc. of the 29th Workshop on Geothermal Reservoir Engineering, Stanford University, Stanford, California, SGP-TR-175.*

Mahon, W.A.J., 1966: Silica in hot water discharged from drillholes at Wairakei, *New Zealand Jour. Sci. 9,* 135-144.

Marshall, W.L., and Chen, C.T.A., 1982: Amorphous silica solubilities -V. Predictions of solubility behaviour in aqueous mixed electrolyte solutions to 300˚ C. *Geochim. Cosmochim. Acta, 46,* 289-291

Marshall, W.L., and Warakomski, M.J., 1980: Amorphous silica solubilities–II. Effects of aqueous salt solutions at 25˚C. *Geochim. Cosmochim. Acta, 46,* 289-291.

Meeker, K.A., and Haizlip, J.R., 1990: Factors controlling pH and optimum corrosion mitigation in chloride-bearing geothermal steam at the Geysers. *GRC Transactions, 14,* 677-1684

Mercerdo, S., Bermejo, F., Hurtado, R., Terrazas, Hernández, L., 1989: Scale incidence on production pipes of Cerro Prieto geothermal wells. *Geothermics, 18,* 225-232.

Moya, P., Nietzen, F., Rivera, E.S., 2005; Development of the neutralization system for production wells at the Miravalles Geothermal Field. *Proc. World Geothermal Congress 2005, Antalya- Turkey.*

Mungania, J., 1992: *Geology of the Olkaria geothermal complex*. Kenya Power Company Ltd., internal report, 38 pp.

Mwangi, M.N., 2005: Country update report for Kenya 2000-2005. *Proc. of the World Geothermal Congress 2005, Antalya, Turkey.*

Naylor, W.I., 1972: *Geology of Eburru and Olkaria prospects.* U.N. Geothermal exploration project, report.

Nouralie, J., 2000: Borehole geology and hydrothermal alteration of well NJ-20, Nesjavellir high-temperature area, SW-Iceland. Report 15 in: *Geothermal training in Iceland 2000. UNU-GTP, Iceland,* 303-330.

Ogoso-Odongo, M.E., 1986: Geology of the Olkaria geothermal field. *Geothermics, 15,* 741-748.

Omenda, P.A., 1998; The geology and structural controls of the Olkaria geothermal system, Kenya. *Geothermics, 27*, 55-74

Opondo, K.M., and Ofwona, C.O., 2003: *Investigations of unusual scale deposition in Olkaria well OW-34*. Kengen, Nairobi, unpublished internal report, 11 pp.

Parlaktuna, M., and Okandan. E., 1989: The use of chemical inhibitors for prevention of calcium carbonate scaling. *Geothermics, 18, 241-248*

Pieri, S., Sabatelli, F., and Tarquin, 1989: Field testing results of downhole scale inhibitor injection. *Geothermics, 18, 249-258.*

Plummer, L.N., and Busenburg, E., 1982: The solubilities of calcite, aragonite and vetrite in CO_2-H_2O solutions between 0 and 90˚ C, and an evaluation of the aqueous model for the system $CaCO_3$-CO_2-H_2O: *Geochim. Cosmochim. Acta, 46*, 1011-1042.

Potter, R.W., and Brown, D.L., 1977*:* The volumetric properties of aqueous sodium chloride solutions NaCl solutions from 0˚C at 500˚C up to 2000 bars based on a regression of available data in the literature. *USGS Bulletin, 1421 C,* 36 pp.

Preuss, C., 2002: *Mathematical modelling of fluid flow and heat transfer in geothermal systems. An introduction in five lectures.* UNU-GTP, Iceland, report 3, 84 pp.

Reshef, T., and Citrin, D., 2003; Review of Olkaria III geothermal project, history, present status and salient characteristics of Kenya's pioneering private geothermal project. *Proc. of 2nd KenGen Geothermal Conference, Nairobi-Kenya.*

Rimstidt, J.D. and Barnes, H.L., 1980: The kinetics of silica reactions. *Geochim. Cosmochim. Acta, 44,* 1683-1699.

Rosell, J.B., and Ramos, S.G., 1998: Origin of acid fluids in the Cawayan sector Bacman Geothermal production field*. Proc. of 23rd Workshop on Geothermal Reservoir Engineering, Stanford University, Stanford, Ca.*

Rothbaum, H.P., Anderton, B.H., Rhode, A.G., Slatter, A., 1979: Effect of silica polymerisation and pH on geothermal scaling. *Geothermics, 8,* 1-20.

Ruaya, J,R., and Seward, T.M., 1987; The ion pair constant and other thermodynamic properties of HCl up to 350˚C. *Geochim. Cosmochim. Acta, 51,* 121-130.

Saemundsson, K., and Fridleifsson, I.B., 1980: Application of geology in geothermal research in Iceland. *J. Iceland Nat. Hist., 50,* 157-188 (In Icelandic with English Summary).

Siega, F.L., Herras, E.B., and Bunig, B.C., 2005: Calcite scale inhibition: The case of Mahanadong wells in Lyete geothermal production field, Philippines. *Proc. of World Geothermal Congress 2005, Antalya, Turkey*

Simmons, S.F., and Christenson, B.W., 1993: Towards a unified theory on calcite formation in boiling geothermal systems. *Proc. of 15th New Zealand Geothermal Workshop, Auckland. 145-148*

Simmons, S.F., and Chritenson, B.W., 1994: Origins of calcite in boiling geothermal systems. *Am. J. of Sci. 294,* 361-400.

Simonson, J.M., and Palmer, D.A., 1993; Liquid-Vapour partitioning of HCl (aq) to 350 ˚C. *Geochim. Cosmochim. Acta, 57,* 1-7.

Solis, P.R., Bondc, E.L., Fragata, J.J., and See, F.S., 2000: Calcite deposition in two phase lines of Bacman Geothermal production field, Philippines. *Proc. of World Geothermal Congress 2000, Kyushu-Tohuku, Japan*.

Sugiaman, F., Sunio, E., Mollin, P. and Stimac, J., 2004: Geochemical response to production of the Tiwi geothermal field, Philippines, *Geothermics, 33, 57-86.*

Thain, I.A., Stacey,R.E., Nicholson., 1981: Zero solids condensate corrosion in steam pipes at Wairakei. *GRC, Transactions, 7, 71-73.*

Thórhallsson, S., 2005: *Personal communication.*

Thórhallsson, S., Mattíasson, J., and Kristmannsdóttir, H., 1979: *Inspection of the steam gathering systm and the turbine of the Krafla power station in June 1979 and comparison with the turbines of the Laxá and Svartsengi power plants.* Orkustofnun, Reykjavík, report OS79041/JHD19, 100 pp.

Thórhallsson, S., Ragnars, K., Arnórsson, S., and Kristmannsdóttir, H., 1975: Rapid scaling of silica in district heating systems. *Proceedings of the 2nd United Nations Symposium on the development and use of geothermal resources, San Francisco, 2,* 1445-1449.

Thórólfsson, G., 2005: Maintenance history of a geothermal plant: Svartsengi Iceland. *Proc. of World Geothermal Congress 2005, Antalya,Turkey.*

Todaka, N., Kawano,Y., Ishii, H., Iwai, N., 1995: Prediction of calcite scaling at the Oguni geothermal field, Japan. Chemical modelling approach. *Proc.of World Geothermal Congress,Florence, Italy, 2475 - 2480.*

Tomasson, J., 1971: *Analysis of drill cuttings from Reykjanes*. Orkustofnun, report, July 1971 (in Icelandic), 91 pp.

Truesdell,A.H.,1991: Origin of acid fluids in geothermal reservoirs. *GRC Transactions, 15*, 289-296.

Truesdell, A.H., and Haizlip, J.R., 1988: Hydrogen chloride in superheated steam and chloride in deep brine at the Geysers Geothermal Field, California. *Proc. of 13th Workshop on Geothermal Reservoir Engineering, Stanford, Ca,* 93-99.

Truesdell, A.H., Haizlip, J.R., Ármannsson,H., and D'Amore, F., 1989: Origin and transport of chloride in superheated geothermal steam. *Geothermics, 18, 295-304.*

Villa, R.R. Jr., and Salonga, N.D., 2000: Corrosion induced by steam condensates in Upper Mahio pipeline, Leyte, Phillipines. *Proc. of World Geothermal Congress 2000, Kyushu-Tohuku, Japan, 5,* 3335-3340.

Villa,R.R.,Jr., Alcober, E.H., Paraon, V.J.R., and Talens,M.A., 2001: Corrosion rates in different condensate lines of Leyte geothermal production field,Philipines. *Proc.of 22nd Annual PNOC.EDC Geothermal Conference, Manila, Philippines,* 239-245.

Weisberg, B.G., Browne, P.R.L., and Seward, T.M., 1979: Ore metals in active geothermal systems; In: Barnes, H.L. (ed), *Geochemistry of hydrothermal ore deposits* (2nd Edition). Wiley Interscience, 738-780.

Weres, O., and Tsao, L., 1981: Chemistry and Silica in Cerro Prieto brines. *Geothermics, 10,* 255-276.

Yakoyama T., Takahashi, Y., Yamanaka, C., Tarutani., 1989: Effect of aluminium on the polymerisation of silicic acid in aqueous solution and the deposition of silica. *Geothermics, 18,* 321-326.

Yanagase,T., Suginohara, Y., and Yanagase, K., 1970: The properties of scales and methods to prevent them. Proc. U.N. Symp. Devel. Util. Geother. Res., Pisa, *Geothermics, 2,* 1619-1623.

Zang, and Dawe, R.W., 1998: The Kinetics of calcite precipitation from high salinity water. *Appl. Geochem., 13,* 177-184.

Zarouk, S.J., 2004: External casing corrosion in New Zealand's Geothermal Fields. *Proc. of the 26th New Zealand Geothermal Workshop, Auckland.*

TABLE 1a (Karingithi, 2002): Chemical analysis of weirbox water and steam samples from selected Olkaria geothermal wells; component concentrations for water samples in mg/kg and mmoles/kg for steam sample

Well	Date of sampling	Aquifer temp. [a] °C *	GSP [b] bar-g	WHP [c] bar-g	Discharge enthalpy kJ/kg	pH at 20°C	Corrected pH	SiO_2	B	Na	K	Ca	Mg	Al	Fe	CO_2	SO_4	H_2S	Cl	F	TDS	CO_2 mmoles /kg	H_2S mmoles /kg	H_2 mmoles /kg	CH_4 mmole s/kg	N_2 mmol es/kg	O_2 mmoles /kg
OW-02	1.2001	251	4.8	5.8	1839	9.07	8.6	643	6.8	557	92	0.73	0.01	0.66	0.02	74	28	1.02	764	69	2198	101	5.61	2.94	0.722	1.94	0
OW-05	1.2001	240	4.8	5.5	2599	8.75	8.36	624	8.7	668	102	1.08	0.01	1.11	0.03	73	70	1.19	933	71	2515	101	5.61	2.33	0.111	2.28	0
OW-10	1.2001	261	4.8	6	(2531[x]) 2730	8.57	8.2	773	12.9	805	144	2.46	0.05	0.83	0.05	78	61	0.17	1190	76	3104	70.5	4.33	1	1.443	5	0
OW-11	1.2001	246	5	5.1	1894	8.94	8.49	597	5.7	497	81	0.58	0	0.7	0.02	69	21	0.34	696	64	1997	53.3	9.27	2.61	0.611	1.72	0
OW-15	1.2001	242	4.5	5	2140	9.43	9.06	576	5.9	526	83	0.56	0.01	0.79	0.02	92	54	9.89	658	57	2007	55	5.44	3.55	0.444	2.83	0
OW-16	1.2001	228	4.8	6	1534	9.37	8.57	502	4.9	503	67	0.35	0.03	0.49	0.01	97	44	7.14	586	64	1820	68.3	4.83	4.27	0.278	6.16	0
OW-19	1.2001	230	5.2	5.5	(1871[x]) 2684	9.51	8.84	548	4.6	425	54	0.49	0.04	0.91	0.02	126	57	22.1	392	70	1615	58.8	5.77	3.72	0.389	5.44	0
OW-20	1.2001	256	5.4	5.5	2541	8.98	8.77	778	14.3	610	97	0.92	0.05	0.43	0.38	110	22	1.19	822	95	2495	101	6.33	4	0.333	1.28	0
OW-26	1.2001	248	7.2	7.5	1881	9.39	8.49	657	2.2	336	51	0.24	0.04	0.93	0.25	104	24	13.6	309	68	1501	129.3	9.21	4.22	0.222	3.33	0
OW-28	2.2001	234	2.1	8	2446	9.27	8.06	625	6.2	441	61	1.33	0.01	0.86	0.12	72	104	4.59	478	50	1804	41.6	4.88	2.33	0.056	2	0
OW-29	2.2001	241	2.1	8.5	2158	8.87	8.4	609	10.1	417	63	0.75	0.03	0.67	0.06	82	30	3.91	509	84	1765	45	6.66	3.77	0.056	3.33	0
OW-30i	2.2001	260	2.1	8	2196	8.6	8.34	768	3.9	406	71	0.27	0.03	1.6	0.91	48	50	1.03	527	52	1905	55	6.61	0.39	0	2.55	0
OW-30ii	2.2001	256	2.1	8	2196	8.96	8.32	701	3.8	394	70	0.36	0.04	1.55	3.37	61	40	0.68	545	53	1843	37.2	5.94	0.5	0	3.66	0
OW-10	6.1999	242	4.5	5	2535	8.75	8.54	638	8	855	130	3.91	0.18	0.99	0.1	114	57	0.91	1080	81	2911	78.8	4.38	3.55	0.611	3.44	0.722
OW-15	6.1999	247	4.6	5.6	1899	8.69	8.66	604	8.7	709	115	1.67	0.04	0.82	0.02	72	41	2.6	1040	62	2918	57.2	5.33	3.61	0.222	3.61	0.056
OW-16	6.1999	238	4.7	5.9	1384	8.97	8.93	573	5.4	482	69	1.01	0.05	0.69	0.02	83	36	2.06	636	70	1915	61.6	6.22	3.16	0.22	1.61	0
OW-19	6.1999	254	4.6	5.3	1823	9.1	8.71	622	8.9	527	94	1.08	0.03	1.05	0.02	65	39	9.48	700	63	2089	91.6	8.6	4.94	0.389	3.67	0.111
OW-23	6.1999	242	5	6.1	2191	9.44	9.24	653	4	370	52	0.9	0.05	0.71	0.04	132	42	7.88	221	75	1485	81	7.27	5.27	0.167	2.5	0.056
OW-25	6.1999	252	4.9	6.4	2516	9.15	8.57	641	5.5	522	94	1.2	0.11	0.51	0.02	150	28	2.12	671	70	2108	78.3	5.61	4.33	0.167	2.44	0.056
OW-202	6.1999	224	1.5	5.2	1104	9.3	9.4	320	2.5	743	128	0.79	0.04	0.86	0.02	1246	75	2.38	354	53	2300	155.4	0.56	0	0.278	0.89	0.056
OW-301	6.1999	262	1.5	7.4	1653	8.67	8.57	855	6.8	1283	208	0.66	0.07	0.67	0.02	2465	112	3.96	240	105	4044	4260.1	3.55	1.05	0.833	11.3	0
OW-302	6.1999	256	1.8	5.7	1234	9.72	9.4	744	3.5	633	101	1.04	0.08	0.78	0.02	578	54	3.43	505	77	2408	367.5	1.11	0.33	0.389	3.22	0.5
OW-304D	6.1999	189	2.6	3.9	1672	8.13	8.1	364	3.3	959	74	3.48	1.73	0.52	0.14	1752	93	0.97	52	24	2451	11462	2.66	0.94	1.721	17.4	0
OW-306	6.1999	224	1.8	4	1037	9.15	9.01	551	6.3	850	96	1.2	0.08	1.38	0.09	1081	50	2.9	251	62	2410	1136.8	2.89	0.56	0.944	7.83	0
OW-709	6.1999	276	1.9	7.1	1921	9.93	9.55	649	5.1	846	218	1.41	0.04	0.89	0.02	318	73	6.54	770	28	2750	56.1	1.44	1.89	0.278	3.05	0
OW-714	6.1999	267	2.8	14.9	1303	9.54	8.98	739	3.6	557	108	0.88	0.06	1.05	0.01	135	35	8.44	682	66	2260	81	4.38	1.22	0.333	3.39	0
OW-719	6.1999	241	2.9	8	1259	9.38	8.95	588	4.8	536	81	1.09	0.04	1.51	0.02	162	83	4.46	544	46	1966	155.4	5.33	1.05	0.444	4.11	0
OW-901	6.1999	220	1.6	4.3	1854	9.8	9.57	529	2.4	506	57	0.72	0.03	0.68	0.03	566	124	18.3	280	80	1863	186.5	4.94	2.44	0.333	5.16	0.111
OW-902	6.1999	209	1	3.2	1108	9.55	9.3	477	1.5	448	41	1.31	0.05	2.12	0.08	434	100	2	212	52	1552	178.7	0.5	0.06	0.777	13.5	0.333
OW-903	6.1999	206	1.3	4	953	9.43	9.25	443	1.1	493	47	0.71	0.04	1.22	0.02	634	103	3.51	178	46	1630	278.1	1.05	0.22	0.722	19	0.666
OW-34	06 2001	273	4.14	5.6	2672	7.83		924	23.5	2411	549	0	0.015	0.843	0.51	302	77	0.24	4038	262	6780	59.64	5.58	0.04	1.66	5.44	0

TABLE 1b: Chemical analysis of water and steam samples from selected Reykjanes, Svartsengi and Nesjavellir geothermal wells.

	Reykjanes						Water Composition (ppm)														Steam (mmoles/kg)					
Well	Date of sampling	Aquifer temp. °C	GSP bar-g	WHP bar-g	Discharge enthalpy kJ/kg	pH at 20°C	SiO_2	B	Na	K	Ca	Mg	Al	Fe	CO_2	SO_4	H_2S	Cl	F	TDS	CO_2	H_2S	H_2	CH_4	N_2	O_2
RN-10	19-11-2003	290	44.8	44.8	1400	5.09	881	8.82	11275	1703	1812	1.44	0.036	2.26	70.8	12.5	5.98	22340	0.28	39090	240.55	12.147	2.9315	0.299	24.5	0
RN-11	19-09-2002	279	43.5	43.5	1320	5.3	803	8.34	10346	1480	1783	1.53	0.064	1.1	73	16.2	7.54	19800	0.22	34430	353.52	6.6176	0.1677	0.024	7.61	0
	Svartsengi						**Water Composition (ppm)**														**Steam Sample (mmoles/kg)**					
Well	Date of sampling	Aquifer temp. °C	GSP bar-g	WHP bar-g	Discharge enthalpy kJ/kg	pH at 20°C	SiO_2	B	Na	K	Ca	Mg	Al	Fe	CO_2	SO_4	H_2S	Cl	F	TDS	CO_2	H_2S	H_2	CH_4	N_2	O_2
SV-05	05/03/1988	240	14.3	14.3	1029 &	6.51	496.7	8.26	7056	1168	1051	0.48	0.301 #	0.2	33.7	29.42	0.51	13434	0.167	22100	7.2727	0.5588	0.0816	0.008	0.5	0.1015
SV-07	15-11-1988	240	15.3	15.3	1028 &	6.43	493	8.1	6615	1146	1040	0.53	0.5 #	0.05	37.2	29.31	0.58	13010	0.163	23100	54.386	1.1941	0.2229	0.021	0.62	0.0139
SV-11	21-11-1988	240	15.4	15.4	1028 &	6.32	500	8.42	6837	1152	1093	0.59	0.102 #	0.1	42.3	29.7	0.7	13530	0.148	23950	38.409	1.4618	0.1431	0.011	0.48	0.0859
SV-10	05/07/1992	240	23	23	2700	4.36	0.3	0.03	0.55	0.1	0.16	0.004		0.16	1866	1	58	0.12	0.008	9	97.79	1.27	0.41	0.03	0.38	0.01
Nesjavellir (Giroud , 2006, pers. comm.)					**Separated water composition (ppm)**																		**Steam (mmloles/kg)**			
Well	Date of sampling	Aquifer temp. °C	GSP bar-g	WHP bar-g	Discharge enthalpy kJ/kg	pH at 20°C	pH corrected	SiO_2	B	Na	K	Ca	Mg	Al	Fe	CO_2	SO_4	H_2S	Cl	F	TDS	CO_2	H_2S	H_2	CH_4	N_2	O_2
NJ-14	14-12-2000	274.5	16.1	25	1400	9.22	8.67	721	1.819	171	31.2	0.29	0.001	1.818	0.001	18.13	10.7	28.8	182.7	1.136		0.9045	0.2618	0.575	0.009	0.05	0
NJ-22	14-12-2000	295.5	15.6	34	1800	8.55	8.28	859	2.008	153	33.4	0.21	0.008	1.991	0.008	14.33	4.3	56.8	164.1	1.047		0.8886	0.9265	8.945	0.002	0.29	0
	Nesjavellir				**Waste water composition (ppm)**																					
Well	Date of sampling	Aquifer temp. °C	pH at 20°C	SiO_2	B	Na	K	Ca	Mg	Al	Fe	CO_2	SO_4	H_2S	Cl	As	W	Sb	Li	Zn	Mo	Be	Sc	Sr	Mn		
Waste water reinjec. well	14-10-2005	~ 46	8.88	783.50	2.0764	153	30.70	0.2648	0.0012	1.90	0.030	35.1		71.29	137.4	0.039	0.05	0.03	0.27	3.E-03	2.E-03	1.E-04	5E-05	2.E-03	0.002		
Retention tank	14-10-2005	~ 54	8.89	783.11	2.0721	155	30.88	0.2640	0.0026	1.88	0.011	38.8		75.47	138.6	0.048	0.04	0.03	0.28	2.E-04	3.E-03	2.E-04	8E-05	3.E-03	0.003		

\# Aluminium values estimated from wells SV-06 and SV-04 fluids from (Kristmansdottir,1989). In data made available the values were not indicated

& Enthalpy of fluids used is estimated to be close to wells SV-06 and SV-04 (from Kristmansdottir,1989) since Svartsengi fluids homogenous at a temperature of 240°C

* Aquifer temperatures recalculation are shown in Table 2 in the Appendix

** Enthalpy taken from Olkaria East production field data base

SV-10 Dry steam well

GSP: Gas Sampling Pressure

WHP : Well Head Pressure

Reykjanes and Svartsengi well data (Ármannsson, 2005 pers comm.)

Nesjavellir well data (Giroud, 2006 pers comm.)

Nesjavellir waste water data (Analysed at Geochemistry Laboratory, Institute of Earth Sciences, University of Iceland, 2005)

TABLE 2a : Calculated gas composition for a selected Olkaria East production wells

Well no.	Date of sampling	Aquifer temp. °C	GSP [b] bar-g	WHP [c] bar-g	Discharge enthalpy kJ/Kg	X at separator using well discharge enthalpy	X between separator & silencer	X (acquifer to separator + separator to silencer (CASE 1)	CO_2 mmoles/kg in total steam	H_2S moles/kg in total steam	H_2 mmoles/kg total steam	CH_4 mmoles/kg in total steam	N_2 mmoles/kg in total steam	O_2 mmoles/kg in total steam
OW-02	1.2001	251	4.8	5.8	1839	0.56	0.05	0.61	93.11	5.17	2.71	0.67	1.79	0.00
OW-05	1.2001	240	4.8	5.5	2599	0.93	0.01	0.93	100.14	5.56	2.31	0.11	2.26	0.00
OW-10	1.2001	261	4.8	6	(2531**) 2730	0.89	0.01	0.91	69.60	4.27	0.99	1.42	4.93	0.00
OW-11	1.2001	247	5	5.1	1894	0.59	0.05	0.63	49.40	8.59	2.42	0.57	1.60	0.00
OW-15	1.2001	243	4.5	5	2140	0.71	0.03	0.74	52.75	5.22	3.40	0.43	2.72	0.00
OW-16	1.2001	231	4.8	6	1534	0.42	0.06	0.48	59.25	4.19	3.70	0.24	5.34	0.00
OW-19	1.2001	230	5.2	5.5	(1871**) 2684	0.57	0.05	0.62	54.23	5.32	3.43	0.36	5.02	0.00
OW-20	1.2001	256	5.4	5.5	2541	0.89	0.01	0.91	99.64	6.24	3.95	0.33	1.26	0.00
OW-26	1.2001	248	7.2	7.5	1881	0.57	0.06	0.62	117.05	8.34	3.82	0.20	3.01	0.00
OW-28	2.2001	234	2.1	8	2446	0.87	0.01	0.88	41.19	4.83	2.31	0.06	1.98	0.00
OW-29	2.2001	241	2.1	8.5	2158	0.74	0.02	0.75	43.96	6.51	3.68	0.05	3.25	0.00
OW-30i	2.2001	260	2.1	8	2196	0.75	0.02	0.77	53.84	6.47	0.38	0.00	2.50	0.00
OW-30ii	2.2001	257	2.1	8	2196	0.75	0.02	0.77	36.42	5.81	0.49	0.00	3.59	0.00
OW-10	6.1999	242	4.5	5	2535	0.90	0.01	0.91	77.84	4.33	3.51	0.60	3.40	0.71
OW-15	6.1999	247	4.6	5.6	1899	0.59	0.04	0.64	53.35	4.97	3.37	0.21	3.37	0.05
OW-16	6.1999	238	4.7	5.9	1384	0.34	0.07	0.42	51.12	5.16	2.62	0.18	1.34	0.00
OW-19	6.1999	254	4.6	5.3	1823	0.56	0.05	0.60	84.53	7.94	4.56	0.36	3.38	0.10
OW-23	6.1999	243	5	6.1	2191	0.73	0.03	0.76	77.76	6.98	5.06	0.16	2.40	0.05
OW-25	6.1999	253	4.9	6.4	2516	0.89	0.01	0.90	77.20	5.53	4.27	0.16	2.41	0.06
OW-34	06 2001	276	4.14	5.6	2672	0.20	0.04	0.23	233.06	0.88	0.18	0.61	15.91	0.56

TABLE 2b: Calculated gas compostion for a selected exploration wells in Olkaria West, North East and Domes

Well	Date of sampling	Aquifer temp. °C	GSP [b] bar-g	WHP [c] bar-g	Discharge enthalpy kJ/Kg	X at separator using well discharge enthalpy	X at P_{atm} for 100°C using well discharge enthalpy (Case 2)	CO_2 mmoles/kg	H_2S moles/kg	H_2 mmoles/kg	CH_4 mmoles/kg	N_2 mmoles/kg	O_2 mmoles/kg
OW-202	6.1999	225	1.5	5.2	1104	0.26	0.304	133.47	0.48	0.00	0.24	0.76	0.05
OW-301	6.1999	262	1.5	7.4	1653	0.51	0.547	3991.78	3.33	0.98	0.78	10.56	0.00
OW-302	6.1999	257	1.8	5.7	1234	0.31	0.361	320.00	0.97	0.29	0.34	2.80	0.44
OW-304D	6.1999	189	2.6	3.9	1672	0.50	0.555	10423.22	2.42	0.85	1.57	15.80	0.00
OW-306	6.1999	224	1.8	4	1037	0.22	0.274	928.55	2.36	0.46	0.77	6.39	0.00
OW-709	6.1999	278	1.9	7.1	1921	0.63	0.665	53.39	1.37	1.80	0.26	2.91	0.00
OW-714	6.1999	268	2.8	14.9	1303	0.33	0.392	68.27	3.69	1.03	0.28	2.85	0.00
OW-719	6.1999	242	2.9	8	1259	0.31	0.372	128.61	4.41	0.87	0.37	3.40	0.00
OW-901	6.1999	218	1.6	4.3	1854	0.60	0.636	176.78	4.68	2.31	0.32	4.89	0.11
OW-902	6.1999	209	1	3.2	1108	0.27	0.305	160.57	0.45	0.05	0.70	12.17	0.30
OW-903	6.1999	207	1.3	4	953	0.20	0.237	229.82	0.87	0.18	0.60	15.69	0.55

TABLE 3: Calculated aquifer temperatures from tqtz and tNaK geothermometry for selected well fluids from Olkaria, Reykjanes, Svartsengi and Nesjavellir.

Well no.	OW-02	OW-05	OW-10	OW-11	OW-15	OW-16	OW-19	OW-20	OW-26	OW-28	OW-29	OW-30i	OW-30ii	OW-10	OW-15	OW-16	OW-19	OW-23	OW-25
Date	1.2001	1.2001	1.2001	1.2001	1.2001	1.2001	1.2001	1.2001	2.2001	2.2001	2.2001	2.2001	2.2001	6.1999	6.1999	6.1999	6.1999	6.1999	6.1999
Field	OE	OE	OE	OE	OE	OE	OE	OE	OE	OE	OE	OE	OE	OE	OE	OE	OE	OE	OE
Enthalpy kJ/kg	1839	2599	2531	1894	2140	1534	1871	2541	1881	2446	2158	2196	2196	2535	1889	1384	1853	2191	2516
pH at $T_{aquifer}$	6.74	6.526	6.745	6.807	6.968	6.895	7.121	6.825	6.863	7.105	6.937	6.668	6.984	6.775	6.793	6.927	6.781	6.886	7.014
t qtz	250	236	260.2	242	238	228	234	262	252	235	240	262	253	241	244	240	247	250	244
t Na/K	251	242	259.6	250	246	228	224	247	243	231	242	257	260	242	249	236	260	234	262
Mean	251	239	259.9	246	242	228	229	255	248	233	241	260	256	241	246	238	253	242	253
Diff	2	6	-0.6	8	8	0	-11	-15	-9	-3	2	-4	7	1	5	-4	13	-16	18

Well no.	OW-34	OW-202	OW-301	OW-302	OW-304	OW-306	OW-709	OW-714	OW-719	OW-901	OW-902	OW-903	SV-05	SV-07	SV-11	RN-10	RN-11	NJ-14	NJ-22
Date	6.1999	6.1999	6.1999	6.1999	6.1999	6.1999	6.1999	6.1999	6.1999	6.1999	6.1999	6.1999							
Field	OE	OC	OW	OW	OW	OW	ONE	ONE	ONE	OD	OD	OD	SV	SV	SV	RN	RN	NJ	NJ
Enthalpy kJ/kg	2672	1104	1653	1234	1674	1037	1921	1303	1259	1854	1108	953	1029	1038	1028	1400	1320	1400	1800
pH at $T_{aquifer}$	6.61	7.331	6.251	6.785	5.932	6.303	7.637	6.932	6.582	7.145	6.893	6.731	5.553	5.321	5.171	4.826	4.757	7.021	6.779
t qtz	256	193	275	264	200	236	245	263	241	227	223	218	246	246	248	327	315	286	287
t Na/K	289	256	247	248	178	212	309	271	241	212	193	193	256	260	249	247	240	264	286
Mean	272	224	261	256	189	224	277	267	241	220	208	205	251	253	248	287	278	275	286
Diff	33	63	-28	-16	-21	-24	64	8	0	-16	-30	-25	9	14	1	-81	-75	-22	-0.5

OE = Olkaria East
ONE = Olkaria North East
OD = Olkaria Domes
OW = Olkaria West
SV= Svartsengi
RN= Reykjanes
NJ = Nesjavellir

TABLE 4: pH, temperature (°C), chloride, HCl and PCO_2 at aquifer for Olkaria, Reykjanes, Svartsengi and Nesjavellir

Well no.	OW-02	OW-05	OW-10	OW-11	OW-15	OW-16	OW-19	OW-20	OW-23	OW-25	OW-26	OW-28	OW-29	OW-30i	OW-30ii	OW-10	OW-15	OW-16
Date of sampl.	1.2001	1.2001	1.2001	1.2001	1.2001	1.2001	1.2001	1.2001	1.2001	1.2001	1.2001	1.2001	1.2001	6.1999	6.1999	6.1999	6.1999	6.1999
Temperature °C	251	240	261	247	243	231	230	256	243	253	248	234	241	260	257	242	247	238
pH	6.738	6.53	6.742	6.845	7.194	7.149	7.173	6.831	7.107	7.02	6.866	7.116	6.941	6.545	6.99	6.778	6.794	6.836
Cl	527.14	596.51	735.63	486.73	466.82	456.52	288.99	536.69	157.32	439.98	217.92	307.39	347.31	336.79	351.99	703.11	722.59	460.98
HClaq	2.42E-04	3.15E-04	4.67E-04	1.55E-04	5.80E-05	4.40E-05	2.67E-05	2.34E-04	2.49E-05	1.13E-04	7.12E-05	3.59E-05	7.47E-05	3.54E-04	1.18E-04	2.15E-04	2.50E-04	1.13E-04
P_{CO2} partial pressure bar-a	1.66	1.56	1.30	0.87	0.77	0.74	0.59	1.75	1.23	1.27	1.91	0.485	0.65	1.06	0.64	1.18	0.89	0.759

Well no.	OW-19	OW-301	OW-302	OW-304D	OW-306	OW-709	OW-714	OW-719	OW-901	OW-902	OW-903	OW-202	OW-34	RN-10	RN-11	SG-05	SG-07	SG-11
Date of sampl.	6.1999	6.1999	6.1999	6.1999	6.1999	6.1999	6.1999	6.1999	6.1999	6.1999	6.1999	6.1999	6 1999	2003	2002	5.1988	5.1988	5.1988
Temperature °C	254	262	257	189	224	278	268	242	218	209	207	225	276	290	279	240	240	240
pH	6.852	6.549	6.804	5.967	6.32	7.751	7.17	7.15	7.22	6.961	6.835	7.331	7.136	5.113	5.287	5.549	5.314	5.163
Cl	478.04	151.95	346.44	40.82	187.14	466.71	439.65	383.74	201.84	164.94	139.84	266.75	1853.77	15707.9	18481.7	11242.4	10996.9	11600.7
HClaq	1.90E-04	1.45E-04	1.63E-04	2.26E-05	9.62E-05	5.77E-05	1.45E-04	5.13E-05	1.17E-05	1.45E-05	1.56E-05	1.34E-05	7.82E-04	8.09E-01	3.16E-01	3.31E-02	5.61E-02	8.27E-02
P_{CO2} partial pressure bar-a	1.55	96.90	9.05	41.60	23.40	1.00	1.93	3.07	1.97	2.21	4.25	2.64	4.88	6.11E-01	5.00E-01	5.93E-01	1.09E+00	1.49E+00

Well no.	NJ-14	NJ-22
Date of sampl.	14.12.2000	14.12.2000
Temperature °C	276	286
pH	7.546	7.494
Cl	150.2	128.27
HClaq	3.31E-05	5.22E-05
P_{CO2} partial pressure bar-a	9.24E-02	6.62E-02

OW = Olkaria Wells
RN = Reykjanes Wells
SV = Svartsengi Wells
NJ = Nesjavellir Wells

TABLE 5: HCl in vapour at pressures at the wellhead for selected wells in Olkaria, Reykjanes, Svartsengi and Nesjavellir

Well no.	Field/sector	WHP bar-g	Temp °C	pH	Cl (ppm)	HCl in vapour (ppm)
OW-901	Olkaria Domes	4.3	154	8.617	234.28	2.86E-08
OW-301	Olkaria West	7.4	173	7.704	195.36	4.43E-07
OW-306	Olkaria West	4	151	8.061	222.7	8.17E-08
OW-20	Olkaria East	5.5	162	7.928	672.53	5.84E-07
OW-30	Olkaria East	8	176	7.402	421.13	2.55E-06
OW-34	Olkaria East	5.6	163	7.768	2563.01	2.93E-06
OW-709	Olkaria North East	7.1	171	8.553	612.73	1.91E-07
OW-714	Olkaria North East	14.2	201	7.857	534.8	4.07E-06
RN-11	Reykjanes	43.5	257	5.534	17483.5	0.19117
RN-10	Reykjanes	44.8	259	5.339	19538.57	0.6507
SV-05	Svartsengi	14.3	199	6.66	12759.08	0.000617
SV-11	Svartsengi	15.4	203	6.397	13022.57	0.001477
NJ-14	Nesjavellir	25	222	7.607	174.02	5.04E-06
NJ-22	Nesjavellir	34	243	7.488	146.79	1.02E-05

TABLE 6: Chemical composition of scales analysis by the ICP; leaching was done by dissolving a weighed amount of scale in 20 mls 0.16 N HNO_3

Olkaria	Si mg/kg	Na mg/kg	K mg/kg	Ca mg/kg	Mg mg/kg	Fe mg/kg	Al mg/kg	Sr mg/kg	Mn mg/kg	Ti mg/kg	S mg/kg	P mg/kg	As mg/kg	W mg/kg		Scale sample taken, weight mg
Metals-kizito	<0.050	0.03041	0.03052	0.01082	0.00026	1.98903	9.59893	0.00009	<0.001	<0.005	0.03221	2.03815	> 1.98242	0.07507		
OW-34 Scale #1	2.25413	0.31137	0.53138	0.52577	0.10981	3.84641	0.51213	0.00233	0.03799	0.01724	1.34079	0.07564	0.01335	0.47946		105.98
OW-34 Scale #2	1.08255	0.50772	0.63772	0.54694	0.10084	3.2382	2.40753	0.0041	0.04433	0.03143	3.55665	0.05	0.02	0.00695		105.56
OW-34 Scale #3	4.87522	1.1954	0.41043	7.16433	0.47752	1.17545	0.64725	0.0437	0.03457	0.03663	0.44775	0.13449	0.01883	0.00954		105.66
OW-34 Scale #4	0.28968	0.1613	0.24245	0.09391	0.02533	0.69926	0.07223	0.00037	0.00877	0.00144	0.58065	0.01182	0.02	<0.020		106.33
OW-34 Scale #5	26.8955	13.7645	5.53104	7.27349	3.66575	18.4867	6.5851	0.04551	0.26992	0.11612	2.45096	0.14368	1.69483	0.28684		105.48
	Cr mg/kg	Ba mg/kg	Be mg/kg	Sb mg/kg	V mg/kg	Li mg/kg	Mo mg/kg	Cl mg/kg	Br mg/kg	B mg/kg	Co ppm	Zn ppm	Cu ppm	Pb ppm	Ni ppm	
Metals-kizito	<0.005	0.00026	0.00028	<0.050	<0.01	0.00049	<0.01	0.10889	0.02391	0.00732	2.01429	2.02226	1.97034	1.94198	2.01966	
OW-34 Scale #1	0.00224	0.00332	0.00044	<0.050	<0.01	0.00286	0.00897	0.29256	0.07918	0.01824	0.00317	20.5791	0.01453	<0.05	0.02754	105.98
OW-34 Scale #2	0.01144	0.00368	0.00044	<0.050	<0.01	0.00074	0.01055	0.37612	0.09614	0.01714	< 0.005	0.25631	0.01176	<0.05	0.00872	105.56
OW-34 Scale #3	0.005	0.00274	0.01431	<0.050	<0.01	0.00285	0.01423	1.26469	0.05805	0.01249	< 0.005	0.18077	0.00212	<0.05	0.01573	105.66
OW-34 Scale #4	0.005	0.00055	0.00018	<0.050	<0.01	<0.01	0.00492	0.2091	0.22054	0.0035	< 0.005	0.11921	0.00405	<0.05	0.00523	106.33
OW-34 Scale #5	0.05876	0.02069	0.00286	0.90249	0.00824	0.02854	2.32773	2.76244	0.04518	0.0936	0.01002	0.09204	0.05045	<0.05	0.05307	105.48

Nesjavellir scale samples	Si mg/kg	Na mg/kg	K mg/kg	Ca mg/kg	Mg mg/kg	Fe mg/kg	Al mg/kg	Sr mg/kg	Mn mg/kg	Ti mg/kg	S mg/kg	P mg/kg	As mg/kg	W mg/kg		Scale sample taken, weight mg
Coupon # 5 retention tank	8.20388	0.47784	0.35208	1.72217	> 1.27301	> 4.77150	2.90544	0.00671	0.14385	0.04297	0.59565	0.0808	0.29014	<0.020		27.26
Coupon # 16 after heat exchangers	1.21542	0.62053	0.52485	0.31304	0.0461	0.43717	0.18491	0.00098	0.02155	<0.005	0.28553	< 0.01095	0.00648	0.01229		24.27
Coupon # 17 retention tank	1.25478	0.27544	0.24439	0.22991	0.13637	0.84432	0.29171	0.00086	0.02566	<0.005	0.20825	0.03055	<0.020	<0.020		19.27
Coupon # 18 retention tank	6.14523	0.41488	0.36473	1.36699	> 0.96903	> 3.92720	2.17641	0.00499	0.15807	0.02553	0.48217	0.05953	<0.020	<0.020		6.75
Standards																
Metals-kizito	<0.050	< 0.020	0.0385	0.01042	0.0003	1.93728	9.35238	0.0001	<0.001	<0.005	0.01185	1.98718	> 1.91694	0.04535		
Trace element stock	<0.050	< 0.020	< 0.1	0.00133	< 0.001	0.00123	<0.001	0.0002	0.0009	<0.005	0.09603	< 0.050	> 4.87004	4.75005		
Spói-05	99.241	231.815	33.2469	3.85482	0.59855	1.17345	1.92521	1.16465	0.41397	0.35967	89.618	0.51714	0.52071	0.02523		
	Cr mg/kg	Ba mg/kg	Be mg/kg	Sb mg/kg	V mg/kg	Li mg/kg	Mo mg/kg	Cl mg/kg	Br mg/kg	B mg/kg	Co mg/kg	Zn mg/kg	Cu mg/kg	Pb mg/kg	Ni mg/kg	
Coupon # 5 retention tank	0.03593	0.00254	<0.001	<0.050	<0.01	<0.01	<0.01	0.13329	0.10126	0.02344	0.0171	0.17886	0.0442	<0.05	19.5238	27.26
Coupon # 16 after heat exchangers	0.01324	0.0022	<0.001	<0.050	<0.01	<0.01	<0.01	0.31089	0.09456	0.00845	0.00983	0.41985	0.02747	<0.05	7.42167	24.27
Coupon # 17 retention tank	0.01243	0.05329	<0.001	<0.050	<0.01	<0.01	<0.01	<0.001	0.07168	0.0068	< 0.005	0.09024	0.02564	<0.05	2.22503	19.27
Coupon # 18 retention tank	0.04194	0.00224	<0.001	<0.050	0.00533	<0.01	<0.01	<0.001	0.33727	0.02002	0.02426	0.27722	0.04276	<0.05	28.0419	6.75
Standards																
Metals-kizito	<0.005	0.00014	<0.001	<0.050	<0.01	<0.01	<0.01	<0.001	0.03333	0.00478	1.9367	1.95489	1.8971	1.89333	1.9612	
Trace element stock	2.43115	4.84231	2.42464	2.45018	4.80181	<0.01	<0.01	0.10706	<0.1	<0.001	0.00902	< 0.002	0.00481	<0.05	<0.020	
Spói-05	<0.005	0.00268	0.17696	<0.050	<0.01	0.98704	0.49182	115.624	1.99594	3.11916	< 0.005	< 0.002	0.00047	<0.05	<0.020	

TABLE 7: Silica as a scales% analysed in the UV after dissolving in 0.5mls HF + 4.5 mls distilled water and diluting to 100 mls + % silica from ICP

Samples	Conc.	Scale sample weights taken (mg)	% Silica (SiO_2)	% Silica analysed from the ICP	Total Silica in scales
OW-34 #1	42.235	105.98	39.85	0.043	39.895
OW-34 #2	59.471	105.56	56.34	0.021	56.359
OW-34 #3	90.882	105.66	86.014	0.092	86.106
OW-34 #4	55.941	106.33	52.611	0.005	52.616
OW-35# 5	51.294	105.48	48.629	0.510	49.139
cpn # 16	12.647	24.27	52.110	0.602	52.712
cpn # 5	11.588	27.26	42.5100	0.100	42.610
cpn # 18	6.000	19.27	31.136	0.13	31.267
cpn # 17	1.471	6.75	21.786	1.821	23.607

TABLE 8a: Coupon weight changes, change in scale thickness and coupon dimensions

Date of insertion	Sample location	Coupon #	Weight before test	Weight after test	Change in weight	Duration of test	Thickness before test mm	Thickness after test mm	Scale thickness mm	Length mm	Width mm	Area of coupon mm2	Average thickness mm
13/07/2005	Well No 14	10	13.369	13.3755	0.0065	13/07/2005 -14/10/2005	1.997	2.021	0.024	44.55	20.5	913.275	0.012
13/07/2005	Well No 22	25	13.3791	13.386	0.00688	13/07/2005 -14/10/2005	1.998	2.023	0.0253	44.75	20.45	915.138	0.0127
07/06/2005	Heat exchangers	16	13.6349	13.6815	0.04658	13/07/2005 -14/10/2005	2.040	2.099	0.0591	44.5	20.35	905.575	0.0295
07/06/2005	Retention tank entry	17	13.4525	13.5097	0.05718	06/07/2005 -14/10/2005	2.026	2.112	0.0856	44.45	20.5	911.225	0.0428
07/06/2005	Retention tank entry	18	13.2152	13.49689	0.281668	06/07/2005-30/01/2006	1.985	2.27625	0.2913	44.7	20.5	916.35	0.146
07/06/2005	Reinjection well	19	13.4323	13.4465	0.01418	06/07/2005-30/01/2006	2.0123	2.0310	0.0187	44.45	20.5	911.225	0.0078
07/06/2005	Reinjection well	20	13.5042	13.5142	0.00998	06/07/2005 -14/10/2005	2.007	2.022	0.0157	44.6	20.45	912.07	0.0093

TABLE 8b: Caliberation of balances with coupons

	Coupon # 24	Coupon # 24	Coupon # 22	Coupon # 3	Mean	Coupon # 10	Coupon # 25	Coupon # 16	Coupon # 17	Coupon # 18	Coupon # 5	Coupon # 19	Coupon # 20
ISOR Balance (mg)	14002	14001.9	13739.7	13847.7		13393.478	13403.6	13659.4	13477	13239.7	13387	13456.8	13528.7
ASKJA Balance (mg)	13977.21	13977.21	13715.6	13823.36		13369.0	13379.1	13634.9	13452.5	13215.2	13362.5	13432.3	13504.2
Diff (mg)	24.79	24.69	24.09	24.34	24.478								

TABLE 9a: Output of well OW-34 under different throttle conditions (Opondo and Ofwona, 2003)

Pipe size (inch)	WHP (bar-a)	Total mass (t/hr)	Steam (t/hr)	Enthalpy (kJ/kg)	X at 100°C
8	3.28	40.45	38.9	2669	0.9969
6	5.25	29.2	28	2672	0.9982
5	6.65	31.7	30.1	2643	0.9854
4	9.83	25.05	24.2	2675	0.9996
	1996				
Pipe size (inch)	**WHP (bar-a)**	**Total mass (t/hr)**	**Steam (t/hr)**	**Enthalpy (kJ/kg)**	**X at 100°C**
5	8.45	55.3	53.2	2670	0.9973
3	19.83	44	42.5	2673	0.9987
	2003				
Pipe size (inch)	**WHP (bar-a)**	**Total mass (t/hr)**	**Steam (t/hr)**	**Enthalpy (kJ/kg)**	**X at 100°C**
8	4.32	47.4	45.6	2673	0.9987
6	6.1	52.1	50.2	2675	0.9996
5	8.45	55.3	53.2	2670	0.9973
4	12.87	51.3	49.4	2673	0.9987
3	19.83	44	42.5	2673	0.9987

X = Steam fraction WHP = Wellhead Pressure

TABLE 9b: Output for well OW-34 between July 2001 and July 2002

Year	Steam (t/hr)	Water (t/hr)	Mass (t/hr)
2001 July	43.15	0.3	43.45
2001 Sept	37.4	0.8	38.2
2002 mar	7.2	0.2	7.4
2002 July	7.35	0	7.35

TABLE 10: Water composition of well OW-34 fluids, make up wells and wells affected most by boiling (sampled 2000 and 2001)

Well no.	WHP bar-g	SSP bar-g	Enth. kJ/kg	pH at 20°C	SiO_2	B	Na	K	Ca	Mg	Al	Fe	CO_2	SO_4	H_2S	Cl	F
OW-34	5.6	5.6	2672	7.83	924	9.6	2411	715	0	0.02	0.843	0.51	302	77	0.24	4038	262
OW-18	7	5.3	2625	8.75	650	4.8	603	111	0	0	-	-	35	62	0.5	994	89
OW-10	6	4.8	2531	8.57	773	12.9	805	144	2.46	0.05	0.83	0.05	78	61	0.17	1190	76
OW-32	6.5	6.2	2332	8.76	769	0.8	572	138	0	0	-	-	72	56	0.68	849	82
OW-33	5.5	2.07	2418	7.84	825	7.7	715	129	0	0	-	-	90	105	0.95	1031	73

APPENDIX B: Methods for cleaning coupons and studying scales

Cleaning method for the stainless steels coupons used in scaling/corrosion tests

1. The coupons were cleaned using an abrasive paper (silicon carbide) to remove surface oxide film and to condition the surface. A smooth surface does not yield a representative result.
2. Marked coupons are washed carefully, first in hot distilled water and then in cold distilled water.
3. This was rewashed in acetone/isopropyl alcohol.
4. The coupons were dried in an oven at 105°C.
5. These were cooled and stored in a dessicator until weighing.
6. Weigh the coupons, put them back in the dessicator and reweigh to constant weight.

Stereo Binocular Microscope analysis

Binocular microscope analyses of test coupons from Nesjavellir were done using the Wild Heerbrugg binocular microscope. Coupons were placed on the mounting stage of the binocular microscope and among the features noted were colours, size of scale, adherence properties of the scale.

Infrared spectroscopy

The spectra in the IR were obtained in absorbance mode from the KBR pellets with a Brucker IFS 66 FTIR spectrometer. Pellets prepared by weighing about 2 mg samples or less in some instances and these were prepared in ~200 mg of Potassium Bromide (KBr). Resolution in the FTIR was 4 cm^{-1}, 100 scans were taken using Mertz phase correction and Blackman-Harris 3 term apodization function with zerofilling of two.

X-Ray diffraction analysis.

X-ray diffractometer is used to identify individual minerals especially clays and zeolites. Scale samples were prepared to < 4 microns by use of a mechanical shaker. A Brucker series D8 FOCUS diffractometer was used, with CuKά radiation (at 40 kvand 50 mA), automatic divergence slit, fine receiving slit, and graphite monochromator. Count data were collected from 2˚ -14 ˚ at intervals of 0.02˚, 2 θ for a time of 1 second.

Scanning Electron Microscope (SEM)

A type LEO SUPRA 25 Scanning Electron Microscope where the scanning conditions were 20 kv accelerating voltage and scan rates of 100 μm. Scale samples were coated with gold before being placed in the SEM. The SEM is equipped with an energy dispersive spectrometer (EDS) that was used to do several EDS spot analyses on the scale samples. The EDS analyses are semi-quantitative i.e they do not quantify the concentrations of elements, but give an idea of what elements could be present in the scale samples.

Inductively Coupled Plasma (ICP)

Weighed scale samples were leached in 20 mls of 0.16 HNO_3 and filtered. The solutions were run in a multi-element analysis in the ICP SPECTRO AS 500.

TABLE 1: SEM elemental analysis of scales as % elements and as % oxides and sulphide

			O	Na	Al	Si	Cl	K	Cu	Total
Coupon # 16 a	After heat exchanger	Spectrum 1	51.250		0.530	47.510	0.120	0.280	0.310	100
		Spectrum 2	52.840		0.470	46.060		0.240	0.380	100
		Spectrum 3	65.050	0.220	0.340	34.260		0.130		100
				Na_2O	Al_2O_3	SiO_2		K_2O	CuO	
				1.35	1.889	2.139	0	1.205	1.252	
				0	1.001	101.640	0	0.337	0.388	
				0	0.888	98.538	0	0.289	0.476	
				0.297	0.642	73.294	0	0.157	0	
			O	Al	Si	K	Total			
Coupon # 16 b		Spectrum 1	49.35	0.66	49.7	0.29	100			
				Al_2O_3	SiO_2	K_2O				
				1.889	2.139	1.205				
				1.247	106.325	0.349				

			O	Al	Si	S	K	Ca		Cu	Total						
Coupon # 18 a	Reinjection well	Spectrum 1	52.67	0.78	44.25	0.66	0.3	0.11		0.48	100						
			Al_2O_3	SiO_2	K_2O	CaO	Fe_2O_3	CuO	FeS	FeS_2	Fe_3S_4	CuS					
		Oxide & Sulphide ratios	1.889	2.139	1.205	1.399	1.430	1.252	1.574	2.148	1.765	1.505					
Coupon # 18 b		Spec 1 (% Oxides & Sulphides)	1.474	94.666	0.3614	0.1539	1.0723	0.601	1.181	1.611	1.324	0.722					
			O	Na	Al	Si	S	K		Ti	Cr	Fe	Cu	Zn	Mo	Total	
		Spectrum 1	56.890	0.210	0.640	41.180		0.230				0.26			0.58	100	
		Spectrum 2	57.510	0.240	0.590	37.510	1.060	0.140		0.200	0.230	1.920		0.51		100	
		Spectrum 3	53.290	0.280	0.730	42.940	0.880	0.330				1.17	0.38			100	
			Na_2O	Al_2O_3	SiO_2	K_2O	CaO	Cr_2O_3	Fe_2O_3	CuO	ZnO	FeS	FeS_2	Fe_3S_4	CuS	ZnS	PbS
		Oxide & Sulphide ratios	1.348	1.889	2.139	1.205	1.399	1.462	1.430	1.252	1.245	1.574	2.148	1.765	1.505	1.490	1.155
		Spec 1 (% Oxides & Sulphides)	0.283	1.209	88.098	0.277	0	0	0.372	0	0	0.409	0.559	0.459	0	0	
		Spec 2 (% Oxides & Sulphides)	0.324	1.115	80.246	0.169	0.126	0.336	2.745	0	0.635	3.022	4.124	3.390	0	0.7601	
		Spec 3 (% Oxides & Sulphides)	0.377	1.379	91.863	0.398	0	0	1.673	0.476	0	1.842	2.513	0.537	0.572	0.760	102.390

			O	Na	Al	Si	S	K		Cu	As	Total			
Coupon # 5	Retention tank	Spectrum 1	54.55			44.06				0.24	0.78	100			
		Spectrum 2	50.57	0.15	0.17	46.13	0.5	0.1		0.32	1.1	100			
		Spectrum 3	54.58			43.85				0.4	0.96	100			
			Na_2O	Al_2O_3	SiO_2	K_2O	Fe_2O_3	CuO	As_2O_3	FeS	FeS_2	Fe_3S_4	CuS	ZnS	As_2S_3
		Oxide and sulphide ratio	1.348	1.889	2.139	1.205	1.430	1.252	1.320	1.574	2.148	1.765	1.257	1.490	1.642
		Specl (% Oxides & Sulphides)	0	0	94.259	0.446	0.343	1.377	1.030	0.582	0.795	0.653	0.302	0	1.281
		Spec 2 (% Oxides and Sulphides)	0.202	0.321	98.688	1.168	0	0	1.452	1.527	0.294	1.712	0.402	0	1.806
		Spec 3 (% Oxides & Sulphides)	0	0	93.810	0.089	0	0	0	0.315	0.059	0.342	0.503	0	1.576
			O	Al	Si	K	Fe	Cu		Total					
Coupon # 5 b	Rentention tank	Spectrum 1	56.59	0.16	42.92			0.33		100					
		Spectrum 2	61.74		37.22	0.07	0.21	0.24		100					
			Al_2O_3	SiO_2	K_2O	Fe_2O_3	CuO	As_2O_3							
		Oxide ratio	1.889	2.139	1.205	1.430	1.252	1.320							
		% oxides	0	0	113.545	0.637	0.430	1.818							
		% oxides	0.382	0.687	118.880	1.671	0	0							

			O	Si	S	Cr	Mn	Fe		Total							
Coupon # 5c	Retention Tank	Spectrum 1	2.06	0.82	0.43	17.72	1.55	68.77		100							
			SiO_2	Cr_2O_3	MnO	Fe_2O_3	NiO	FeS	FeS_2	Fe_3S_4	NiS						
		Oxide and sulphide ratio	2.139	1.462	1.291	1.430	1.291	1.574	2.148	1.765	1.546						
		spec 1 (% oxides & sulphides)	1.754	25.899	2.001	98.322	11.156	108.249	147.727	121.408	2.397						
			O	Na	Mg	Al	Si	Ca		Cr	Fe	Cu	Hg	Total			
Coupon # 5 fine	Retention tank	Spectrum 1	35.02				63.61				0.7	0.67		100			
		Spectrum 2	63.07	0.19	0.43	0.78	32.3	0.37		0.28	1.89	0.2	0.39	100			
			Na_2O	MgO	Al_2O_3	SiO_2	CaO	Cr_2O_3	Fe_2O_3	CuO							
		Oxide ratio	1.348	1.665	1.889	2.139	1.399	1.462	1.430	1.252							
		spec 1 (% oxides)	0.000	0.000	0.000	136.083	0.000	0.000	1.001	0.839							
		spec 2 (% oxides)	0.256	0.716	1.474	69.101	0.518	0.409	2.702	0.250							
			O	Si	Cr	Mn	Fe	Ni									
Coupon # 5 fine b	Retention tank	Spectrum 1	54.66	45.06			0.28										
		Spectrum 2	5.77	11.66	15.7	1.29	59	6.59									
			SiO_2	Cr_2O_3	MnO	Fe_2O_3	NiO										
		Oxide ratio	2.139	1.462	1.291	1.430	1.273										
		spec 1 (% oxides)	96.398	0.000	0.000	0.400	0.000										
		spec 2 (% oxides)	24.945	22.946	1.666	84.354	8.386										
			O	Mg	Al	Si	S	K		Ti	Fe	Cu	Ag	Te	Total		
Coupon # 17	Retention tank	Spectrum 1	44.81		0.8	49.07	1	0.47			1.25	0.87	0.81	0.91	100		
		Spectrum 2	54.66	0.23	0.76	28.71	5.8	0.12		0.15	8.85	0.44			100		
		Spectrum 3	50.82		0.77	46.97	0.49	0.43			0.54				100		
			MgO	Al_2O_3	SiO_2	K_2O	CaO	Fe_2O_3	CuO	FeS	FeS_2	Fe_3S_4	CuS	Ag_2S			
		Oxide & sulphide ratio	1.665	1.889	2.139	1.205	1.399	1.430	1.252	1.574	2.148	1.765	1.213	1.297			
		spec 1 (% Oxides & sulphides)	0.000	1.512	104.977	0.566	0.000	1.787	1.089	1.968	2.685	2.207	1.056	1.051			
		spec 2 (% Oxides & sulphides)	0.000	1.436	61.420	0.145	0.392	12.653	0.551	13.931	19.011	15.624	0.534	0.000			
		spec 3 (% Oxides & sulphides)	1.282	1.455	100.485	0.518	0.000	0.772	0.000	0.850	1.160	0.953		0.000			
			O	Na	Al	Si	K	Cu									
Coupon # 17 b	Retention tank	Spectrum 1	51.23	0.14	0.63	47.4	0.32	0.28									
			Na_2O	Al_2O_3	SiO_2	K_2O	CuO										
		Oxide ratio	1.348	1.889	2.139	1.205	1.252										
		spec 1 (% oxides)	0.189	1.190	101.404	0.337	0.350										
			O	Na	Al	Si	S	K		Cu	Total						
Coupon # 17 b 2	Retention tank	Spectrum 1	28.85	0.21	0.32	8.62	27.08	0.13		0.35	100						
			Na_2O	Al_2O_3	SiO_2	SO_3	K_2O	Fe_2O_3	CuO	FeS	FeS_2	Fe_3S_4	CuS	ZnS			
		Oxide & sulphide ratio	1.348	1.889	2.139	2.497	1.205	1.430	1.252	1.574	2.148	1.765	1.465	1.490			
		spec 1(% Oxides & sulphides)	0.283	0.605	18.441	67.622	0.157	49.226	0.438	54.195	73.960	60.784	0.513				
			O	Al	Si	S	Cl	K		Mn	Fe	Ni	Cu	Zn	Ag	Total	
Coupon # 19	Reinjection well	Spectrum 1	47.79	0.15	46.59		0.16	0.14			0.42		1.3		3.44	100	
		Spectrum 2	21.69		21.19	0.99				0.68	37.94	4.82	1.23	0.53	1.4	100	
			Al_2O_3	SiO_2	Cr_2O_3	MnO	Fe_2O_3	NiO	CuO	ZnO	FeS	FeS_2	Fe_3S_4	CuS	ZnS	NiS	
		Oxide & sulphide ratio	1.889	2.139	1.462	1.291	1.430	1.273	1.252	1.245	1.574	2.148	1.765	1.465	1.490	1.546	
		spec1 (% Oxides & sulphides)	0.283	99.672	0	0	0.600	0	1.627	0	0.661	0.902	0.741	1.905	0	0	
		spec 2 (% Oxides & sulphides)	0	45.333	13.914	0.878	54.244	6.134	1.540	0.660	59.720	81.500	66.980	1.802	0.790	7.453	
			O	Si	Cr	Mn	Fe	Ni		Total							
Coupon # 19 b	Reinjection well	Spectrum 1	8.49	5.22	23	2.53	58.45	1.08		100							
			SiO_2	Cr_2O_3	MnO	Fe_2O_3	NiO	CuO									
		Oxide & sulphide ratio	2.139	1.462	1.291	1.430	0.969	1.252									
		spec 1(% Oxides & sulphides)	11.167	33.616	3.267	83.568	1.047	1.552									

Coupon # 20	Reinjection well		O	Na	Mg	Al	Si	Cl		Ca	Cu	Total
		Spectrum 1	51.85			0.18	47.96					100
			66.22	0.55	0.14	0.17	15.34	0.54		16.45	0.23	100
				Na_2O	MgO	Al_2O_3	SiO_2		K_2O	CaO	CuO	
		Oxide & sulphide ratio		1.348	1.665	1.889	2.139		1.205	1.399	1.252	
		spec 1 (% Oxides & sulphides)		0.000	0.000	0.340	102.603	0.000	0.000	0.000	0.000	
		spec 2(% Oxides & sulphides)		0.741	0.233	0.321	32.817	0.000	0.434	23.017	0.288	

Coupon # 20 b	Reinjection well		O	P	S	Cl	K	Ca		Total
		Spectrum 1	27.49	21.51	11.24	4.45	4.3	3.35		100
			P_2O_5	K_2O	CaO	ZnO	ZnS			
		Oxide & sulphide ratio	2.290	1.205	1.430	1.245	1.490			
		spec 1 (% Oxides & sulphides)	49.264	5.180	4.790	34.441	41.238			

			O	Na	Mg	Al	Si	S	Cl	K	Ca	V	Cr	Mn	Fe	Ni	Cu	Zn	Total		
Coupon # 25	Well NJ-25	Spectrum 1	32.44	0.54	0.84	5.66	16.59	1.56	0.15	0.22	2.04	0.43	1.13	0.42	35.64	0.33	0.54	1.46	100		
		Spectrum 2	36.41		0.91	5.19	15.04	2.52	0.46	0.26	1.75	0.31	0.83	0.35	31.34	0.51	0.37	3.75	100		
			Na_2O	MgO	Al_2O_3	SiO_2	K_2O	CaO	V_2O_5	Cr_2O_3	MnO	Fe_2O_3	NiO	CuO	ZnO	FeS	FeS_2	Fe_3S_4	CuS	ZnS	NiS
		Oxide & sulphide ratio	1.348	1.665	1.889	2.139	1.205	1.399	1.785	1.462	1.291	1.430	1.273	1.252	1.245	1.574	2.148	1.765	1.465	1.490	1.546
		spec 1 (% Oxides & sulphides)	0.728	1.399	10.694	35.492	0.265	2.854	0.768	1.652	0.542	50.956	0.420	0.676	1.817	56.100	76.560	#####	0.791	2.176	0.510
		spec 2 (% Oxides & sulphides)	0.000	1.515	9.806	32.176	0.313	2.449	0.553	1.213	0.452	44.808	0.649	0.463	4.668	49.331	67.323	#####	0.542	5.589	0.789

			O	Na	Mg	Al	Si	S	Cl	K	Ca	V	Cr	Mn	Fe	Ni	Cu	Total
Coupon # 25 b		Spectrum 1	41.740	0.690	1.000	6.530	18.980	0.780	0.140	0.240	1.520	0.300	0.270	0.270	26.930	0.260	0.350	100
		Spectrum 2	39.250	1.140	1.180	6.460	17.900	1.170	0.360	0.420	1.200	0.360	0.260	0.330	29.330	0.280	0.360	100
			Na_2O	MgO	Al_2O_3	SiO_2	K_2O	CaO	V_2O_5	Cr_2O_3	MnO	Fe_2O_3	NiO	CuO	FeS	CuS	NiS	
		Oxide & sulphide ratio	1.348	1.665	1.889	2.139	1.205	1.399	1.785	1.462	1.291	1.430	1.273	1.252	1.574	1.505	1.202	
		spec 1 (% Oxides & sulphides)	0.930	1.665	12.338	40.605	0.289	2.127	0.536	0.395	0.349	38.503	0.331	0.438	42.390	0.527	0.421	
		spec 2 (% Oxides & sulphides)	1.537	1.965	12.206	38.294	0.506	1.679	0.643	0.380	0.426	41.934	0.356	0.451	46.167	0.542	0.151	

Coupon # 10	Well NJ-14		O	Na	Mg	Al	Si	S	Cl	K	Ca	V	Cr	Mn	Fe	Ni	Cu	Zn	Ag	Total	
		Spectrum 1	13.970		0.160	0.950	2.220	38.880							41.400		0.560	1.840		100	
		Spectrum 2	3.920			0.250	0.800	31.880							59.290	3.060	0.800			100	
		Spectrum 3	6.940	0.000	0.270	1.390	4.620	22.670		0.140	0.430		0.200		60.490		1.130	1.050	0.660	100	
		Spectrum 4	25.800	0.990	0.680	7.030	17.860	2.110	0.610	0.530	1.530	1.870		2.180	37.380	0.510	0.930			100	
		Spectrum 5	8.370	0.480	0.340	1.290	4.030	21.630			0.190	0.200		0.290	61.050		1.160	0.960		100	
		Spectrum 6	22.310	0.910	0.740	3.280	9.550	17.370		0.230	0.640	0.410		0.610	38.950	0.400	2.920	1.230	0.440	100	
			Na_2O	MgO	Al_2O_3	SiO_2	K_2O	CaO	V_2O_5	Cr_2O_3	MnO	Fe_2O_3	NiO	CuO	FeS	FeS_2	Fe_3S_4	CuS	ZnS	NiS	AgS
		Oxide & sulphide ratio	1.348	1.665	1.889	2.139	1.205	1.399	1.785	1.462	1.291	1.430	1.273	1.252	1.574	2.148	1.765	1.505	1.490	1.546	1.297
		spec1 (% Oxides & sulphides)	0.000	0.266	1.795	4.749	0.000	0.000	0.000	0.000	0.000	59.191	0.000	0.701	65.166	88.933	73.089	0.843	2.742	0.000	0.000
		spec 2 (% Oxides & sulphides)	0.000	0.000	0.472	1.711	0.000	0.000	0.000	0.000	0.000	84.769	3.894	1.001	93.327	127.363	104.672	1.204	0.000	4.731	0.000
		spec 3 (% Oxides & sulphides)	0.000	0.450	2.626	9.884	0.169	0.602	0.000	0.292	0.000	86.484	0.000	1.415	95.215	129.941	106.791	1.700	1.565	0.000	0.856
		spec 4 (% Oxides & sulphides)	1.334	1.132	13.283	38.209	0.638	2.141	3.338	0.000	2.815	53.443	0.649	1.164	58.839	80.297	65.992	1.399	0.000	0.789	0.000
		spec 5 (% Oxides & sulphides)	0.647	0.566	2.437	8.622	0.000	0.266	0.357	0.000	0.374	87.285	0.000	1.452	96.097	131.144	107.779	1.745	0.000	0.000	0.000
		spec 6 (% Oxides & sulphides)	1.227	1.232	6.197	20.431	0.277	0.895	0.732	0.000	0.788	55.688	0.509	3.655	61.310	83.670	68.763	4.393	1.833	0.618	0.571

			O	Na	Si	S	Fe	Cu	As	Total		
Coupon # 10 c		Spectrum 1	4.26	0.5	0.58	44.62	49.04	0.53	0.47	100		
			Na_2O	SiO_2	Fe_2O_3	CuO	As_2O_3	FeS	FeS_2	Fe_3S_4	CuS	As_2S_3
		Oxide and Sulphide ratios	1.348	2.139	1.430	1.252	1.320	1.574	2.148	1.765	1.505	1.642
		spec1 (% Oxides and Sulphides)	0.674	1.241	70.114	0.663	0.621	77.192	105.345	86.576	0.797	0.772

Olka-OW 34 # 1		O	Si	Total
	Spectrum 1	58.54	41.46	100
	Spectrum 2	55.67	44.33	100

		SiO_2		
	Oxide ratios	2.1393		
	Spec1 (% Oxides)	88.697		
	Spec 2 (% Oxides)	94.837		
Olka-34 # 1b		O	Si	Total
	Spectrum 1	61.15	38.85	100
		SiO_2		
	Oxide ratios	2.1393		
	Spec1 (% Oxides)	83.113		
Olka OW- 34 # 2		O	Si	Total
	Spectrum 1	58.73	41.27	100
		SiO_2		
	Oxide ratios	2.1393		
	Spec1 (% Oxides)	88.29		
Olka OW-34 no 2 overview		O	Si	Total
	Spectrum 1	63.1	36.9	100
		SiO_2		
	Oxide ratios	2.1393		
	Spec1 (% Oxides)	78.941		
Olka OW-34 #3		O	Si	Total
		51.25	48.75	100
		SiO_2		
	Oxide ratios	2.139		
	Spec1 (% Oxides)	104		
Olka OW-34 #3 b		O	Si	Total
	Spectrum 1	66.67	33.33	100
	Spectrum 2	41.82	58.18	100
		SiO_2		
	Oxide ratios	2.139		
	Spec1 (% Oxides)	71		
	Spec 2 (% Oxides)	124		

Olka- OW 34 # 4 b		O	F	Na	Mg	Al	Si	Cl	K	Ca	Fe	Total
	Spectrum 1	56.36	1.47	0.35	0.26	0.82	36.72	0.46	0.34	1.23	2	100
	Spectrum 2	62.92		0.4		0.76	35.41		0.32		0.18	100
				Na_2O	MgO	Al_2O_3	SiO_2		K_2O	CaO	Fe_2O_3	
				1.34797	1.66526	1.8894	2.13934		1.2046	1.3992	1.4297	
				0.47179	0.43297	1.5493	78.5564		0.4096	1.721	2.8595	
				0.53919	0	1.436	75.7539		0.3855	0	0.2574	

Olka OW-34# 4 d		O	Na	Si	S	Cl	K	Fe	Nb	Total
	Spectrum 1	62.73	0.62	28.78	1.65	0.52	0.86	4.84		100
	Spectrum 2	38.97	0.33	46.42	1.69	0.76	1.16	10.67		100
	Spectrum 3	59.18		40.57				0.25		100
	Spectrum 4	62.62	0.21	37.17					0	100

	Na_2O	SiO_2	Al_2O_3	K_2O	Fe_2O_3	FeS	
	1.348	2.1393	1.88945	1.2046	1.42973	1.5741	
Spec1(% Oxides& Sulphides)	0.8357	61.57	3.11759	1.036	6.91989	7.6185	
Spec 2 (% Oxides&sulphides)	0.4448	99.308	3.19317	1.3973	15.2552	16.795	
Spec3 (% Oxides&Sulphides)	0	86.793	0	0	3.8138	0.3935	
	0.0934	79.519	0	0	0	0	

Olka-OW 34# 5 b

	O	Al	Si	K	Fe	Total
Spectrum 1	64.93	0.3	34.49	0.09	0.19	100
		Al_2O_3	SiO_2	K_2O	Fe_2O_3	
		1.8894	2.13934	1.20461	1.4297	
Spec1 (% Oxides)		0.5668	73.7857	0.10841	0.2716	

Olka-OW-34#5 b

	O	Na	Mg	Al	Si	Cl	K	Ca	Cr	Fe	Ni	Total
Spectrum 1	59.98	0.35	1.02	2.84	28.56	0.34	1.1	0.22	0.33	4.7	0.54	100
Spectrum 2	66.57	0.22		0.44	32.66		0.11					100

	Na_2O	MgO	Al_2O_3	SiO_2	SO_3	K_2O	CaO	Cr_2O_3	Fe_2O_3	NiO	CuO	ZnO	As_2O_3	PbO	Ag_2O	MoO_3
	1.348	1.66526	1.88945	2.1393	2.49714	1.2046	1.3992	1.4616	1.4297	1.2726	1.252	1.2447	1.32032	1.0772	1.074	1.5
	0.4718	1.69856	5.36603	61.099	0.84903	1.3251	0.3078	0.4823	6.7197	0.6872						
	0.2966	0	0.83136	69.871	0	0.1325	0	0	0	0						

Olka OW- 34 #5 c

	O	Na	Al	Si	K	Fe	As	Total
Spectrum 1	63.87	0.35	0.61	33.27	0.25	1.41	0.24	100
Spectrum 2	61.56	0.48	1.26	35.87	0.56	0.27		100
Spectrum 3	55.51	0.34	0.88	41.27	0.62	1.09	0.29	100

	Na_2O	Al_2O_3	SiO_2	K_2O	Fe_2O_3	As_2O_3
	1.348	1.88945	2.13934	1.2046	1.42973	1.3203
Spec1 (% Oxides)	0.4718	1.15256	71.1757	0.3012	2.01592	0.3169
Spec 2 (% Oxides)	0.647	2.38071	76.738	0.6746	0.38603	0
Spec 3 (% Oxides)	0.4583	1.66271	88.2904	0.7469	1.55841	0.3829

SCALE SPECTRA

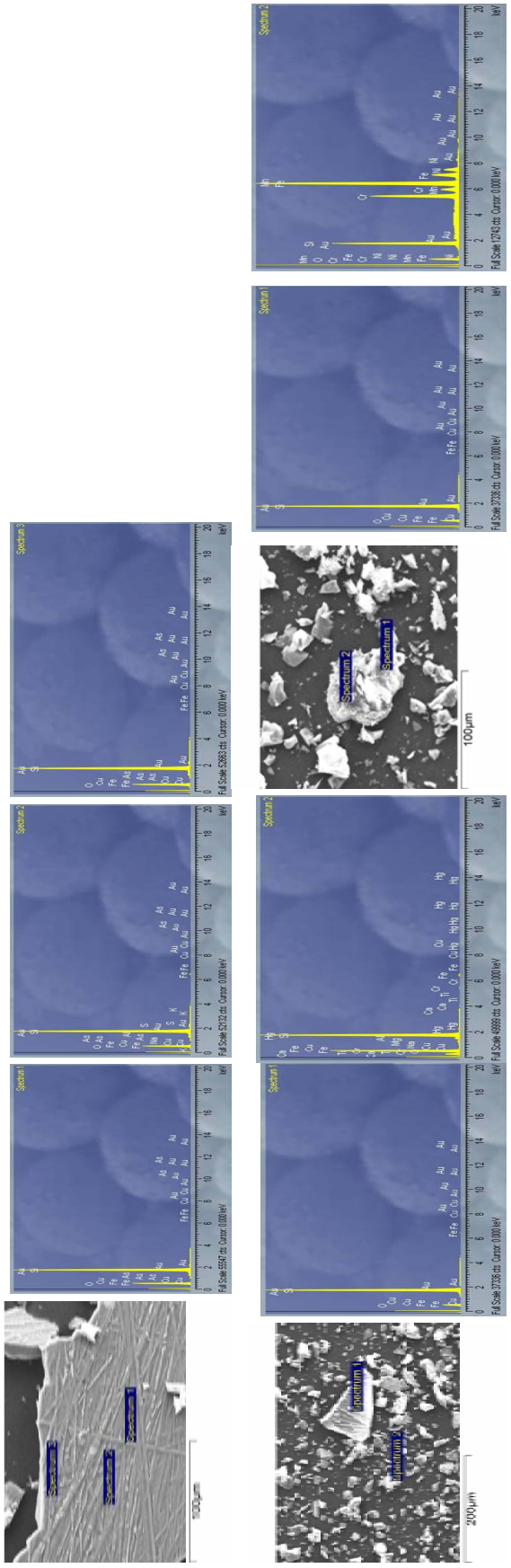

Spectra for scale from coupon # 5

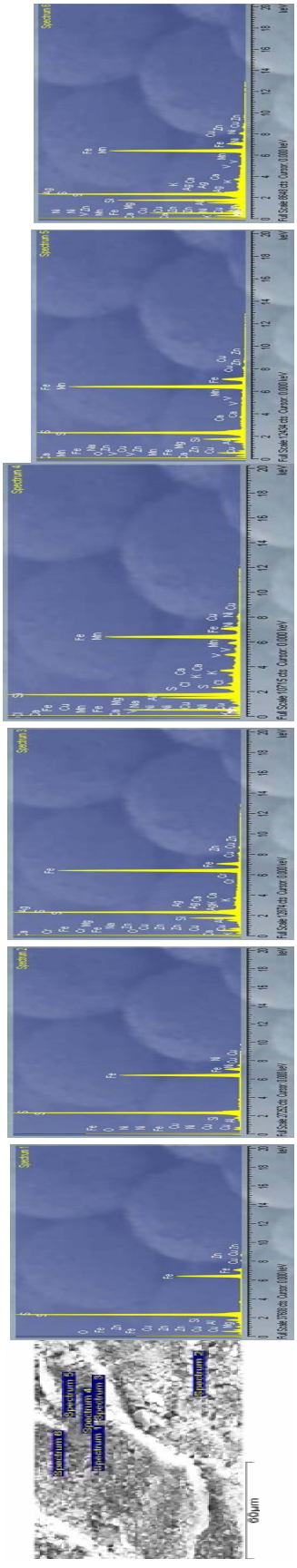

Spectra for scale from Coupon # 10

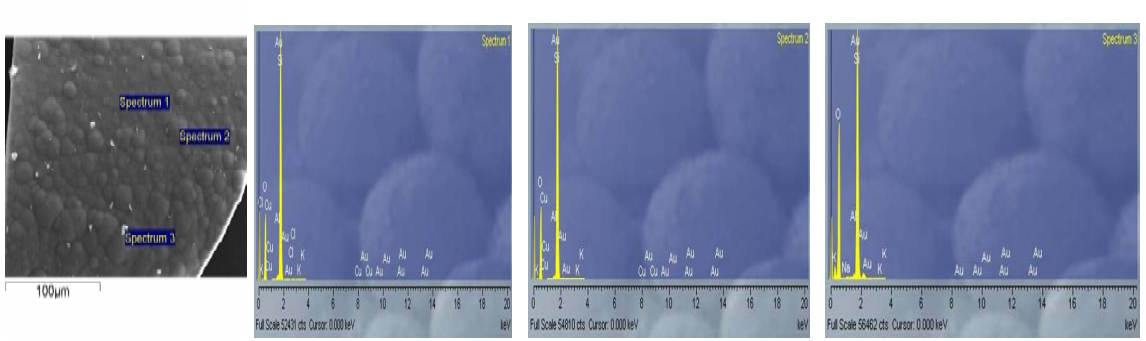

Spectra for scales from coupon # 16

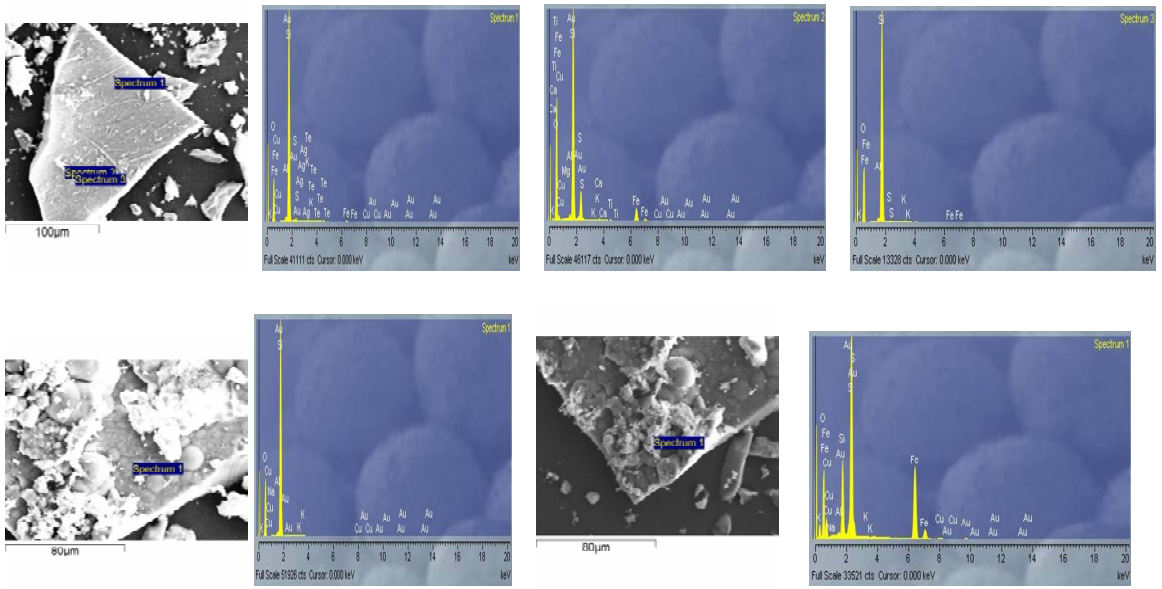

Spectra for scale from coupon # 17

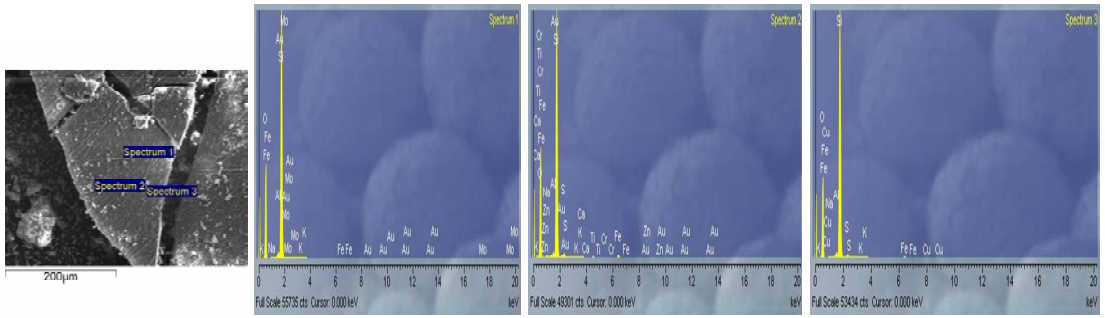

Spectra for scales from coupon # 18

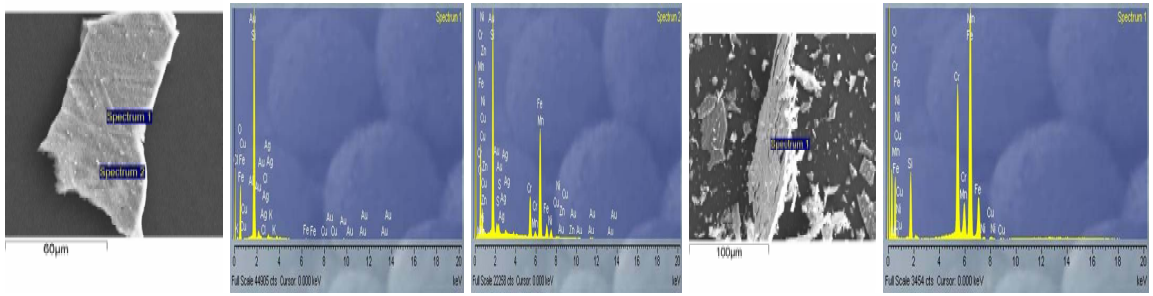

Spectra for scales from coupon # 19

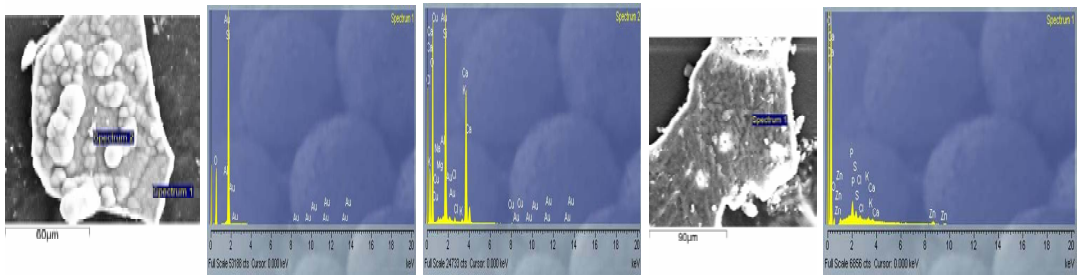

Spectra for scale from coupon # 20

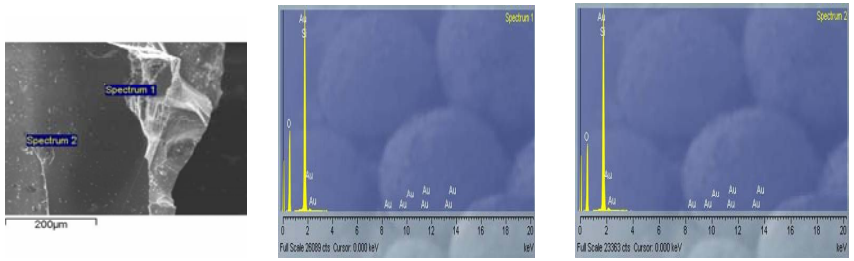

Spectra for Olkaria OW-34 scale # 1

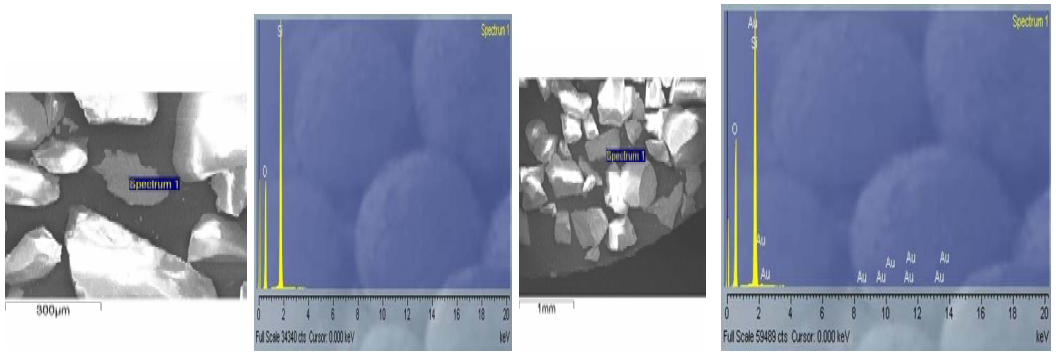

Spectra for Olkaria OW-34 scale # 2

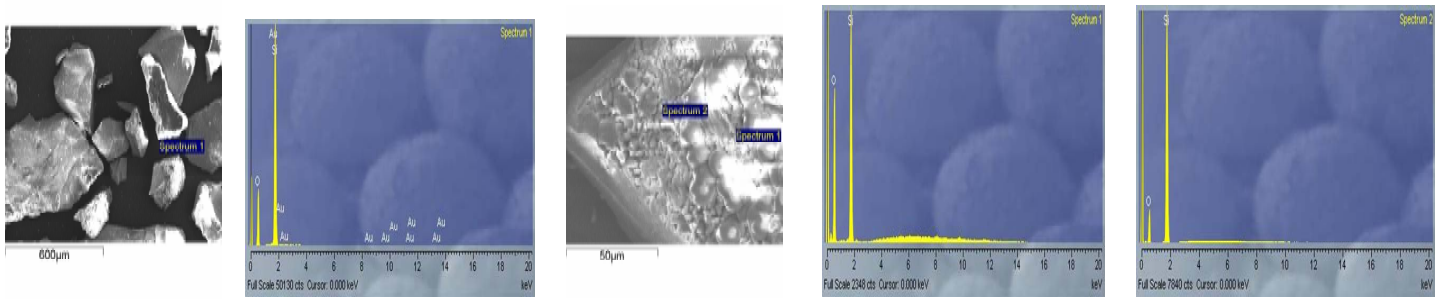

Spectra for Olkaria OW-34 scale # 3

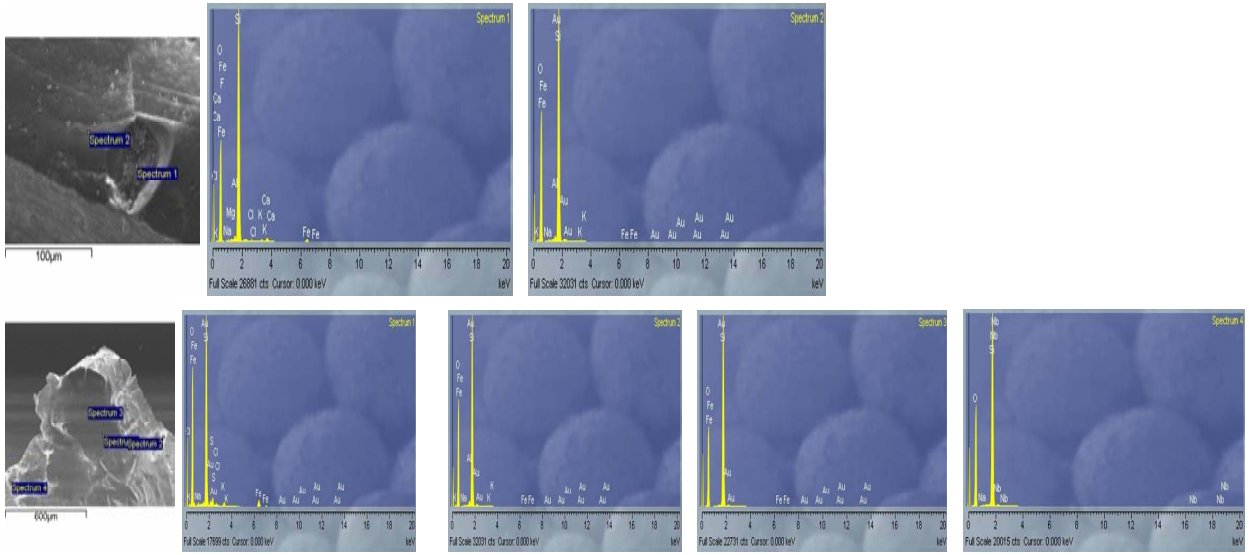

Spectra for Olkaria OW-34 Scale # 4

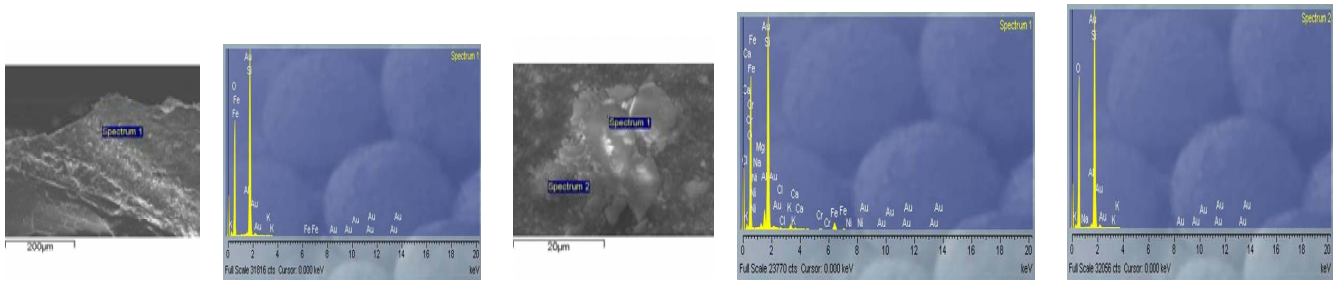

Spectra for Olkaria OW-34 Scale # 5

TABLE 2: Summary of some selected spectra of scales from Nesjavellir in SEM recalculated as oxides and sulphides

Test sites and coupon # no.	Na_2O	MgO	Al_2O_3	SiO_2	CaO	K_2O	V_2O_5	MnO	Fe_2O_3	CuO	Total	FeS	CuS	ZnS	NiS	AgS	As_2S_3	Total
Well NJ-14 coupon # 10	0.65	0.57	2.44	8.62	0.27	0.28	0.36	0.37	87.3	1.45	102.28	96.10	1.75	1.83	0.618	0.57	0.77	101.64
Well NJ-22 coupon # 25	1.54	1.97	12.21	38.29	0.51	1.68	0.64	0.43	41.9	0.45	99.64	46.17	0.54	5.59	0.421			52.72
After heat exchanger # 16	0.30		0.64	98.54		0.29					99.77							
Retention tank # 5,	0.20		0.32	98.69	1.17						100.38	1.53	0.40				1.81	3.74
Retention tank entry # 17	1.28		1.45	100.48	0.39	0.145					103.76							
Retention tank entry # 18	0.38		1.38	91.86		0.398			0.77		94.79	1.84	0.57	0.76				3.17
Re-injection well # 19	0.74	0.23	0.32	99.67					0.60		101.57	0.66	1.9					2.57
Re-injection well # 20			0.34	102.60							102.94							

TABLE 3: Percent as oxides in well OW-34 scales on a semi-quantitative basis on SEM elemental analysis

Sample #	Na2O	MgO	Al2O3	SiO2	K2O	CaO	Fe2O3
1	-	-	-	100	-	-	-
2	-	-	-	100	-	-	-
3	-	-	-	100	-	-	-
4	0.47	0.43	1.55	78.56	0.41	1.72	2.86
5	0.46	1.7	1.66	88.29	0.75	0.31	1.56

Samples # s1 to # 3 showed only silicon and oxygen could be ~100% silica